NGU REPORT 2018.002

Reprocessing of ERT data from Åknes,
Stranda Municipality,
Møre & Romsdal County

GEOLOGY FOR SOCIETY

SINCE 1858

GEOLOGICAL SURVEY OF NORWAY

- NGU -

NORGES GEOLOGISKE UNDERSØKELSE
- NGU -

REPORT

Geological Survey of Norway
P.O.Box 6315 Torgard
NO-7491 TRONDHEIM
Tel.: 47 73 90 40 00

Report no.: 2018.002

ISSN: 0800-3416 (print)
ISSN: 2387-3515 (online)

Grading: Open

Title:
Reprocessing of ERT data from Åknes, Stranda Municipality, Møre & Romsdal County

Authors:
Georgios Tassis, Jan Steinar Rønning

Client: NVE, Norwegian Water Resources and Energy Directorate

County:
Møre & Romsdal

Commune:
Stranda

Map-sheet name (M=1:250.000)
Ålesund

Map-sheet no. and -name (M=1:50.000)
1219 II Geiranger

Deposit name and grid-reference:
Åknes, UTM 32 395800 – 6895200

Number of pages: 85 **Price (NOK):** 300,-
Map enclosures:

Fieldwork carried out:	**Date of report:**	**Project no.:**	**Person responsible:**
2004 -2007, 2017	12.04.2018	329500	Marco Brönner

Summary:

NGU performed consecutive geophysical investigations in the Åknes area from 2004 until 2007 in connection with the Åknes/Tafjord project. These investigations consisted of 10 km of ERT profiling distributed in 10 profiles, 8 km of georadar profiling distributed in 10 profiles and 1.8 km refraction seismic profiling distributed in 4 profiles. All results were presented in NGU reports (Rønning et al. 2006; Rønning et al. 2007), interpretations were made on these results and conclusions were drawn regarding the extent of unstable bedrock in the area. Processing of resistivity data took place with the Res2DInv software version available at the time (versions 3.54j and 3.55.48) whereas traditional Hagedoorn's plus-minus method was applied on refraction seismic. In this report we focus on the ERT profiling since this method helped determining the dimensions of the unstable masses to 500 x 1200 meters spread and 40-60 meters thickness and gave indications on possible vertical or inclined fracture zones.

The ERT data were processed and interpreted using *Standard inversion* (L2-norm) and a V/H filter equal to 0.5 to favour horizontal structures and thus map the lower resistivity layer more accurately. During the last ten years new and more powerful inversion algorithms have been developed and implemented in Res2DInv. The ten existing ERT profiles from Åknes were reprocessed using a larger variety of approaches i.e. enabling *Robust* (L1-norm) in addition to *Standard inversion* and by using various V/H filters. It is expected that *Robust inversion* and values for V/H filter larger than 1.0 could help accentuate possible sub-vertical fracture zones. Moreover, another 1 km long ERT profile has been added to the ten old ones and has also been processed and interpreted using the newest Res2DInv version available (ver. 4.07.11). This profile was measured with Gradient Plus array in addition to Wenner and Dipole-Dipole arrays which were used in the old investigations.

Along with reprocessed data and new interpretations, this report presents a methodology for extracting a modified logarithmic scale for color distribution which is more suitable for the highly resistive environment in Åknes than the one automatically chosen by any plotting software. All results were also exported accordingly to be compatible with a 3D model for Åknes compiled in a modified version of Schlumberger's PETREL software package. This demanded an in-depth reevaluation of how topography should be sampled and incorporated in Res2DInv tied with accurate UTM coordinates for inversion results to match detailed DEMs such as ones based on LiDAR data.

Keywords:	Geophysics	Resistivity
Reprocessing	Unstable rock	Fracture zones
Rock quality	Groundwater	Scientific report

CONTENTS

1. INTRODUCTION

The Norwegian Water Resources and Energy Directorate (NVE) has obtained a budget to evaluate methods for stabilizing the unstable bedrock masses in Åknes by means of groundwater drainage. To achieve that, it is necessary to increase the knowledge of how groundwater operates within the bedrock masses. Earlier surveys between 2004 and 2007 consisted both of ground geophysics (Rønning et al. 2006; Rønning et al. 2007) and borehole logging measurements (Elvebakk 2008, Elvebakk 2013). The results of these investigations contributed to a better understanding of how big the volume of unstable masses is and how the groundwater moves beneath the mountainside. However, as already mentioned it is now suggested that slope stabilization can be improved by draining out groundwater and to evaluate this, more geophysical and geological investigations must be performed.

This report is focused on three tasks i.e. the reprocessing of already existing ERT data, the acquisition and processing of new resistivity data and the formatting of the results to be compatible with a 3D model of Åknes, built up in PETREL software (Schlumberger 2017). As previously stated, the NGU has performed intensive work with the ERT data collected in Åknes in 2004 and 2007 and the results obtained have already been published in NGU reports referenced above. However, this report is contributing to the already acquired knowledge by producing better and more reliable results with the use of the latest version of Res2DInv (Loke 2017) with recently developed more powerful inversion algorithms, which allow to perform different inversions with a larger selection of parameters as opposed to the singular approach of the old reports, by using more detailed LiDAR topography and by plotting the results in Surfer 15 (Golden Software 2018) program package, where more flexibility with color scales and plotting options is available.

2. RESISTIVITY MEASUREMENTS

2.1 Data Collection

Measurements for profiles 1 to 10 (**figure 2.1**) were acquired with a cable system developed at the Faculty of Engineering in Lund (LUND system - Dahlin 1993). The system consists of a relay box (Electrode Selector ES464) and two or four multi-electrode cables. The measurement sequence was controlled by a data file which was uploaded in the instrument, ABEM Terrameter SAS 4000 (ABEM 1999). In that survey, a 4-cable with 5 and 10 m electrode spacing was used which amounts to a total cable length of 400 and 800 meters respectively. All profiles were measured with both Wenner and Dipole-Dipole arrays, since Wenner is more suitable for mapping horizontal layers and Dipole-Dipole is more sensitive to vertical structures such as faults or weakness zones. Depth coverage with these electrode configurations is about 65 and 130 meters by default, with the highest resolution achieved in the upper half of the sections.

Profile 11 (**figure 2.1**) which was carried out in 2017 and covers the western flank of the slope, was measured with the Terrameter ABEM-LS system (ABEM 2012) using

the Lund system and an electrode spacing equal to 10 m and Wenner, Dipole-Dipole and Multiple Gradient arrays. Electricity was inserted in the ground in 1 second pulses and with shifting polarity. Measuring of resistivity in Ωm started 0.4 seconds after the current was turned on while the measurement time was 0.6 seconds. All profiles were marked during the measurement phase and their coordinates measured with GPS. The old profiles were measured every 50 meters whereas Profile 11 had every electrode marked.

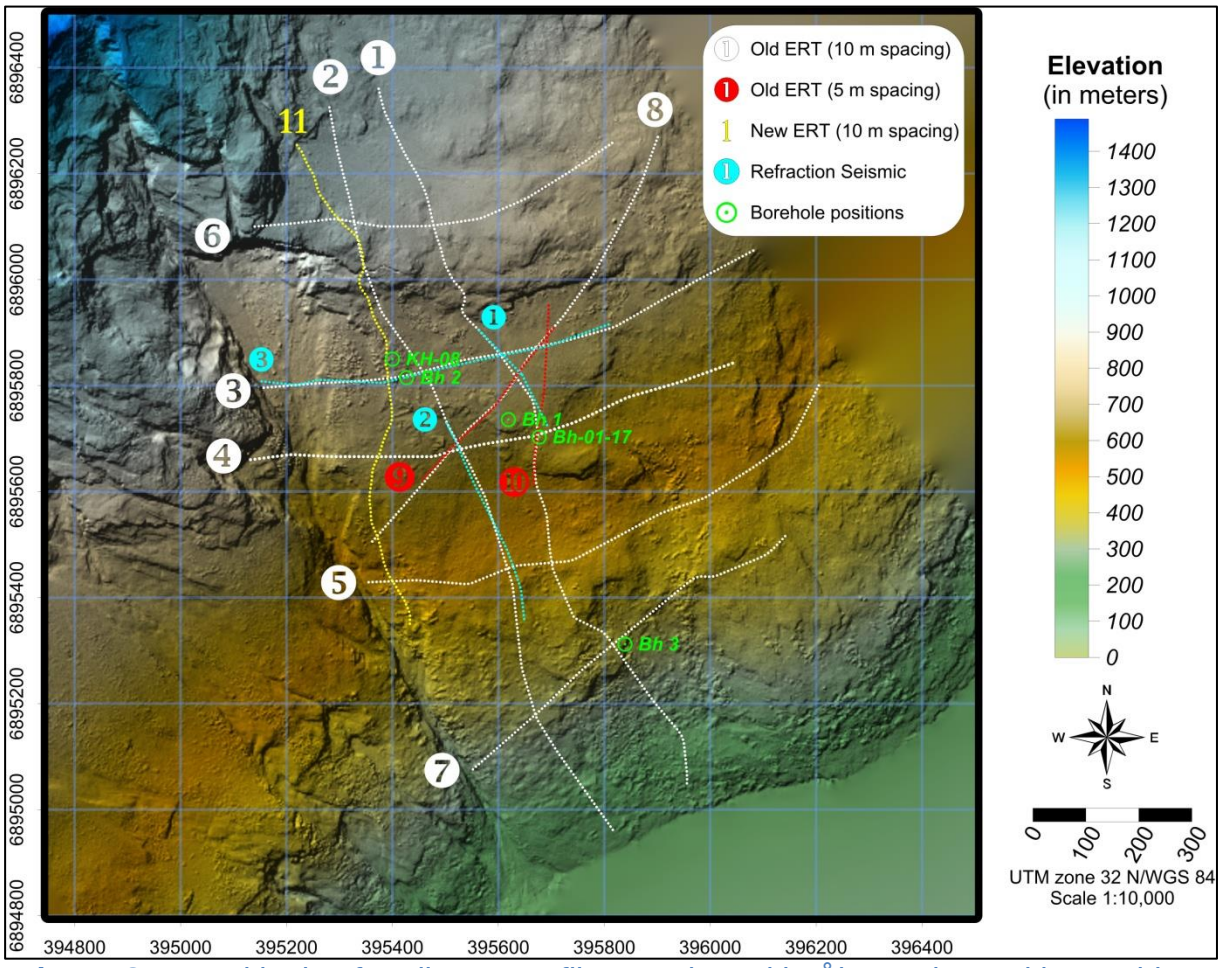

Figure 2.1: Positioning for all ERT profiles conducted in Åknes along with matching Refraction Seismic profiles and Borehole positions. LiDAR elevation relief.

2.2 Data Quality, Preparation & Preprocessing

The ground conditions were very poor due to loose stones and boulders in several places, and extra time was spent on improving the electrode contact (sponges / moss with saltwater). Even with these improvements, a current of only 1 or 2 mA could be achieved for some measurements, but most were at the 10 and 20 mA level. Despite of these problems, the data quality was very good even with the very low current levels. Some measurements were above acceptable noise levels, and these were deleted before processing.

Before undergoing inversion, all data had topography and UTM zone 32 coordinates assigned to them. Topography was sampled from detailed LiDAR data with the

elevation point spacing set equal to the electrode spacing used for each profile. The reason for not choosing a more detailed spacing is that due to the very steep topographic conditions, there are too many consecutive elevation points which form angles higher than 60^{o} which is a condition Res2DInv does not accept. Instead, the program scans topography and when it detects such a pair of points, it gives a warning message and then proceeds to modifying the angle to become 60^{o}. This results in distorted topographic surfaces which translates into a mismatch between the resulting profiles and the DEM model from LiDAR. Therefore, for the profile topography to match the LiDAR data, all points with inclination higher than 60^{o} were deleted from the raw data files (*.dat files). Furthermore, to avoid assigning wrong topographic values due to inaccurate surface distances between electrodes, the real electrode spacing was extracted by calculating the true distance along topography and dividing by the total number of electrodes per profile. This resulted in a slight error due to a small elongation of the profiles. However, this doesn't affect the overall positioning of the inversion results and subsequent interpretations. Eventually, by doing these topographic calculations, we were able to accurately link the ERT profiles with real world coordinates as best as possible, although not perfectly.

Preprocessing of data took place in two steps within Res2DInv. The first step consisted of exterminating obvious bad data points and then running standard inversion. The second step included a RMS error statistical analysis which allowed us to delete points with errors higher than an intuitively selected percentage of maximum error. The second stage of preprocessing took place on the inversion results, but the edited data were saved in raw format so that inversion can be reapplied to these files. Additionally, the maximum error percentage was not constant for each profile and heavily depended on the array used and the number of point data per file. Finally, after cleaning all data files and saving them in general array format, it was possible to merge Wenner and Dipole-Dipole data and create unified data files with more points and subsequently higher resolution.

2.3 Inversion

What is measured in all resistivity surveys, is an apparent resistivity. This represents a weighted means of all resistivities within the influence range of each point measurement. To find the true resistivity in different parts of the subsurface, data must be inverted. This is done by dividing the ground into blocks and by assigning to each of them a certain resistivity starting value. Then, these values are adjusted in several stages (iterations) until the response from the theoretical model fits the measured data as good as possible. The remaining misfit is described mathematically with the use of an RMS error percentage.

Resistivity measurements were reinverted using Res2DInv, version 4.07.11 (Loke 2017). Originally, the old ERT data measured in 2004 to 2007 were inverted using Res2DInv versions 3.54j and 3.55.48 respectively. Furthermore, while the old processing only utilized *Standard inversion* (L2-norm) and V/H filter equal to 0.5 to highlight horizontal layering, this report presents six different results for each array. These results represent processing with both *Standard* and *Robust inversion* (L1-norm) and V/H filters equal to 0.5, 1 and 2. This was done to display the variety of results ERT inversion can provide and also to investigate the possibility of unveiling fracture zones not possible to detect in the old inversions. The other inversion

parameters were kept to the default values the software developer M.H. Loke suggests for *Standard* and *Robust inversion*. One extra feature that does not affect the result that much, is the use of setting a range of accepted values within inversion to avoid the calculation of extremely high resistivity values. This range was set equal to 5 times the average resistivity after the first iteration.

2.4 Statistical Analysis & Color Scale

After ensuring that the correct topography and accurate UTM coordinates were affixed to the raw data and that bad data points have been successfully removed, inversion became a straight-forward procedure. Inversion parameters used for each of the six different approaches were saved in respective files (*.ivp) and loaded automatically for each profile array. This automatisation allowed us to run i.e. 204 individual inversions, in a very reasonable time. These 204 inversions amount to almost 600,000 point values (**table 2.2**) which outline the geoelectrical conditions over the whole survey area and therefore can be used for constructing a representative resistivity color scale for Åknes. This helped emphasizing the critical point where bedrock becomes water saturated and/or fractured.

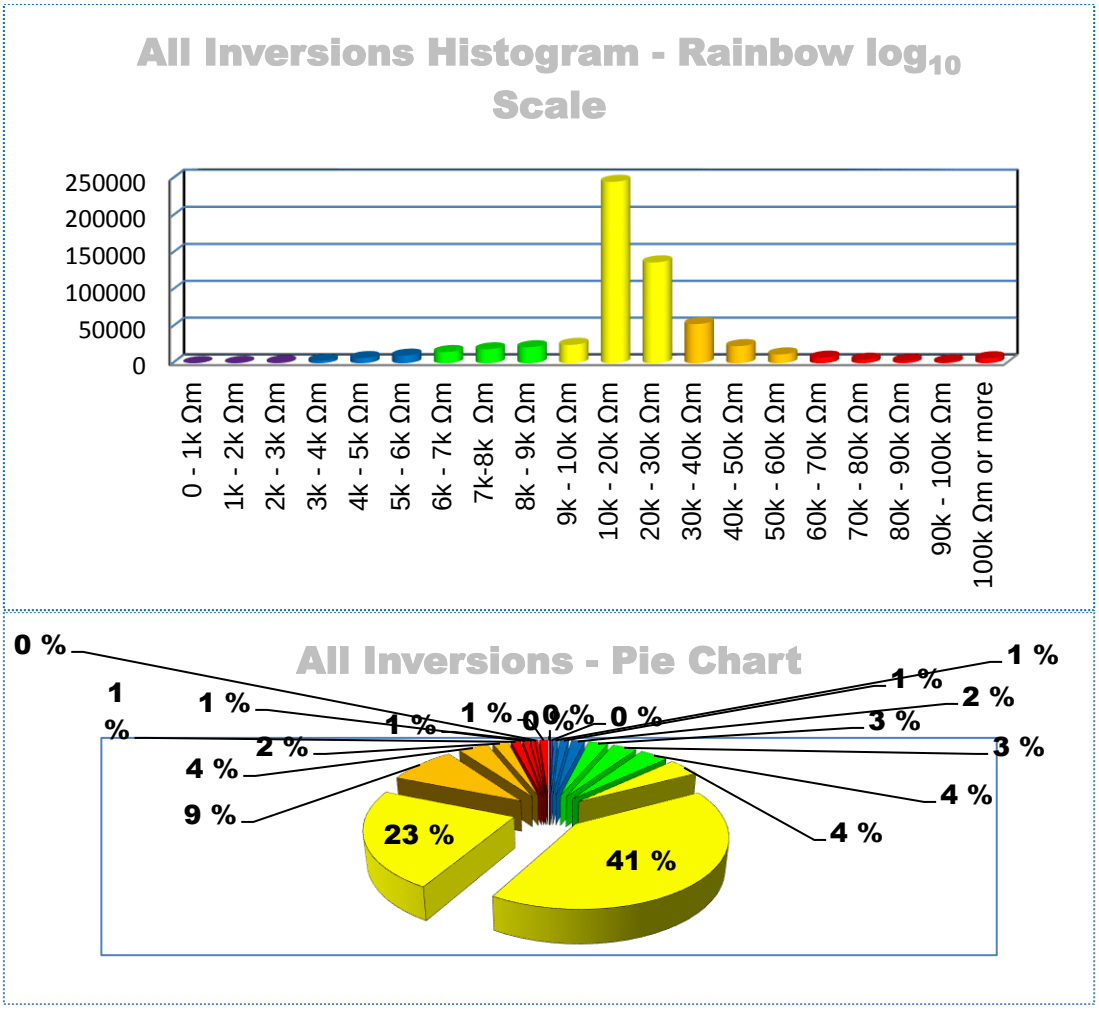

Figure 2.2: Top: Histogram depicting the statistical characteristics of all inversion results. Bottom: Pie chart depiction of the same data. Colors in both plots exhibit how a typical rainbow logarithmic scale would group resistivity values up to 100,000 Ωm.

Top side in **figure 2.2** shows a histogram for all resistivity point values obtained with inversion while bottom side in **figure 2.2** displays the same information in the form of a pie chart which also provides an outlook of the portion of the total each grouping represents. Both figures also portray how an automatically picked logarithmic scale using the typical rainbow color succession would classify the resulting resistivity values. It becomes obvious that resistivity values between 10 and 20 thousand Ωm represent 41 % of the obtained results while using an automatic grouping, values between 9 and 30 thousand Ωm are put together which amounts to 68 % of the total. **Figure 2.2** proves exactly how dominant the yellow color would be in an automatically picked rainbow color scale such as this and how randomly the color changes are if we do not establish quantitative rules when choosing a color scale.

Range	*No. Of values*
0 - 1k Ωm	222
1k - 2k Ωm	586
2k - 3k Ωm	1498
3k - 4k Ωm	3430
4k - 5k Ωm	7048
5k - 6k Ωm	10373
6k - 7k Ωm	15258
7k-8k Ωm	18978
8k - 9k Ωm	21824
9k - 10k Ωm	25053
10k - 20k Ωm	245724
20k - 30k Ωm	137120
30k - 40k Ωm	53295
40k - 50k Ωm	23265
50k - 60k Ωm	12025
60k - 70k Ωm	7635
70k - 80k Ωm	4906
80k - 90k Ωm	3230
90k - 100k Ωm	2242
100k Ωm or more	6801

Table 2.1: Logarithmically distributed statistics for all inversion results.

Table 2.1 shows that the environment in Åknes is highly resistive and that only a few values can be found below 1,000 Ωm. On the other hand, there is still a considerable number of values over 60,000 Ωm but such values represent highly fractured bedrock which is drained or bedrock with extremely low porosity. Talus (scree material) will also have an extremely high resistivity since it is probably drained. These high values might also be caused by bedrock with permafrost but this is less likely. Further differentiation is of no interest. Therefore, our color scale spectrum is dictated by the environment to be between 1,000 and 60,000 Ωm.

The second step is assigning critical resistivity values where experience predicts condition changes. Interpretation in the old reports has been done manually and has tried to set the limit for water-saturated fractured bedrock possibly unstable at around 10,000 Ωm and downwards. However, we have to place the first critical point at 12,000 Ωm to set the upper limit for water-saturated fractured areas prone to movement and

the lower limit for gradually increasing bedrock mass quality. The color change at 7,500 Ωm represents a further classification of water-saturated bedrock while 37,500 Ωm represents the critical point where bedrock starts becoming extremely fractured and drained. Essentially, the resistivity spectrum is divided in such a way that it represents three main classes of Åknes bedrock with a few extra sub-classes i.e. water-saturated fractured (12,000 Ωm or less), varyingly unfractured bedrock (12,000 - 37,500 Ωm) and increasingly drained fractured bedrock (37,500 Ωm or more).

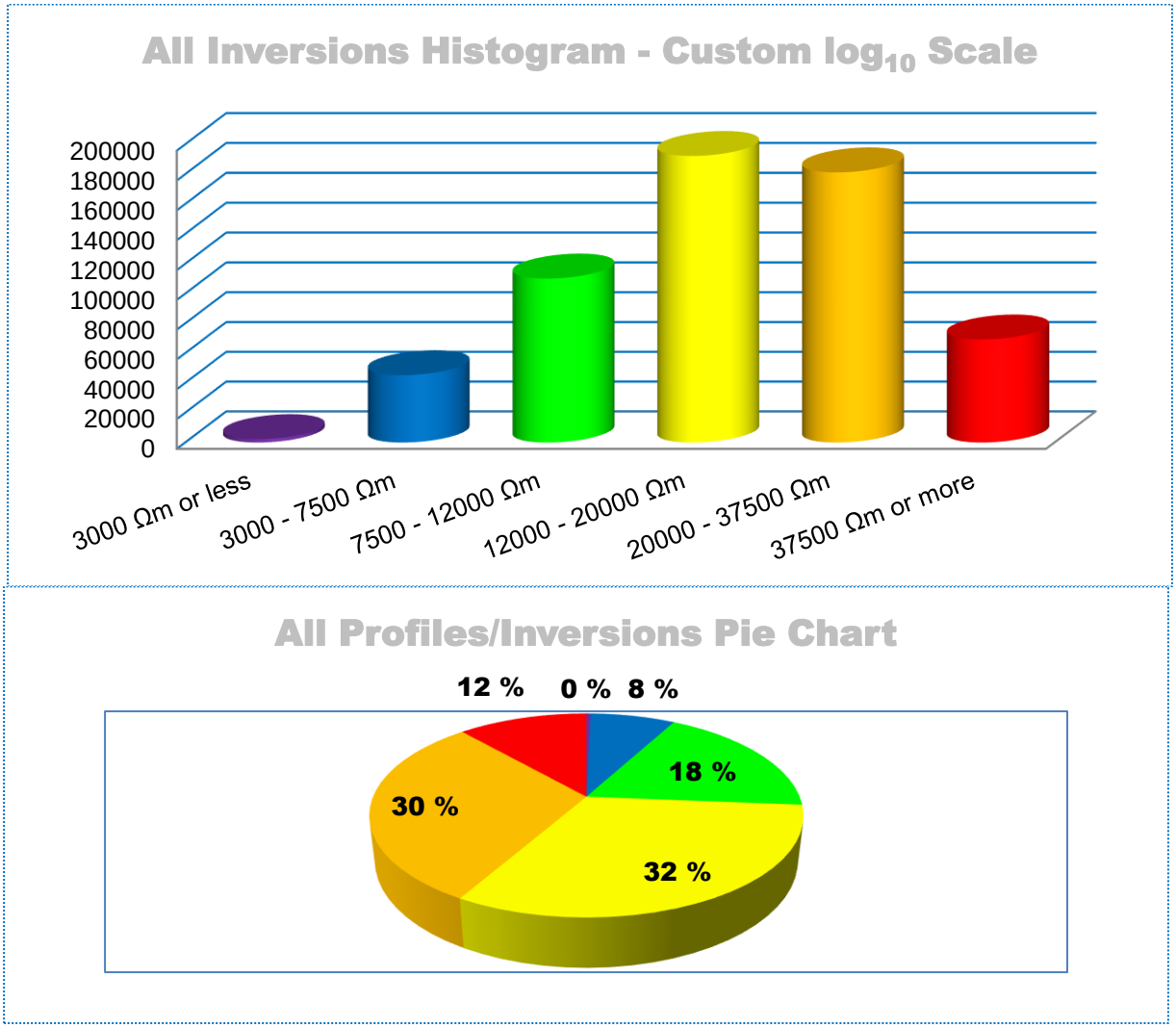

Figure 2.3: Top: Histogram depicting the statistical characteristics of all inversion results. Bottom: Pie chart depiction of the same data. The color choice in both plots exhibits how a custom-made rainbow logarithmic color scale would group resistivity values up to 60,000 Ωm with critical point values at 12,000 and 37,500 Ωm.

Figure 2.3 shows how the new critical point establishment modifies the grouping and distribution of the resistivity values after inversion with several different parameters. Bottom side in **figure 2.3** shows that our data are roughly categorized now in three parts which approximately form up one third of the total number each. This kind of statistical depiction and the fact that the profiles conducted in Åknes are almost placed in a grid which covers the entire mountainside (**figure 2.1**), enables us to make a rough assumption on the bedrock quality for the whole survey area. Therefore, 26 % can be considered as possibly water-saturated fractured bedrock, 62 % as unfractured healthy

bedrock and 12 % as drained fractured bedrock. As can be seen, the new value grouping which essentially also means a new custom-made color scale, presents a more balanced distribution of inversion results and gives more emphasis to the values below 12,000 Ωm where water-saturated fractured bedrock is more likely to occur. The new color scale is still logarithmic, but it is not using equal distribution of colors on the chosen data spectrum (1 to 60 thousand Ωm) but a more geoelectrical aware modified version instead. It should also be noted that our results will be presented with the use of filled contours and this means that there is going to be a gradual change in hue between colors instead of the sharp changes we see in **figure 2.3**. Finally, **table 2.2** gives the numerical values on which the plots in **figure 2.3** were based on.

Range (Ωm)	***Number***	***Portion (%)***
3000 or less	2,306	0.4
3000 - 7500	45,312	7.6
7500 - 12000	110,145	18.3
12000 - 20000	192,231	32.0
20000 - 37500	181,238	30.2
37500 or more	69,281	11.5

Table 2.2: Custom logarithmic distribution for all inversion results.

2.5 Effect of the New Color Scale

It is essential to show here the effect of the use of the new custom log scale on the depiction of our results. The comparison will also include the typical Res2DInv color scale which has also been tampered on the reporting of the old inversion results. **Figure 2.4** presents the comparison between two versions of both old and new inversion results for Profile 01 (L2-norm & V/H filter = 0.5) and the same results with use of two color scales i.e. old / automatic vs. new. Profile 01 was chosen to be the focus point in this comparison because it is one of the longest profiles (1800 meters along topography or 1500 meters of projected distance) and covers the entire slope from almost top to bottom. Furthermore, the Dipole-Dipole measurements for Profile 01 were utilized for essentially the same reason. Dipole-Dipole array produces more measurements than Wenner. Ideally, a mixed Wenner & Dipole-Dipole array would be the best option, but no such data fusion took place in the original processing.

Right hand side in **figure 2.4** shows the merit connected with using the new custom-made logarithmic scale. Left hand side in the figure shows the exact same data plotted with an automatically generated rainbow color scale in Surfer (top) and a slightly tampered but still frigid Res2DInv color scale (bottom). On the new inversion results, a typical log scale is plotting all data which could represent our Area Of Interest (AOI) in similar hues between green and yellow, making it hard to distinguish anything in these relatively low-resistivity areas. However, when the new log scale is used, the color contrast in the AOI becomes more intense and the differences more vivid. Same stands for the old inversion results. The default Res2DInv color scale is also dominated by green or light blue colors and the contrast is hardly distinguishable. Again, the implementation of the new color scale on the same data brings about the same effect as before: stronger contrast and more vivid colors in AOIs. Finally, if we take a closer look at the bars on the top of the figure, it can be clearly seen that with the new color scale, the resistivity area between 6,000 and 20,000 Ωm now contains the biggest color variation (from blue to red) which helps the AOIs to be more emphasized.

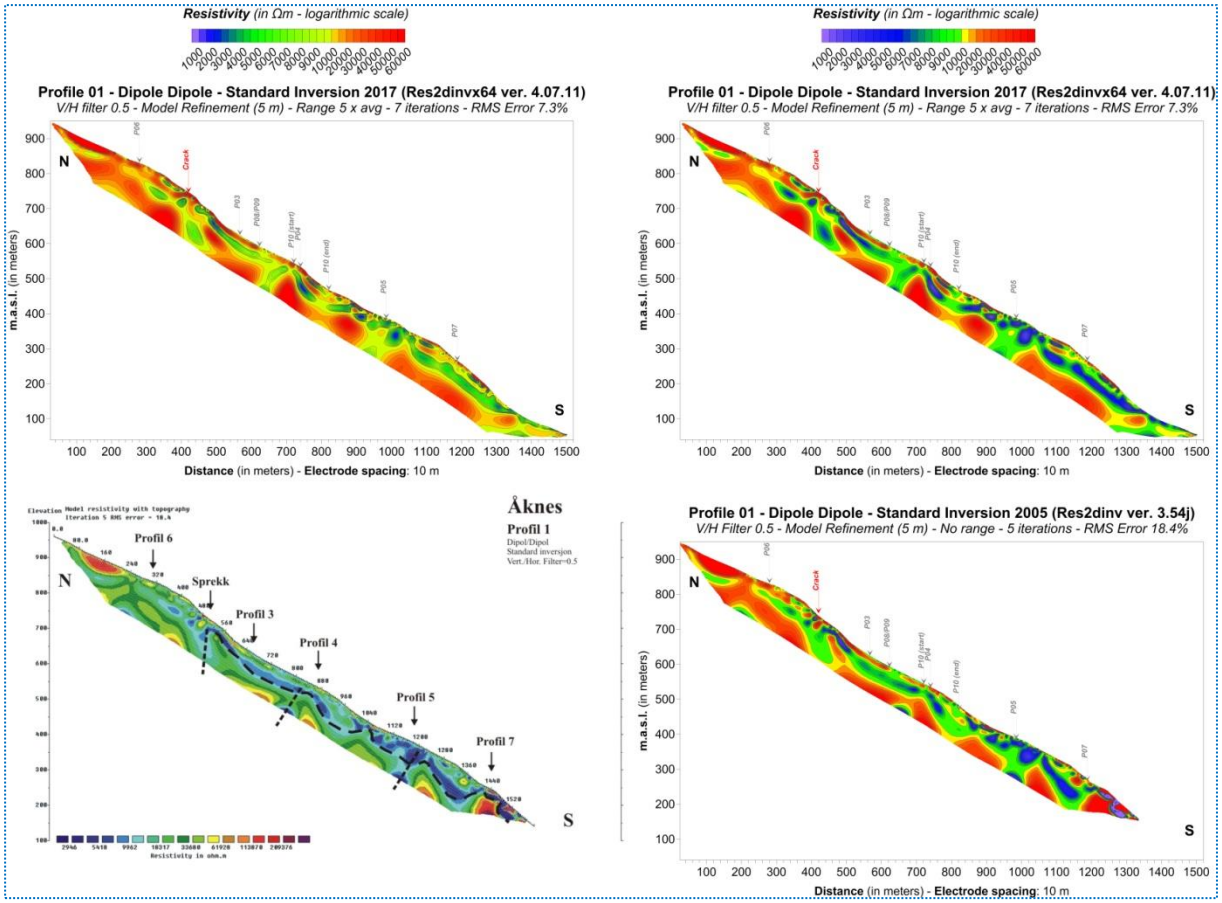

Figure 2.4: Top: Inversion result using the latest Res2DInv software with an automatically generated rainbow color scale (left) and the new custom-made color scale (right). Bottom: Inversion result using the old Res2DInv software with the built-in color scale (left) and the new custom-made color scale (right). All profiles represent Profile 01 processed with Standard (L2-norm) inversion and V/H filter = 0.5. Note that Profile 1 is extended after the first inversion.

3. REPROCESSING RESULTS, PRESENTATION AND DISCUSSION

In this section, we will present the results after reprocessing the ERT data from Åknes in two stages. First, we will be comparing the part of the results which matches the old inversion in parameters utilized to discern what kind of differences the newest Res2DInv version can bring about on the results. Old inversion results are presented in the same way that they were presented in the respective NGU reports i.e. with interpretations made by E. Dalsegg incorporated in the profiles. The same interpretations are also plotted with the reprocessing results to give out a first impression on how interpretations can change after the new inversion results. However, the old ERT data suffer from the same topographic mismatch we have explained in **section 2.2** due to the steep slope conditions in Åknes. Therefore, it was essential to apply corrections to the old interpretations to be accurately incorporated in the reprocessing results. It should be noted that this comparison only takes place for the old ten profiles since profile 11 was only conducted in 2017 and no old inversion results exist.

Secondly, all six inversion results we obtained for each profile and array will be presented to highlight the variety of different outcomes one may acquire with the use of different parameters in Res2DInv. All results will share the same structure i.e. left side will display the *Standard inversion* (L2-norm) results and the right side the *Robust inversion* (L1-norm) results. Then, the vertical to horizontal ratio filter (or V/H filter) will be increasing from top to bottom from 0.5 to 1.0 and finally to 2.0 for both inversion norms. Results are grouped according to array which essentially means three sets of results for the old profiles (Wenner, Dipole-Dipole and Mixed) and four for profile 11 (Wenner, Dipole-Dipole, Gradient Plus and Mixed).

Before we focus on the reprocessing results for each profile and array separately, it is necessary to point out how the use of L2- or L1-norm affects the inversion. *Standard inversion* (L2-norm) is generally creating higher contrasts between high and low-resistivity values and is followed by slightly higher RMS error percentages. *Robust inversion* (L1-norm) on the other hand produces lower RMS errors, cleaner and less pronounced resistivity contrasts and pushes the calculated features to acquire rectangular shapes with more abrupt angles as opposed to *Standard inversion*. Theoretically, this should benefit vertical structures but in practice, the use of *Robust inversion* helps formulate vertical zones better, but *Standard inversion* assigns lower resistivities to these zones making them more pronounced in these results. Finally, higher V/H filters result in higher fragmentation and therefore a higher frequency of fracture zone formulation. The intensity of this effect has to be evaluated at the interpretation stage and not all indicated weakness zones are necessarily real.

All profiles are plotted with the use of the custom-made log color scale, which was presented in the previous section. The most important inversion parameters used are listed on the title of each profile together with the RMS error percentage. Positions where profiles are intersected by other profiles or ground features such as a big crack located in the northern part of the slope and visible in **figure 2.1** a bit south of profile 6, are marked with arrows while the general direction is stated at the start and end of each profile.

3.1 ERT Profile 01

Profile 01 is the easternmost profile conducted in Åknes and crosses the whole slope from top to bottom in very steep topography and with a North-Northwest / South-Southeast orientation (see **figure 2.1**). The mean inclination is about 35^{o} thus even though the distance along topography is 1800 meters if we consider the 181 electrodes used with a 10 m spacing, the horizontal or projected distance of the profile becomes 1496 meters. This profile is intersecting the back-scarp to the north of the area at about 420 meters while all the East-West profiles are cutting across Profile 01 in various locations. Refraction seismic Profile 01 matches part of ERT Profile 01 while several boreholes are in close proximity to its course like Bh-01-17 and Bh-03 (see **figure 2.1**). Parts of Profile 01 and 10 also match even though the direction of Profile 10 is almost pure North-South.

Figure 3.1.1 presents the comparison between the inversion done with Res2DInv ver. 3.54j and the inversion done with ver. 4.07.11. The newest inversion is conducted with more iterations compared to the old ones (seven instead of five) and the RMS error change varies with array used. More specifically, the percentage compared to the 2005

processing appears to be higher when Wenner is inverted (2. 9 % versus 1.9 %) but much lower with Dipole-Dipole (4.6 % versus 18.4 %). The RMS deviation in the case of Wenner is negligible but the relatively higher value in the new processing may be caused by less intense data cleaning. Moreover, the level of detail is higher in the old results, but this is due to the fewer iterations used which also is reflected in a significantly higher error in the case of Dipole-Dipole. As expected, both results are very close in qualitative terms, but they are not identical.

The new inversion of the Wenner data returns fewer areas of very high resistivity (bedrock) whereas the lower resistivity areas appear to be quite alike both in terms of value and distribution. However, the new inversion calculates a much less resistive southern end for this profile with a highly resistive area which is only present in the 2005 inversion. Possible vertical structures are still apparent in both results even though neither the array nor the inversion scheme is proper for such interpretations.

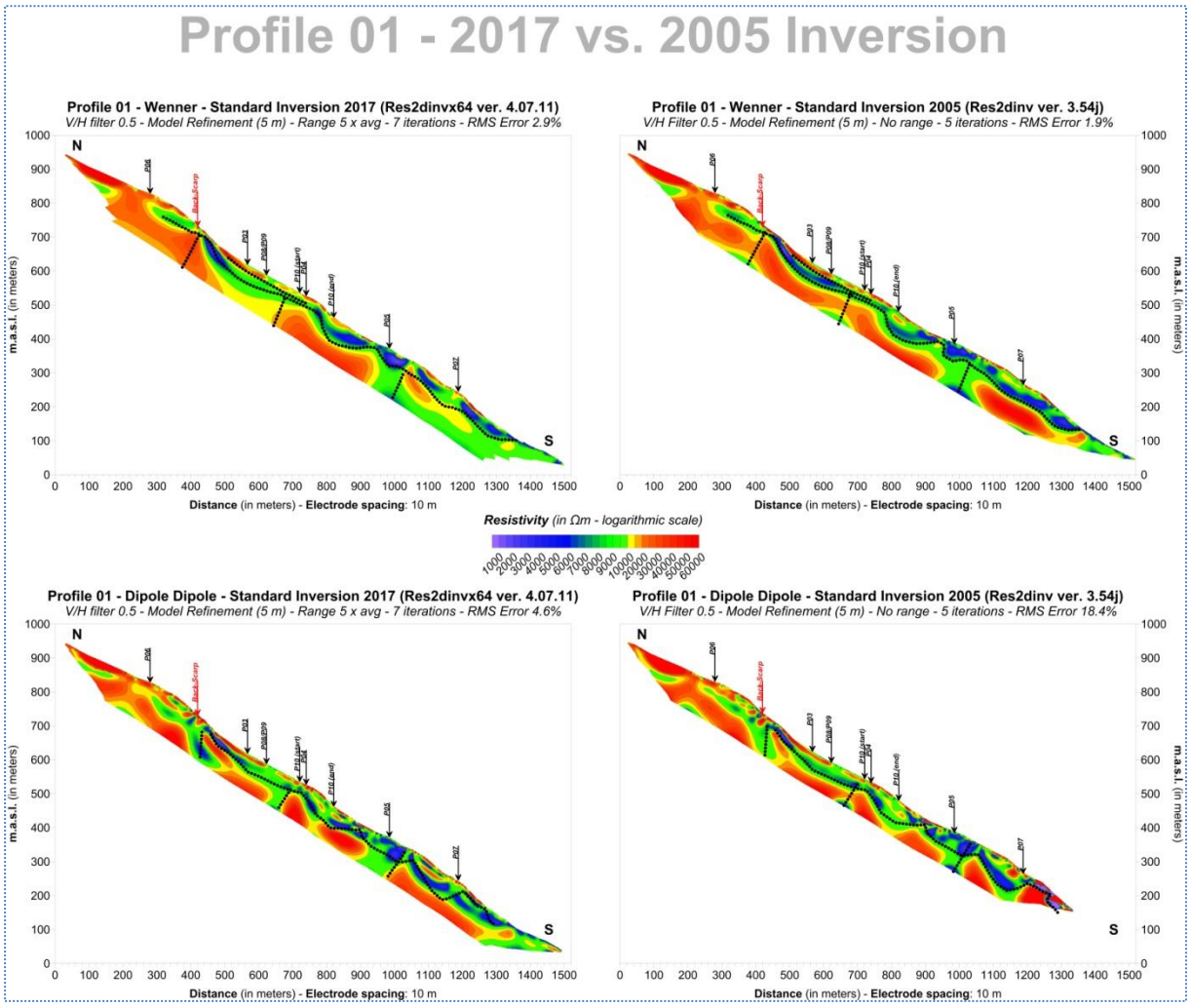

Figure 3.1.1: Wenner (top) and Dipole-Dipole (bottom) inversion results for **Profile 01** with the use of new (left) and old (right) Res2DInv versions. Black dotted lines represent interpretations based on the old results. Note: 2005 inversion of Profile 01 Dipole Dipole configuration (lower right) is shorter than the rest.

When Dipole-Dipole inversion results are examined at the bottom side of **figure 3.1.1**, more similarities than differences can be seen. It should be noted though that the last part of the profile was conducted a year after the 1st field expedition and hasn't been

included in the old inversion. Regardless, the part of the results that matches shows a good agreement but with some deviations as well. First and foremost, the area below the crack vividly stands out in both inversions, but with a lower resistivity in the reprocessing result. An interesting feature is that even though this zone is detected inclined, when topography is applied in both results, it acquires an almost vertical form. This is something that does not happen with the rest of the possible weak zones in Profile 01 which appear more vertical in the original inversion but become inclined after the implementation of topography. Low-resistivity zones are generally better formed and more continuous in the new inversion, especially at 660 meters. Another interesting feature is that the southern part of Profile 01 now appears to be fragmented in the old inversion but more continuous in the new one, which is the opposite behavior than we saw with Wenner.

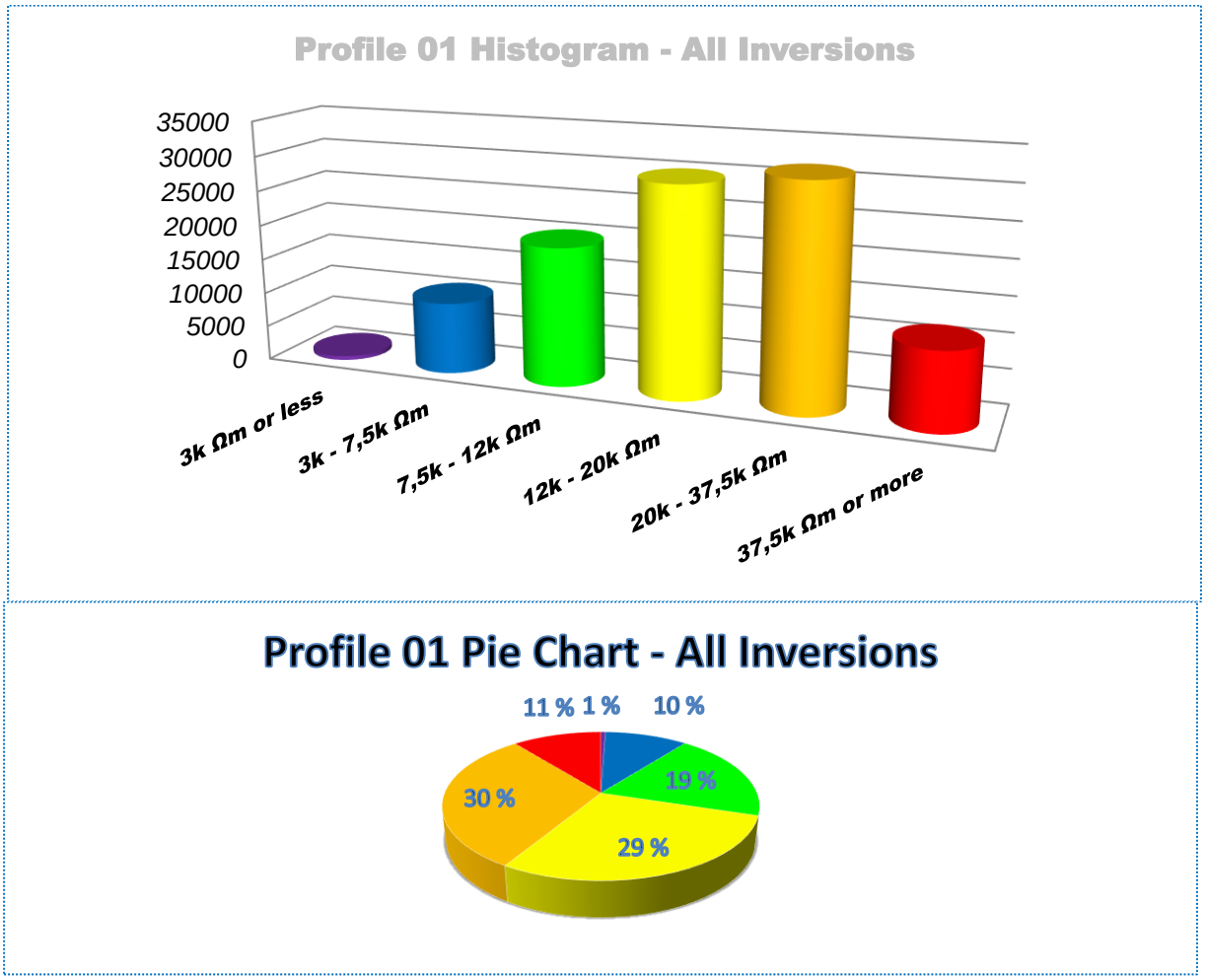

Figure 3.1.2: Top: Histogram depicting the statistical characteristics of all inversion results for **Profile 01**. Bottom: Pie chart depiction of the same data (custom rainbow $\log_{10}$ color scale).

Figure 3.1.2 presents the aggregated inversion statistics for Profile 01 and **figures 3.1.3**, **3.1.4** and **3.1.5** display the six different results for Wenner, Dipole-Dipole and Mixed arrays. The number of data points per array are 929, 2498 and 3427 which automatically constitutes the Mixed array to be the highest in resolution. **Figure 3.1.2** shows a statistical distribution which is identical to the statistics for all the profiles shown in **figure 2.3** and this is natural since Profile 01 is a profile which covers the

entire length of the survey area in the North-South orientation. However, we need to examine the different inversion results individually to identify patterns in the profile.

Figure 3.1.3 presents six inversion results for Wenner array using the format mentioned in the beginning of this section. Theoretically, this is the array which is more suitable for highlighting horizontal layering, especially when *Standard inversion* and V/H equal to 0.5 is used. Nonetheless, all six results indicate a wider spread of low-resistivity values in the southern part of Profile 01 or in other words, a more resistive environment on the northern half. *Standard inversion* calculates lower resistivities in the southern end of the profile than *Robust inversion* while the lowest calculated resistivity distribution does not change much with the use of various V/H filters. However, increasing values for V/H filters cause fragmentation in the high resistivity areas, especially when *Standard inversion* is employed. In any case, Dipole-Dipole and Mixed array results are more suitable for interpreting such features.

Figures 3.1.4 and **3.1.5** present results for Dipole-Dipole and Mixed arrays respectively. These results appear to be quite similar since the majority of the Mixed array data points are coming from Dipole-Dipole. However, the Mixed array also contains a significant number of Wenner data points which make results more balanced in relation to horizontal versus vertical structures. In Profile 01, three possible weakness zones can be identified: the first at 420 meters which matches the superficial crack, a second at 650 meters and a third at 960 meters. These zones are appearing in most profiles sometimes more pronounced than others, especially when *Standard inversion* is used which assigns lower resistivities to them than *Robust inversion*. The lowest RMS error which is 2.93 % can be found with Mixed array *Robust inversion* with V/H filter equal to 1.0. This profile seen in the middle and to the right of **figure 3.1.5** shows that the first and third possible zones are clearer than the one in the middle and with lower resistivities. Same goes for the result seen in the top and to the left of **figure 3.1.4** which presents the most sensitive to vertical structures array which is Dipole-Dipole but with a balancing factor being the V/H filter equal to 0.5. *Standard inversion* again causes high contrast in values but still the zone in the middle appears somewhat dubious compared to the other two. Finally, both Dipole-Dipole and Mixed arrays validate the pattern identified in Wenner where resistivities present a southward decrease in value.

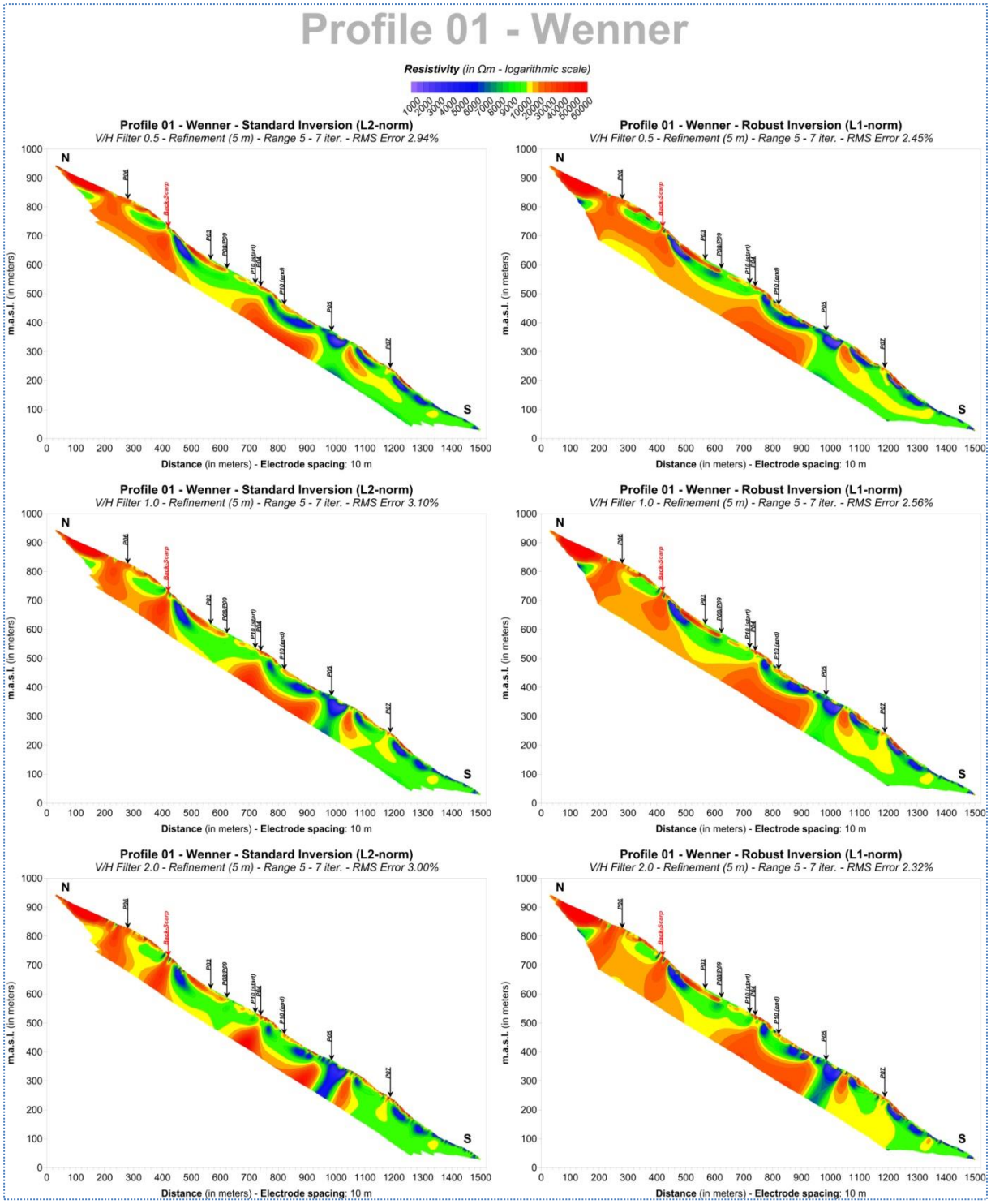

Figure 3.1.3: Reprocessing of **Profile 01** - **Wenner array** using various inversion schemes: Standard or L2-norm (Left) and Robust or L1-norm (Right) inversion with V/H filters equal to 0.5, 1.0 and 2.0 (from top to bottom).

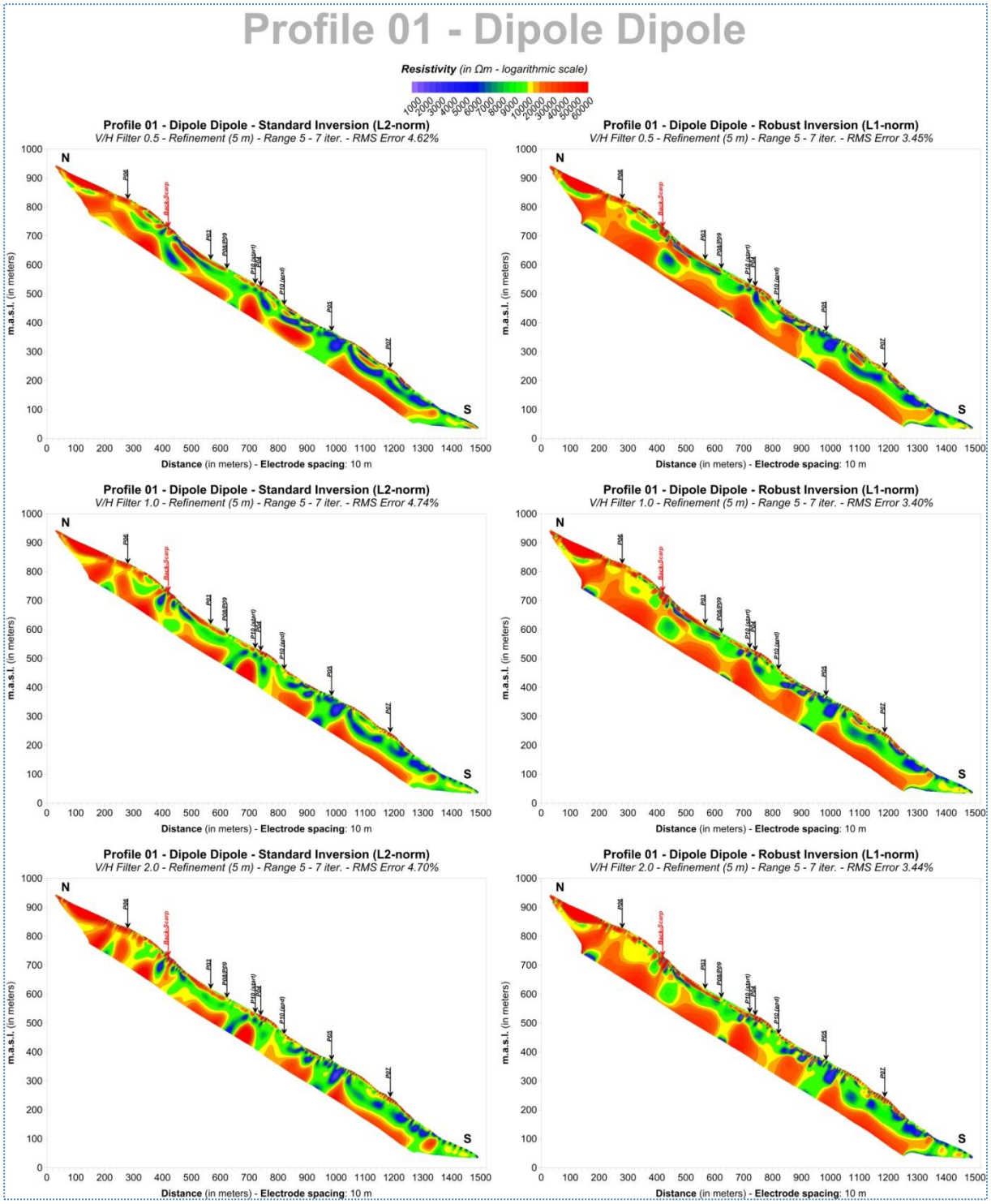

Figure 3.1.4: Reprocessing of **Profile 01** - **Dipole-Dipole array** using various inversion schemes: Standard or L2-norm (Left) and Robust or L1-norm (Right) inversion with V/H filters equal to 0.5, 1.0 and 2.0 (from top to bottom).

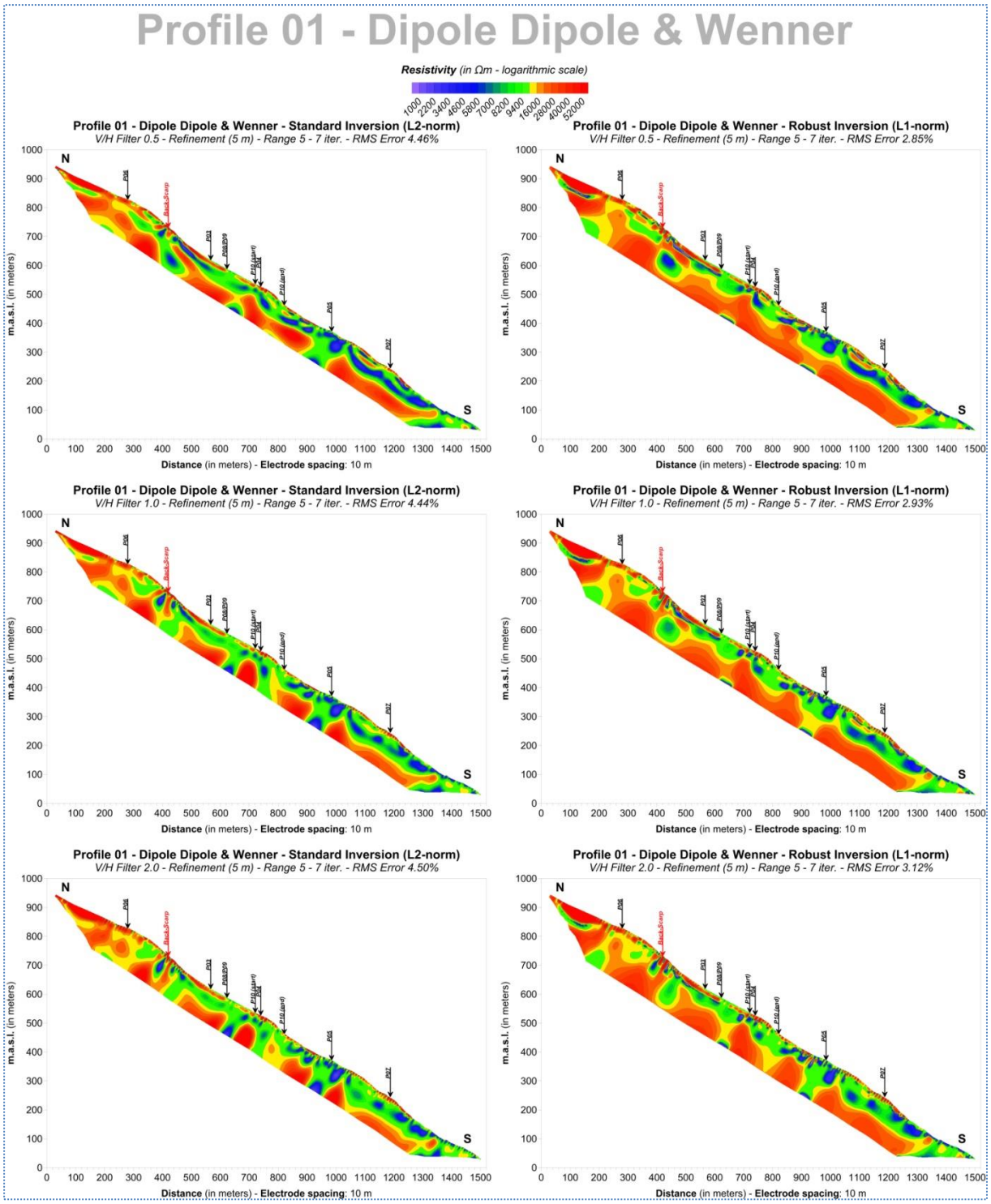

Figure 3.1.5: Reprocessing of **Profile 01** - **Mixed array** using various inversion schemes: Standard or L2-norm (Left) and Robust or L1-norm (Right) inversion with V/H filters equal to 0.5, 1.0 and 2.0 (from top to bottom).

3.2 ERT Profile 02

Profile 02 is very similar to Profile 01, positioned about 100 meters to its West and follows the same general North to South orientation (see **figure 2.1**). Its total length is 1490 meters (1800 meters along topography) and covers the entire central extent of the survey area, at a 35^{o} angle as in Profile 01. The back-scarp is again vertically intersected by Profile 02 but this time a little bit sooner within the profile at about 320 meters. As seen in **figure 2.1** it is crosscut by many other ERT lines and its middle part also coincides pretty well with the refraction seismic Profile 02 except for the second half of the profile (deviation equal to 15 meters). Borehole Bh-2 (see **figure 2.1**) is located relatively close to the profile's course (30 m to its west) but no borehole was placed precisely on the path of Profile 02.

The comparison between the respective inversion results from 2005 and 2017 is shown in **figure 3.2.1**. The results for both Wenner and Dipole-Dipole are much more similar than in Profile 01. The RMS errors obtained with the new inversion are 3.1 % against 4.9 % for Wenner and 4.7 % against 10.9 % for Dipole-Dipole and this shows a small but considerable improvement when the newest Res2DInv version is used. The fact that the reprocessing utilized more iterations (seven instead of five) is also a factor in the improved error percentages, but the qualitative differences in the final results are small. The area near the southern end of Profile 02 is also appearing to be less resistive compared to the northern one and the possible bedrock masses appear to be discontinued by relatively wide low-resistivity areas. Considering the Wenner results, the new inversion calculates lower resistivities for the southern part of Profile 02 but not that much lower than in the 2005 inversion. Overall, Wenner inversion with the latest Res2DInv algorithm doesn't seem to inflict a big change in Profile 02.

The bottom part of **figure 3.2.1,** presenting the Dipole-Dipole reprocessing results, also shows no major differences between inversions. The main features are all still apparent in both results and only small changes in the highest resistivity areas are formulated especially in the middle part of the profile can be detected. At the position of the back-scarp, both inversions reveal two similar low-resistivity areas, one horizontal ending at where the fracture is located and one vertical to topography with a lower resistivity contrast than in the old inversion. However, this is not happening with all other vertical low-resistivity areas to be found in both results. Some are more pronounced in the 2017 inversion and some in the 2005, but their positions, dimensions and geometry are very much alike.

It is important to comment on an obvious interpretation mistake done in the old Wenner inversion result (black dotted lines). As can be seen in **figure 3.2.1**, the first two weak zones interpreted are marked along high resistivity features. We believe that the reason for this mistake is due to the illustration based on the standard Res2DInv color scale. The inversion result presented in Rønning et al. (2006) shows the entire lower part of the profile illustrated in green hues. Considering that these high resistivity areas appear as vertical structures and that the color contrast is not clear, such misinterpretations are easy to occur. When the new color scale is used (top **figure 3.2.1)**, these two areas consist of high resistivity values and therefore cannot be interpreted as possible weak zones. To avoid such unfortunate errors, we will interpret the reprocessed images in two stages. One pure quantitative and an ensuing qualitative. More about interpretation can be found in following sections focused on this subject alone.

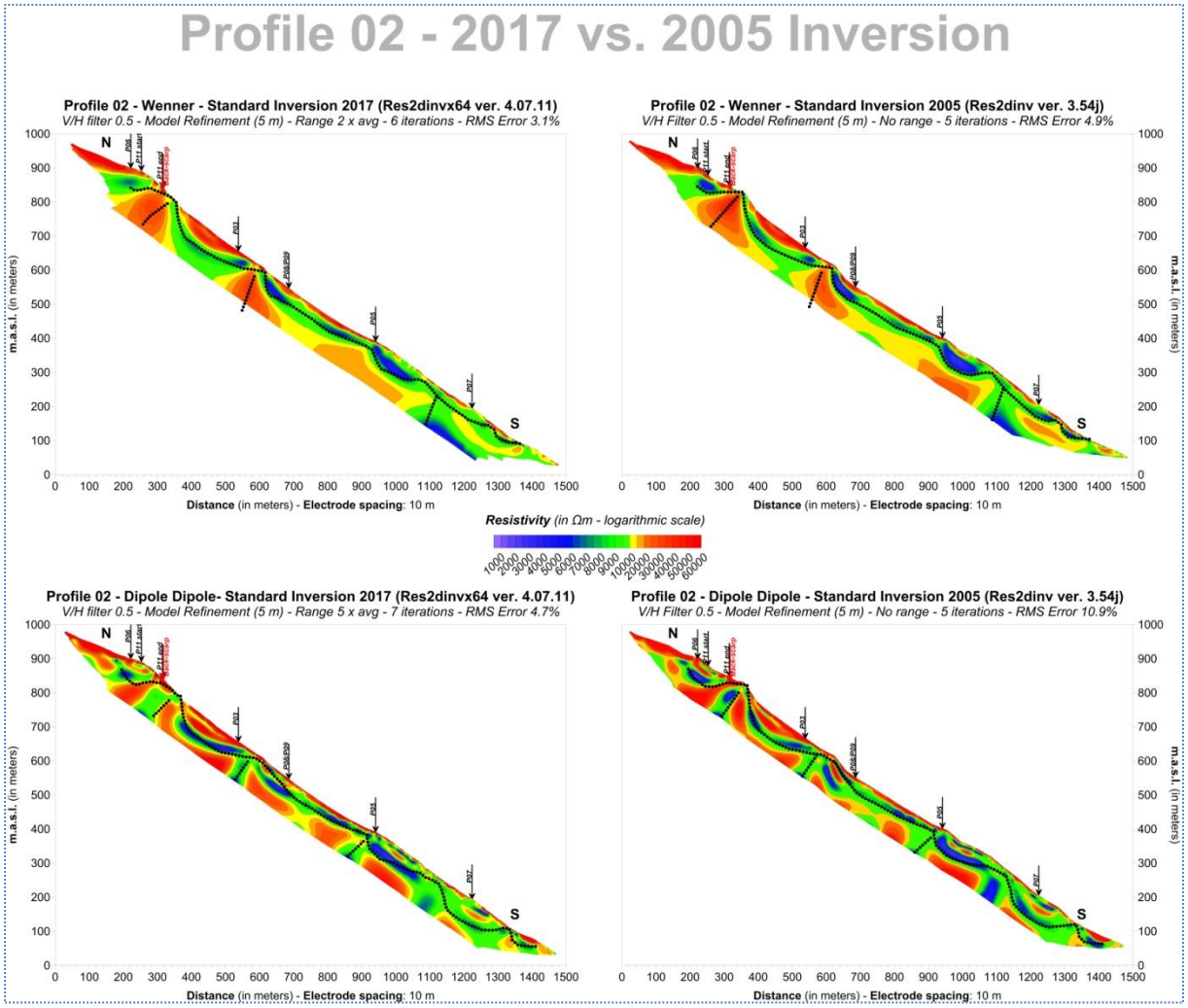

Figure 3.2.1: Wenner (top) and Dipole-Dipole (bottom) inversion results for **Profile 02** with the use of new (left) and old (right) Res2DInv versions. Black dotted lines represent interpretations based on the old results.

Figure 3.2.2 shows a histogram and a pie chart with statistics for all the resistivity values obtained after reprocessing Profile 02. The number of point values for each array are: 873 points for Wenner, 2263 points for Dipole-Dipole and 3136 points for Mixed. The data distribution is very similar to Profile 01 but the percentage of values between 3,000 and 7,500 Ωm is almost half in Profile 02 (6 % instead of 10 %) balanced by a higher drained fractured bedrock percentage (15 % instead of 11 %). This indicate a slightly less water-saturated environment, but conditions are not changing drastically towards the western flank of the slope.

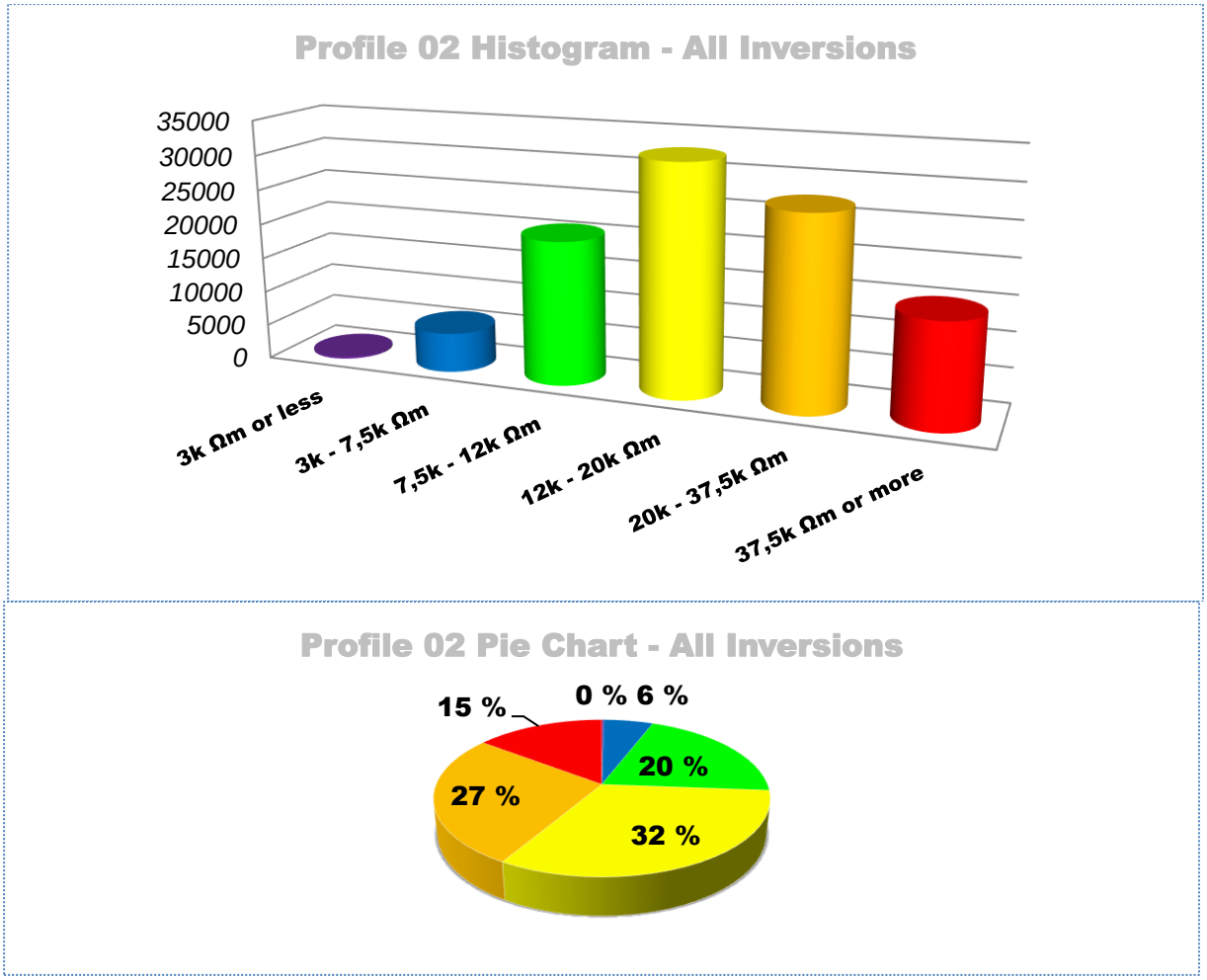

Figure 3.2.2: Top: Histogram depicting the statistical characteristics of all inversion results for **Profile 02**. Bottom: Pie chart depiction of the same data (custom rainbow $\log_{10}$ color scale).

Figure 3.2.3 shows the different results obtained for Wenner array along Profile 02 where it is easy to discern that different inversion parameters do not alter the inversion results much. This is due to both the small number of measurements that Wenner array produces and the environment. A less resistive situation near the fjord is again portrayed but similar low areas can also be found in the northern part of the profile. An interesting feature could be the generation of very low resistivities in depth near the southern end of Profile 02 which could be an artificial effect. RMS error percentages are quite small for all inversion schemes (between 2.28 and 3.24 %) but using *Standard inversion* with a V/H equal to 0.5 still is the most trustworthy approach for interpreting water-saturated or fractured bedrock.

Figures 3.2.4 and **3.2.5** present the results obtained for Dipole-Dipole and Mixed arrays and show similar results as expected. In both these sets of results, the less resistive environment in the south is more clearly pronounced while a higher number of possible fracture zones can be interpreted at 320 meters (superficial back-scarp position), 550 meters, 730 meters, 880 meters and 1080 meters. Those fracture zones appear consistently both in Dipole-Dipole and Mixed array reprocessing results and are very much alike in geometry when *Standard* and *Robust inversion* with V/H filter equal to 1.0 are compared. Finally, RMS errors are below 5 % which is a quite satisfying mathematical discrepancy for 2 or 3 thousand points.

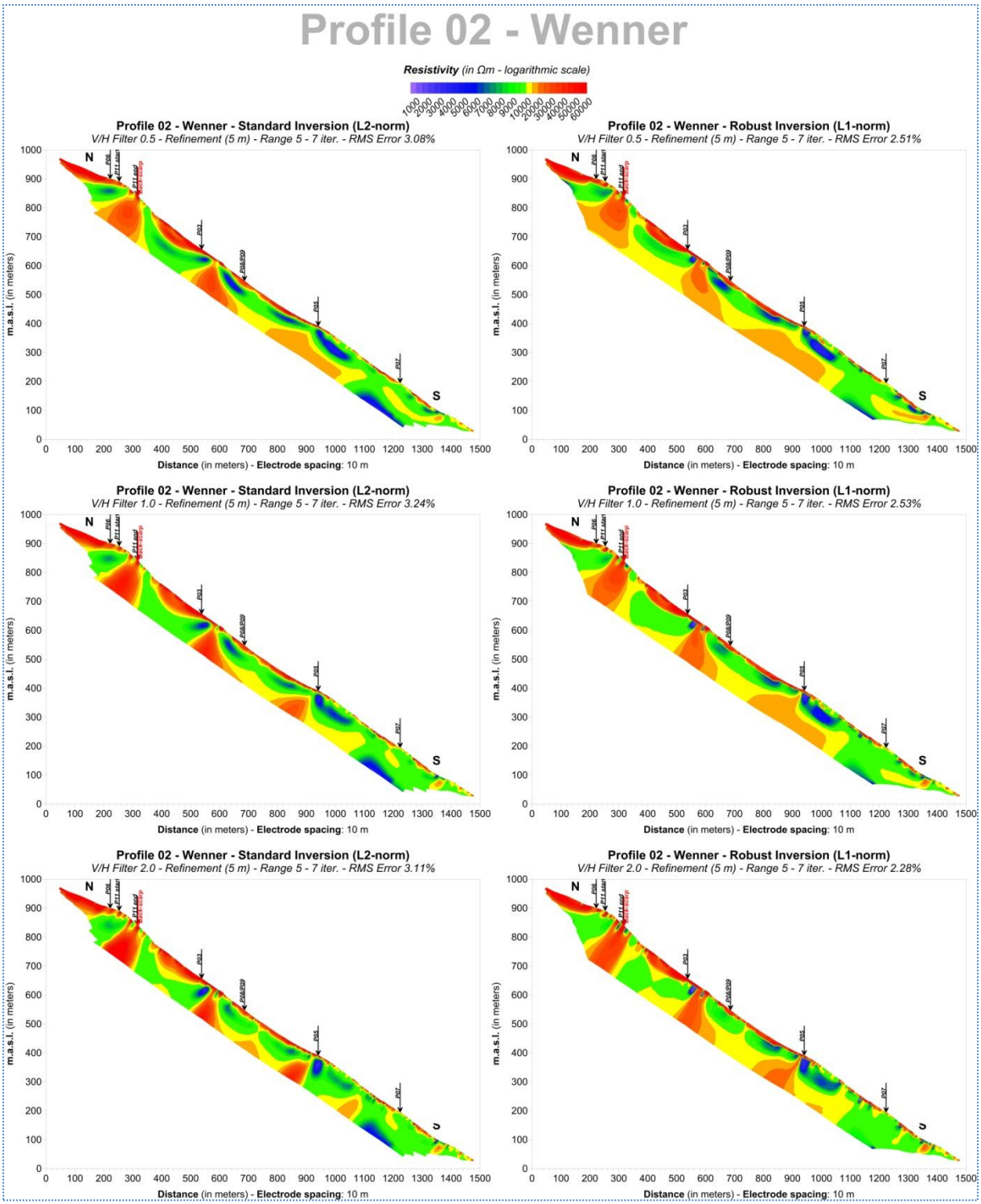

Figure 3.2.3: Reprocessing of **Profile 02** - **Wenner array** using various inversion schemes: Standard or L2-norm (Left) and Robust or L1-norm (Right) inversion with V/H filters equal to 0.5, 1.0 and 2.0 (from top to bottom).

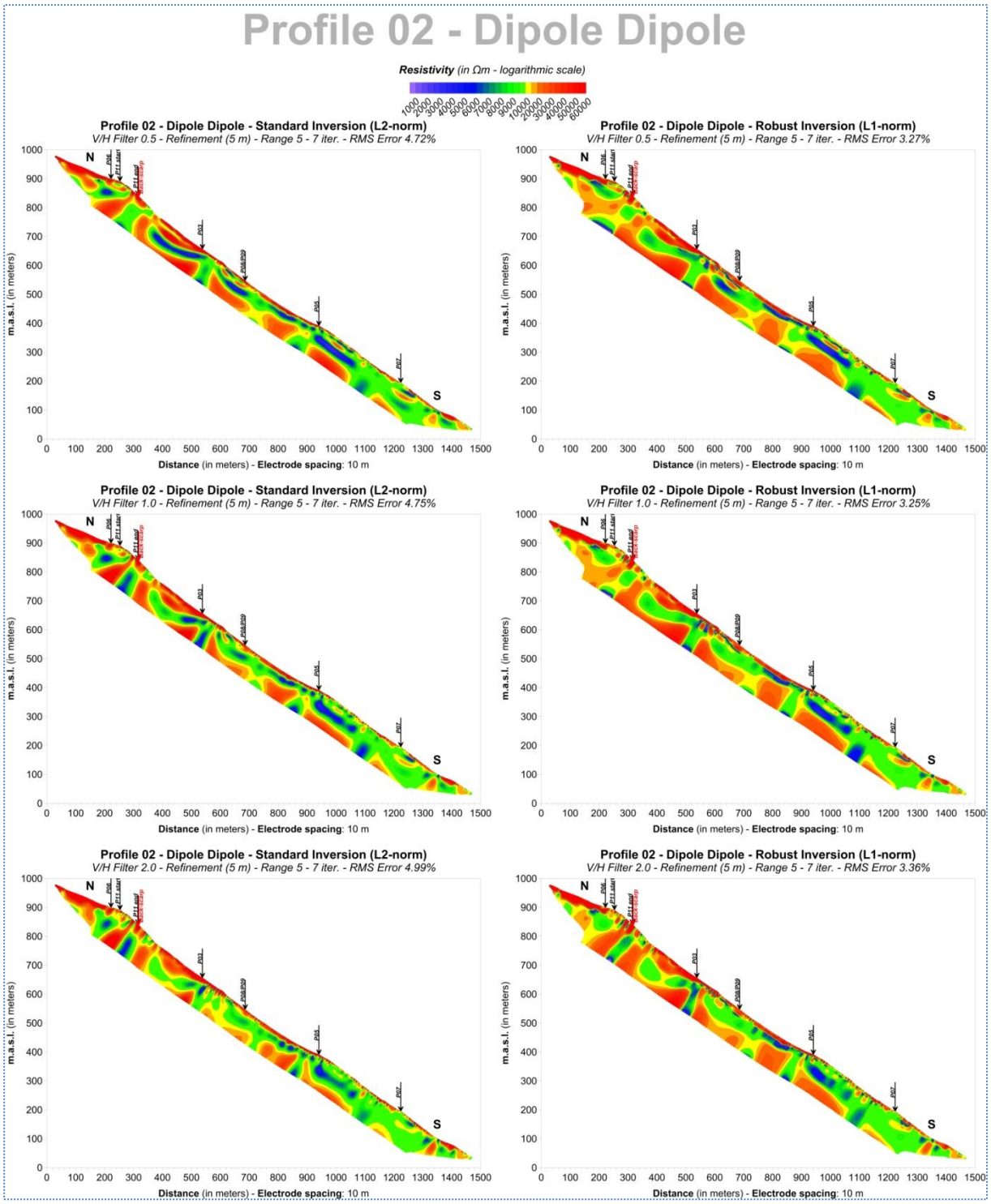

Figure 3.2.4: Reprocessing of **Profile 02** - **Dipole-Dipole array** using various inversion schemes: Standard or L2-norm (Left) and Robust or L1-norm (Right) inversion with V/H filters equal to 0.5, 1.0 and 2.0 (from top to bottom).

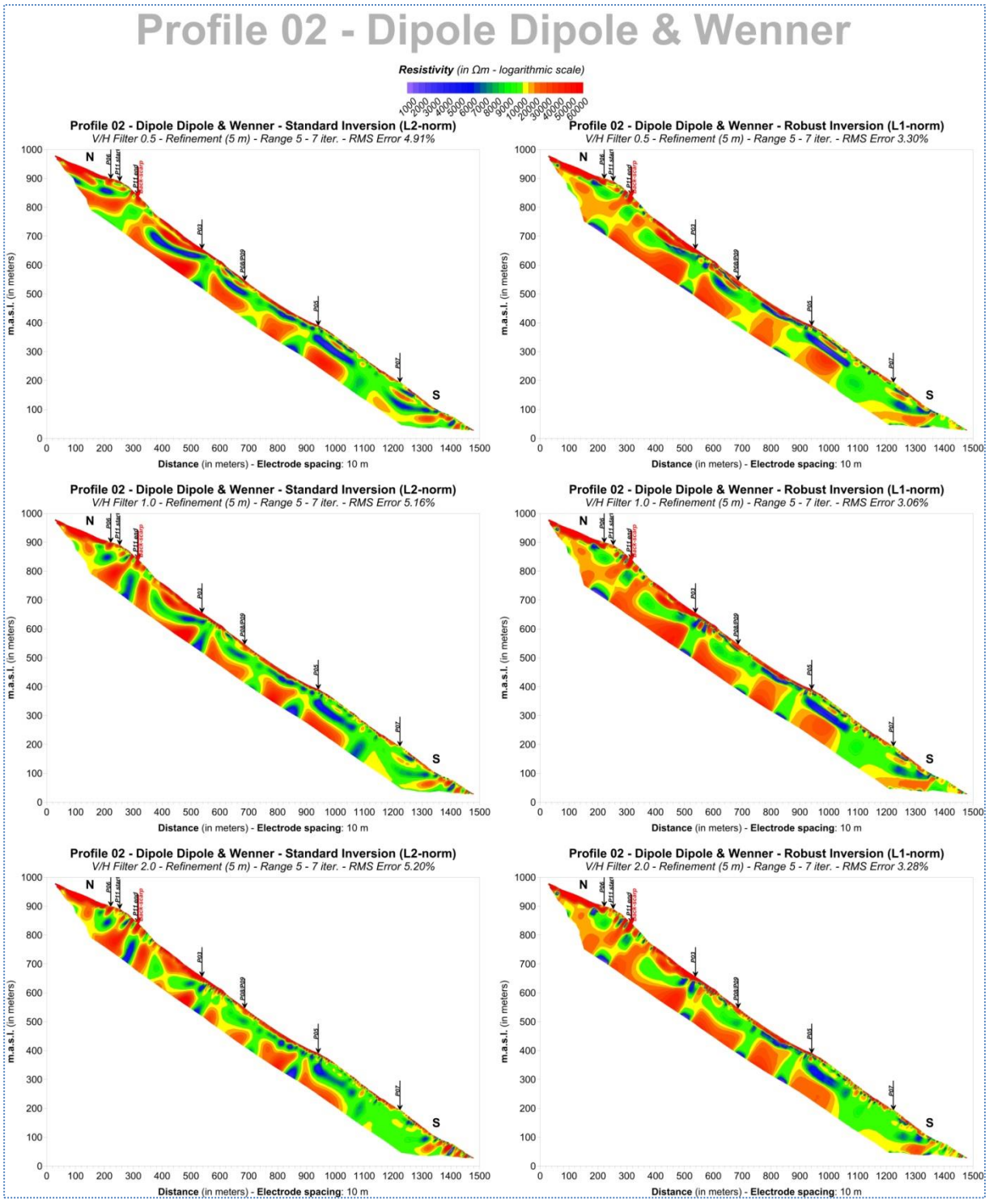

Figure 3.2.5: Reprocessing of **Profile 02** - **Mixed array** using various inversion schemes: Standard or L2-norm (Left) and Robust or L1-norm (Right) inversion with V/H filters equal to 0.5, 1.0 and 2.0 (from top to bottom).

3.3 ERT Profile 03

Profile 03 is the first profile which is following a direction from West to East, crossing Profiles 01 and 02 almost perpendicular and is roughly located ca. 150 meters South of the back-scarp to the North of the survey area. Since this profile is extending across the slope, the topography is relatively flat, and this means that its projected length being 974 meters is not that different from the length along topography which is equal to 1000 meters (101 electrodes with 10 m spacing). Additionally, Refraction Seismic Profile 03 matches two thirds of the length of ERT Profile 03 while Bh-2 (see **figure 2.1**) can be found at 270 meters of horizontal distance exactly on the profile's course.

Figure 3.3.1 compares the 2017 reprocessing results against the 2005 inversion for Wenner and Dipole-Dipole arrays. Examining the results for Wenner, we detect a different general outlook and a reshaped high resistivity distribution. The first half of Profile 03 is still characterized by the clustering of low resistivities, however, possible bedrock at the base of the profile is now more unified. Interpretation by Dalsegg (Rønning et al. 2006) is intuitively matching the 2017 inversion, too (probably even better), but now it seems that the low-resistivity area to the West is not continuous but is interrupted by a possible healthy bedrock high at about 350 meters. This effect, now visible with Wenner, was already apparent in Dipole-Dipole, although placed a little bit sooner in the profile at about 300 meters. On this subject, it is expected that the bedrock high between 250 and 300 meters can be better imaged with Dipole-Dipole. Further commenting on this particular array, we can say that the new inversion is not much different than the 2005 result, but the RMS error percentage is much lower (6.3 % versus 16.2 %), which indicates that the inversion results better fits the observed data.

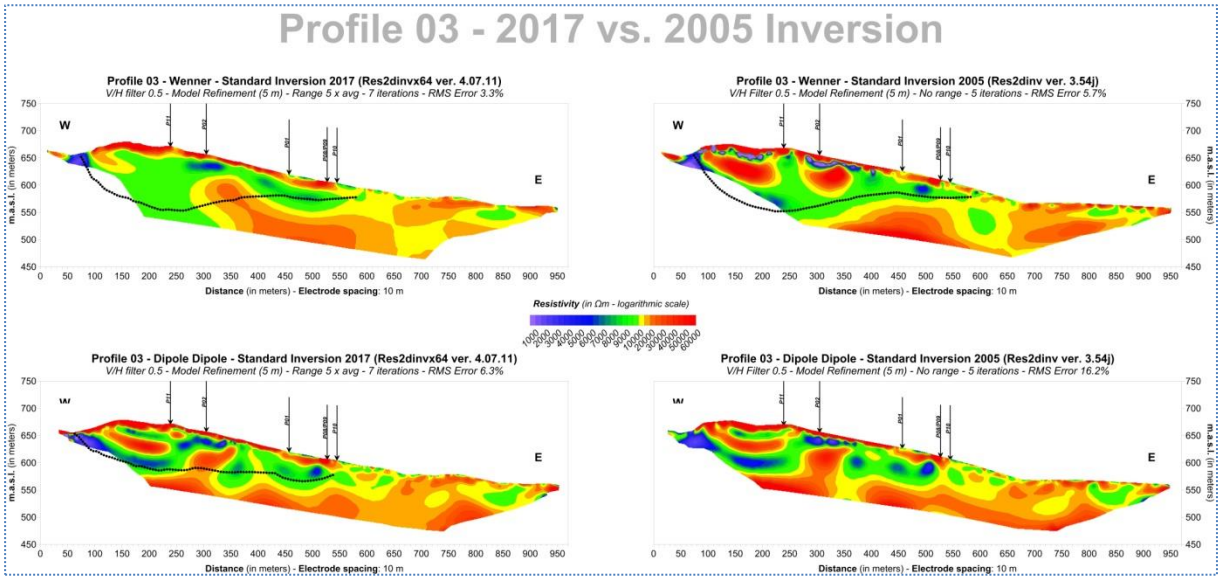

Figure 3.3.1: Wenner (top) and Dipole-Dipole (bottom) inversion results for **Profile 03** with the use of new (left) and old (right) Res2DInv versions. Black dotted lines represent interpretations based on the old results.

Figure 3.3.2 exhibits a statistical aspect of the reprocessing results for Profile 03. Inversion was implemented on 425 points for Wenner, 1030 points for Dipole-Dipole and 1455 points for Mixed array. These statistics indicate that Profile 03 is covering an

area where bedrock is only slightly fractured and water-saturated (4 %), that 87 % of it is consisting of high resistivity values which represent varyingly healthy bedrock and that 9 % of its values can be attributed to fractured drained bedrock (< 37500 Ωm). This was already hinted by Profiles 01 and 02 which demonstrated a more resistive environment for the northern part of the study area. Profile 03 on the other hand, reveals a less resistive domain on its western half, even though such values constitute only 16 % of the total.

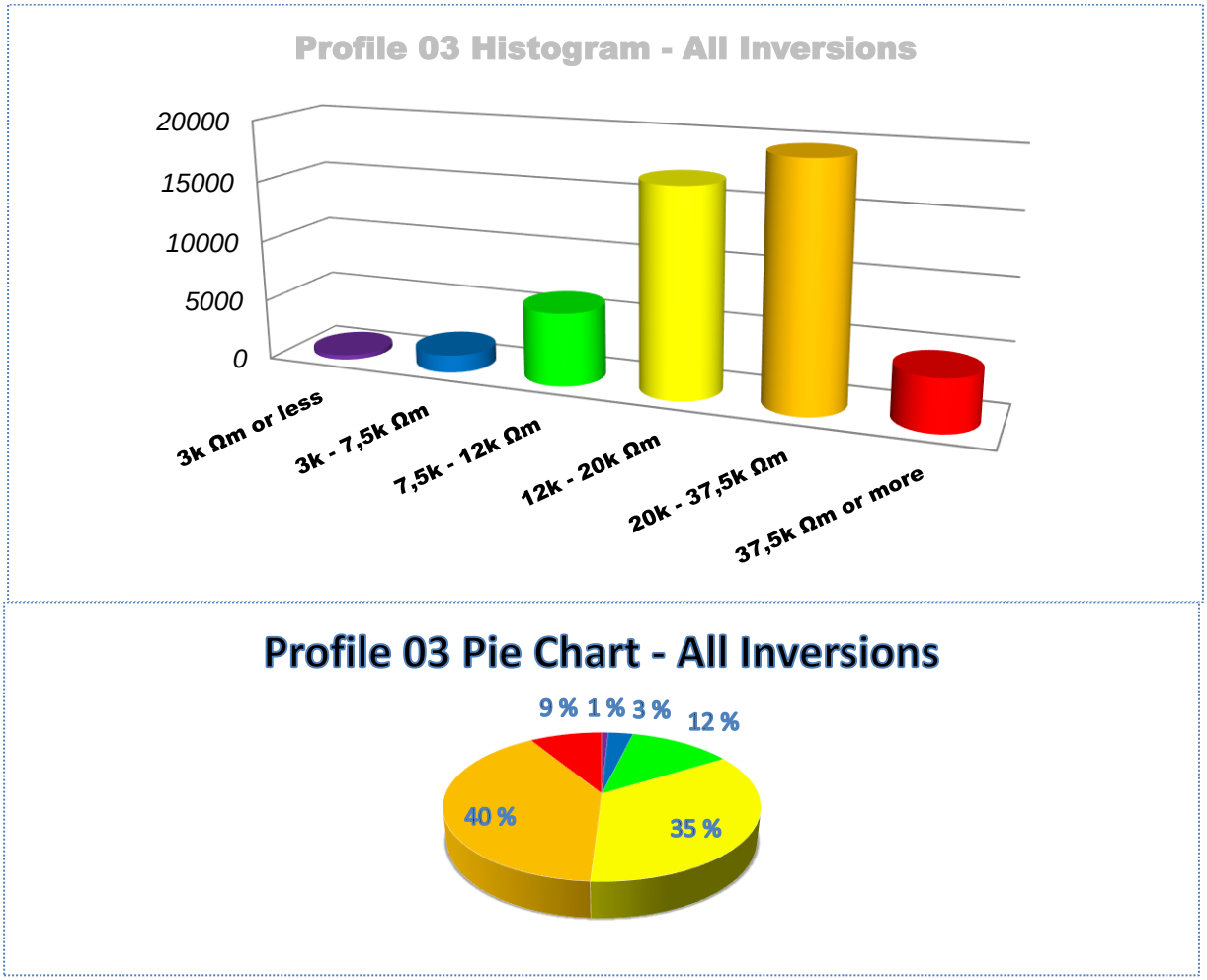

Figure 3.3.2: Top: Histogram depicting the statistical characteristics of all inversion results for **Profile 03**. Bottom: Pie chart depiction of the same data (custom rainbow $\log_{10}$ color scale).

Figures 3.3.3, **3.3.4** and **3.3.5** shows six different inversion products for Profile 03 using six different inversion parameter sets for Wenner, Dipole-Dipole and Mixed array respectively.

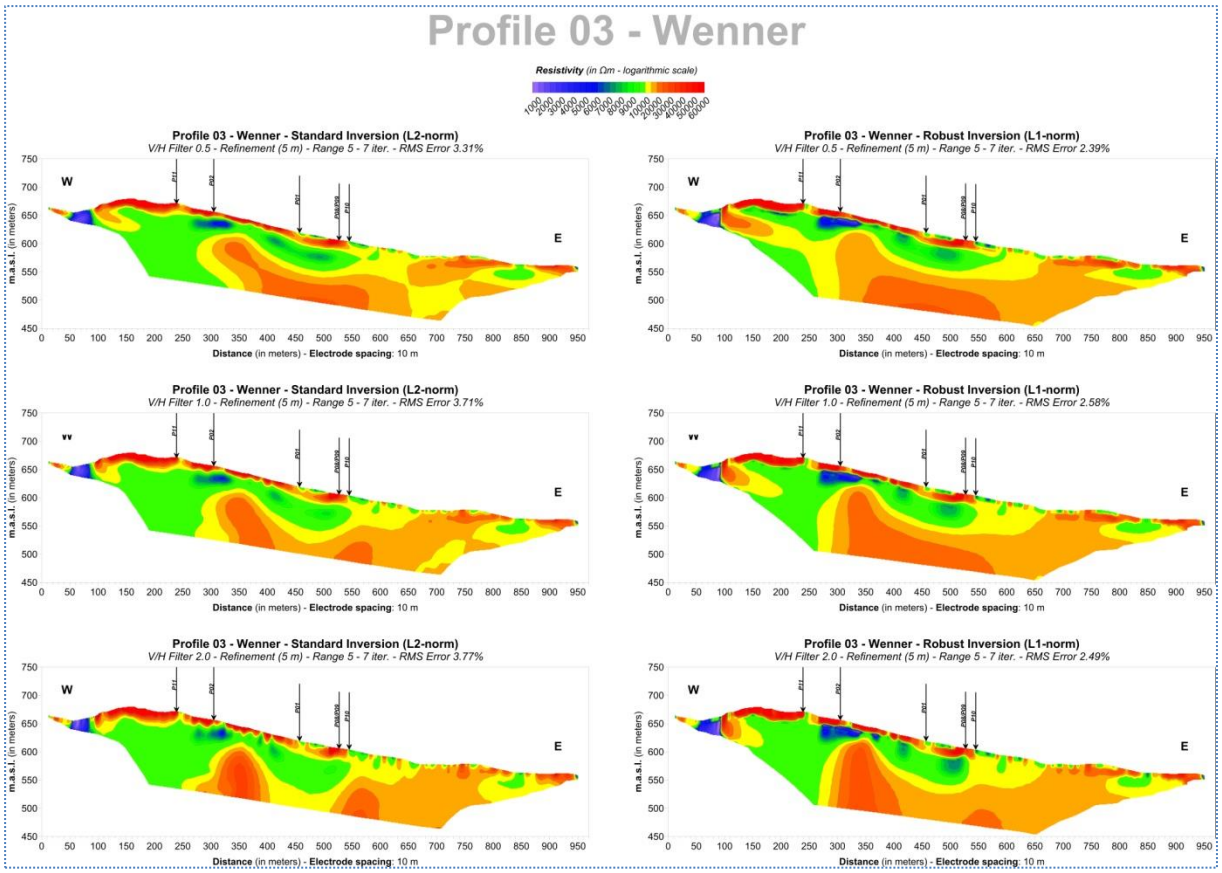

Figure 3.3.3: Reprocessing of **Profile 03** - **Wenner array** using various inversion schemes: Standard or L2-norm (Left) and Robust or L1-norm (Right) inversion with V/H filters equal to 0.5, 1.0 and 2.0 (from top to bottom).

Figure 3.3.3 illustrates the reprocessing for Wenner array and differences are only linked to the shape of the high resistivity area in the eastern counterpart of the profile. It should be noted that *Robust inversion* gives out more consistent results in relation with Dipole-Dipole (and Mixed), positioning the bedrock uplift we talked about earlier at a similar position i.e. around 300 meters. Lastly, *Robust inversion* with V/H filter equal to 0.5 is the only Wenner result which splits the low-resistivity area in the western half of the profile into an upper and a lower counterpart. This is intriguing since it is something more commonly observed with Dipole-Dipole and Mixed array as we'll see on the following paragraph.

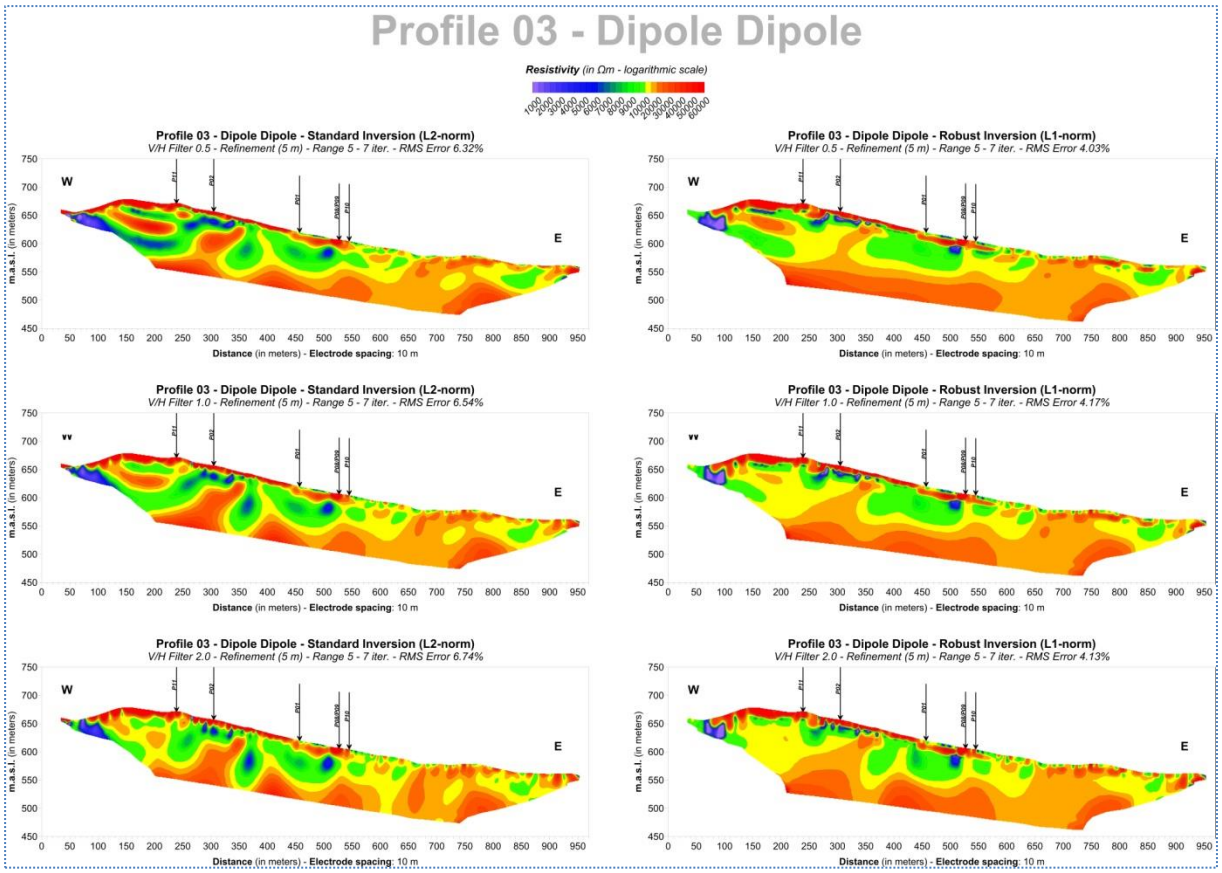

Figure 3.3.4: Reprocessing of **Profile 03** - **Dipole-Dipole array** using various inversion schemes: Standard or L2-norm (Left) and Robust or L1-norm (Right) inversion with V/H filters equal to 0.5, 1.0 and 2.0 (from top to bottom).

Figures 3.3.4 and **3.3.5** display the results for Dipole-Dipole and Mixed arrays and reveal variations in results depending on the implementation of *Standard* or *Robust inversion*. *Standard* (L2-norm) *inversion* is forming a sequence of high-low-high-low-resistivity values on the westernmost part of Profile 03 which is diminishing with the increase of V/H filter. *Robust inversion* (L1-norm) on the other hand, produces smoother results with lower contrasts and higher resistivities overall. Moreover, a possible fracture zone seen at around 350 meters with *Standard inversion*, is not formulating with *Robust inversion* except for the extreme case where V/H filter equal to 2.0 is used. In any case, Dipole-Dipole and Mixed array results show that indeed the low-resistivity expansion in Profile 03 is limited.

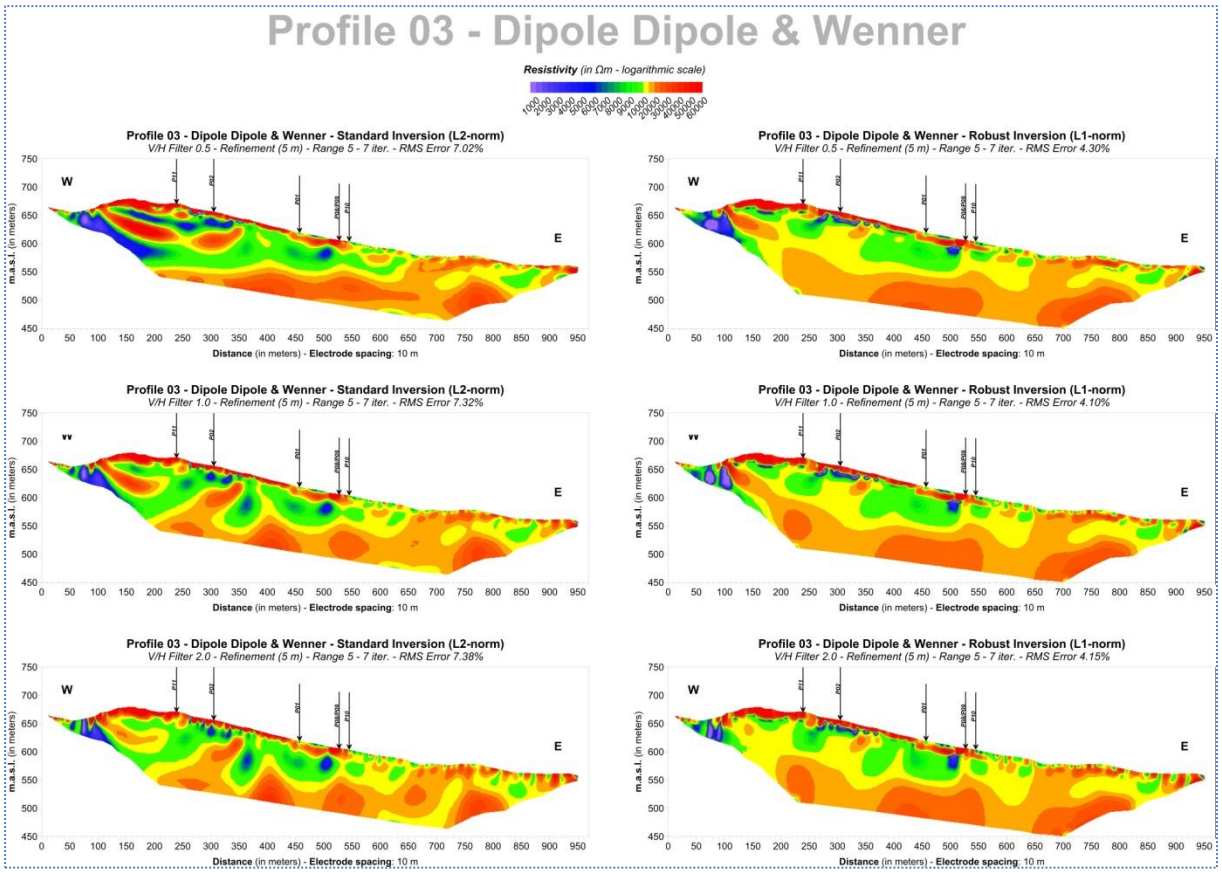

Figure 3.3.5: Reprocessing of **Profile 03** - **Mixed array** using various inversion schemes: Standard or L2-norm (Left) and Robust or L1-norm (Right) inversion with V/H filters equal to 0.5, 1.0 and 2.0 (from top to bottom).

3.4 ERT Profile 04

Profile 04 is almost parallel to Profile 04 and is positioned ca.150 meters to the South. Its length along topography is also 1000 meters but when projected, it becomes 945 meters. Profile 04 investigates the middle part of the Åknes area in a West - East direction and its course only coincides with borehole Bh-01-17 as seen in **figure 2.1** while Bh-01 is positioned about 35 meters north of it.

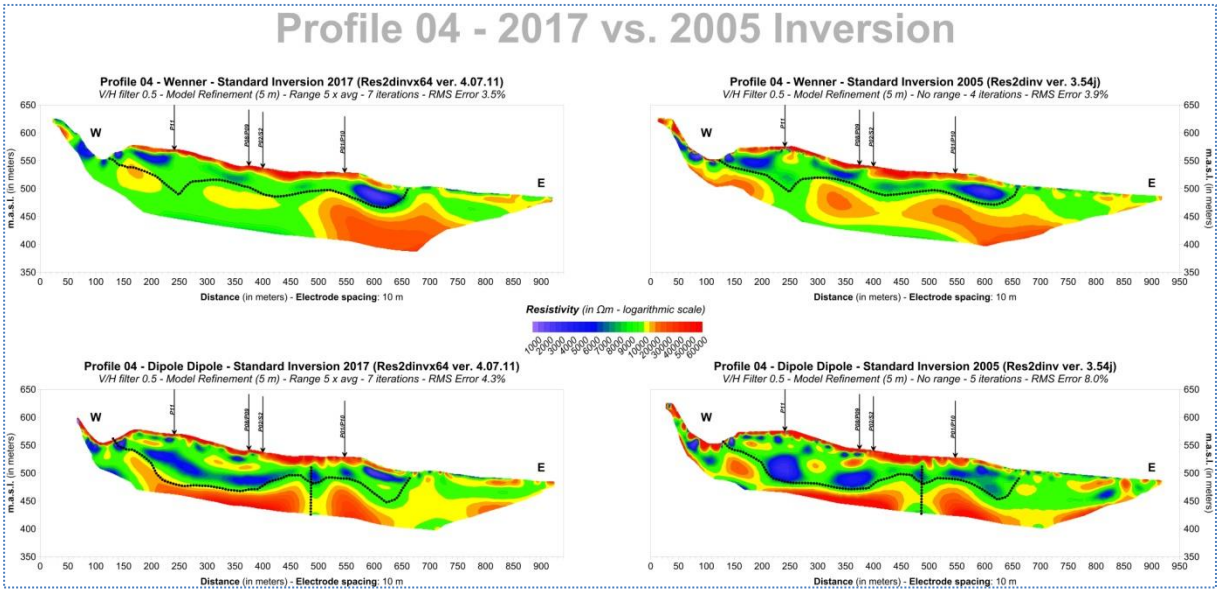

Figure 3.4.1: Wenner (top) and Dipole-Dipole (bottom) inversion results for **Profile 04** with the use of new (left) and old (right) Res2DInv versions. Black dotted lines represent interpretations based on the old results.

In **figure 3.4.1** we may observe differences in results connected with the use of Res2DInv version 4.07.11 (2017) and 3.54j (2005). As in previous cases, this effect is stronger with Wenner whereas Dipole-Dipole looks more consistent although with some dissimilar key features. The new Wenner inversion yields a rather simple structure for Profile 04 as opposed to the old processing, which is partly related to the use of only four iterations in 2005. The old inversion presents a more dominant high resistivity setting overall with a thinner low top resistivity layer. The new inversion on the other hand displays a rather homogeneous low-resistivity environment for the western half of the profile while the eastern half is characterized by a general bedrock high. The RMS errors between these two results are comparable (3.5 versus 3.9 %) but the mean resistivity level in the new inversion is obviously lower.

Qualitatively, what we obtained for Wenner with the new inversion is more or less validated with the new inversion on Dipole-Dipole. On top we have a thin but highly resistive layer representing drained fractured bedrock. The next layer (resistivity green and blue) is the possibly fractured and water-saturated layer which is thicker on the western half while the resistivity level seems to be rising on the eastern half. Interpretation on the old inversion result only takes into account the lowest resistivity areas (blue or purple), but it is remarkable how good this interpretation matches the new inversion result. A possible fracture zone at around 475 meters is validated in both inversions even though appearing to be thinner in the new one. Lastly, the new

inversion illustrates the very low-resistivity areas (blue or purple) to be more flattened out and homogeneous compared to the 2005 result.

A look at the statistics for all inversions referring to Profile 04 in **figure 4.3.2** shows that as we move towards the base of the slope, the conditions are becoming less resistive with the green-blue-purple resistivity spectrum to rise to one third of the total i.e. 33 % as opposed to the 16 % at Profile 03 yielded 150 meters to the North. In addition to that, high resistivity values take up a smaller portion of the profile i.e. 56 % instead of 75 % for Profile 03 whereas extremely high resistivity percentage is also slightly higher (11 % instead of 9 %). Still, Mixed array is the most populous here with 1481 points, Dipole-Dipole follows with 1048 and Wenner is of course the sparsest of all with 433 points.

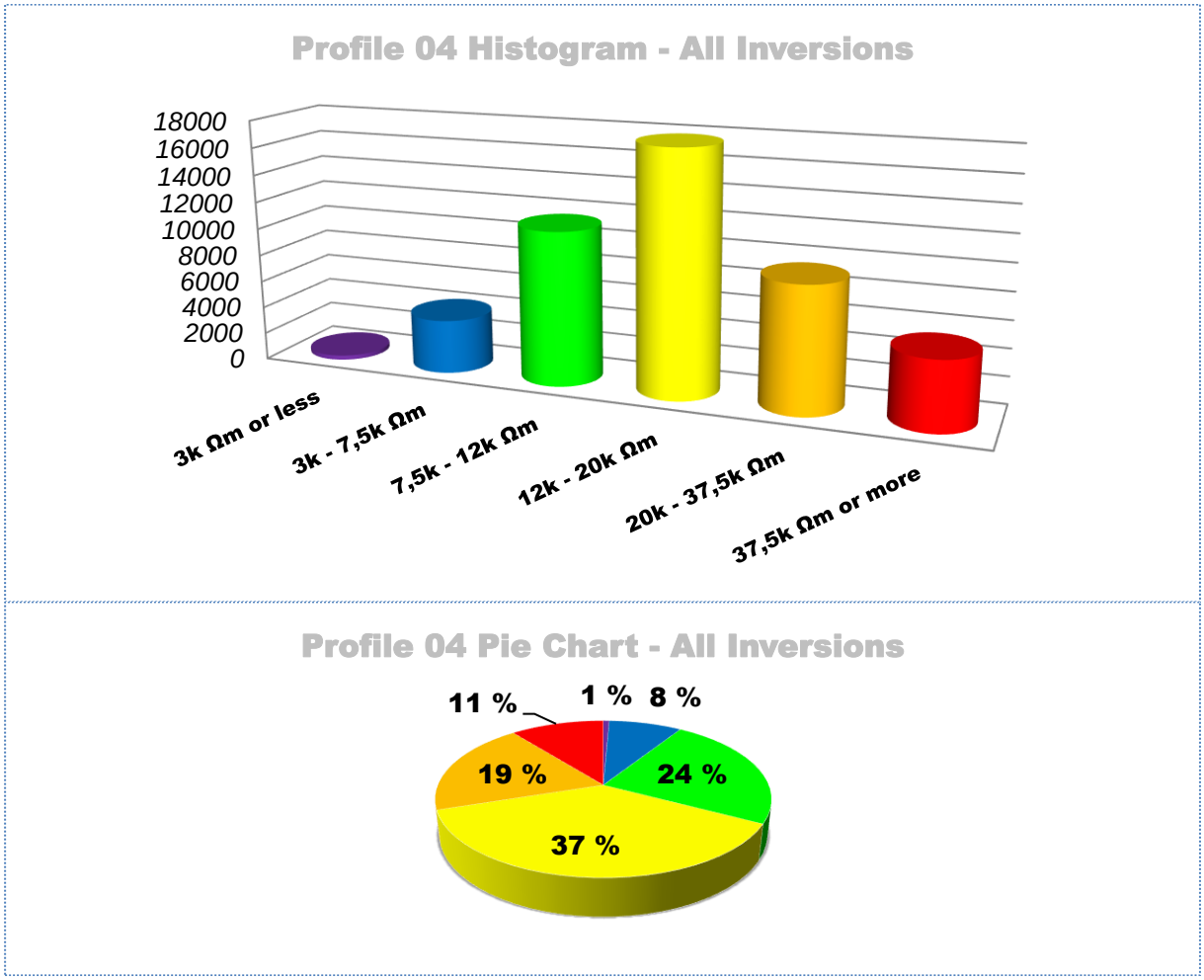

Figure 3.4.2: Top: Histogram depicting the statistical characteristics of all inversion results for **Profile 04**. Bottom: Pie chart depiction of the same data (custom rainbow $\log_{10}$ color scale).

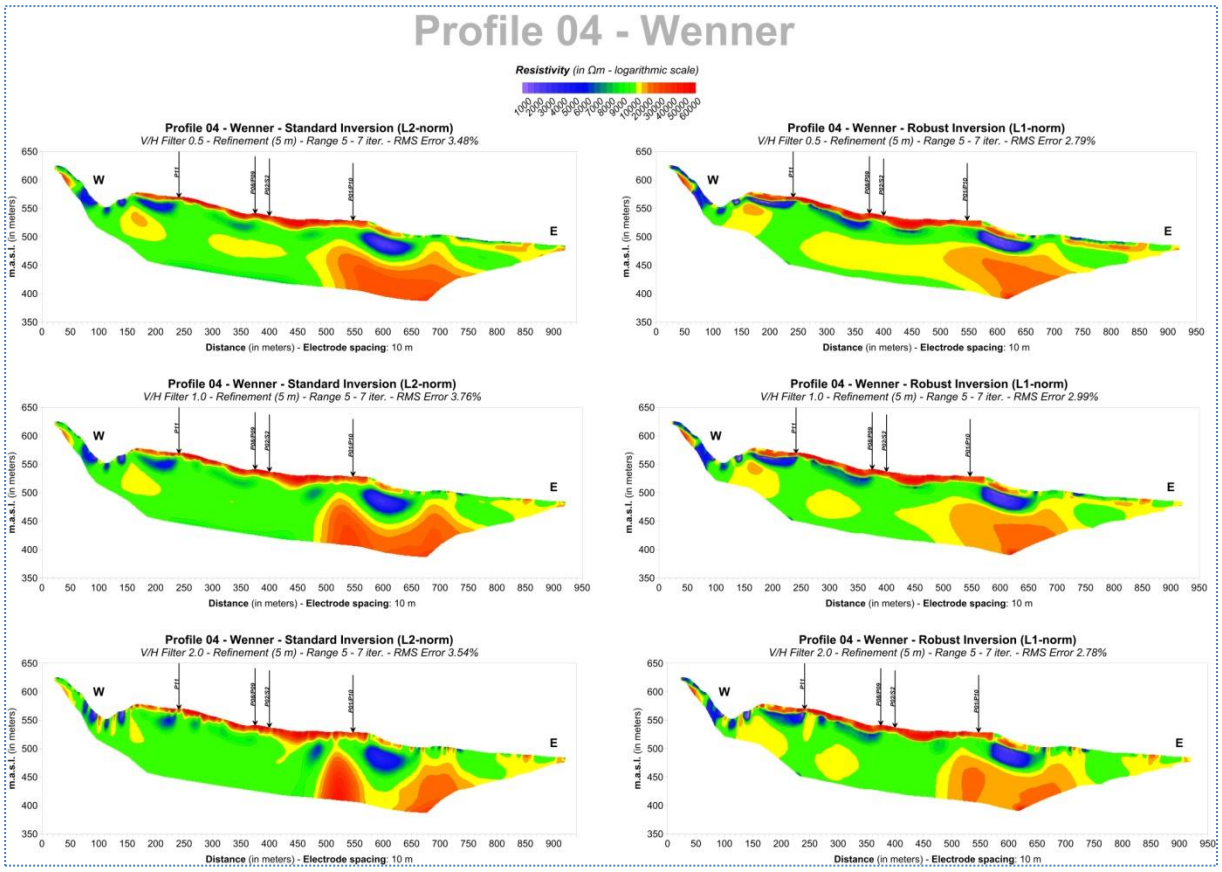

Figure 3.4.3: Reprocessing of **Profile 04** - **Wenner array** using various inversion schemes: Standard or L2-norm (Left) and Robust or L1-norm (Right) inversion with V/H filters equal to 0.5, 1.0 and 2.0 (from top to bottom).

Figure 3.4.3 shows that different ways of inverting Wenner array measurements does not affect the result much. There is a clear separation in resistivity between the western and the eastern half of Profile 04 and this is followed through regardless of *Standard* or *Robust inversion* used as well as V/H filter value. Yet, *Robust inversion* results present smaller resistivity contrasts and show a relatively wider expansion of very low-resistivity areas (blue or purple). It is also noticeable that Wenner array fails to formulate any healthy bedrock surface in depth at the western part of the profile and there are only hints found of such a high resistivity concentration in *Robust inversion*. This is due to the low resolution of the array and bedrock is expected to appear near the bottom of the profile but still lower than in the eastern flank (see inversion results for Mixed and Dipole-Dipole arrays).

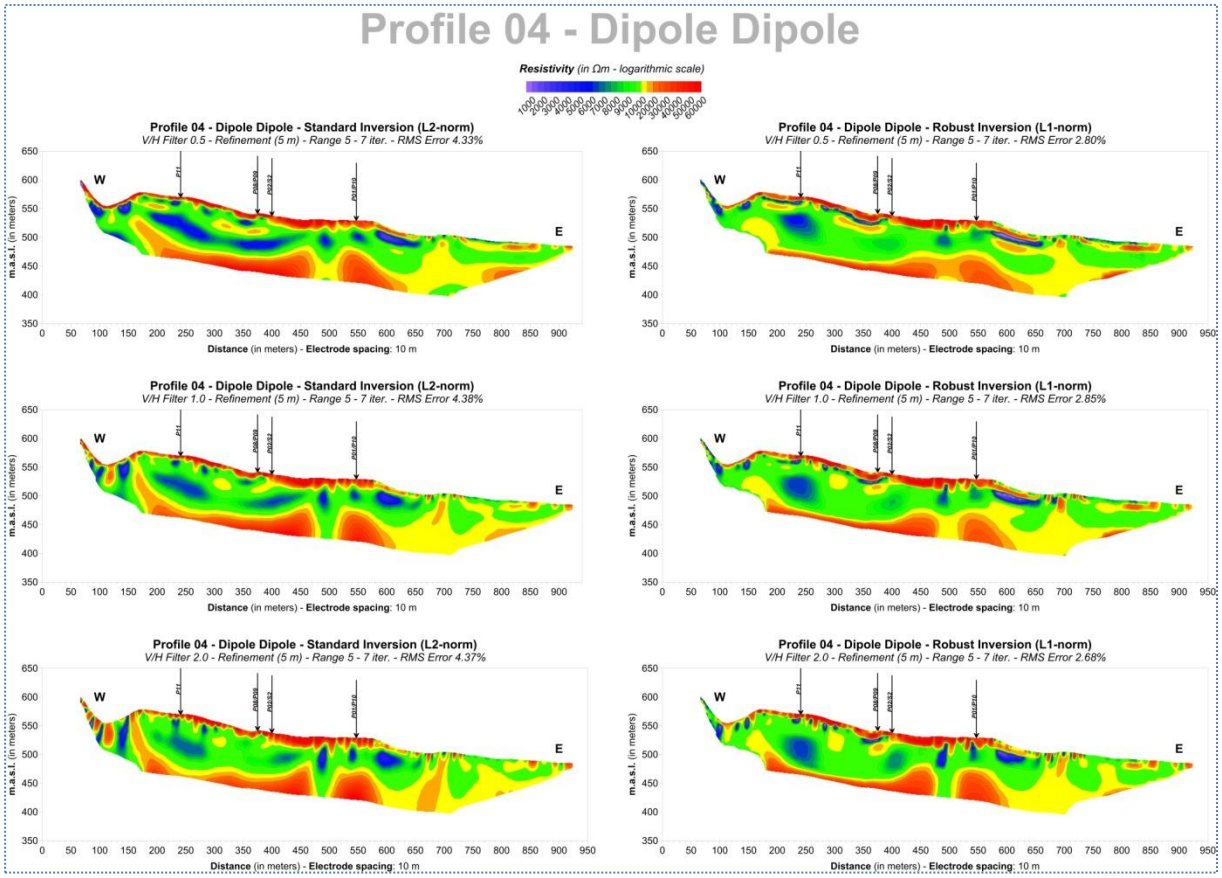

Figure 3.4.4: Reprocessing of **Profile 04** - **Dipole-Dipole array** using various inversion schemes: Standard or L2-norm (Left) and Robust or L1-norm (Right) inversion with V/H filters equal to 0.5, 1.0 and 2.0 (from top to bottom).

Figures 3.4.4 and **3.4.5** presenting the results for Dipole-Dipole and Mixed arrays are once again comparable in their outcomes since the biggest part of the Mixed array is practically values copied from the Dipole-Dipole raw data file. However, the inclusion of Wenner values in the Mixed array is bringing about some small changes after inversion and Profile 04 is a fine example for that. As can be seen in **figure 3.4.4** applying various inversion schemes on Dipole-Dipole yields the same qualitative results as Wenner, but it also unveils a possible weak zone at 475 meters which is apparent in all schemes and becomes more apparent as the V/H filter increases. If we look at **figure 3.4.5** though, this zone seems to become dubious especially with a V/H filter equal to 0.5. Of course, the increase of V/H filter makes this vertical feature to stand out better.

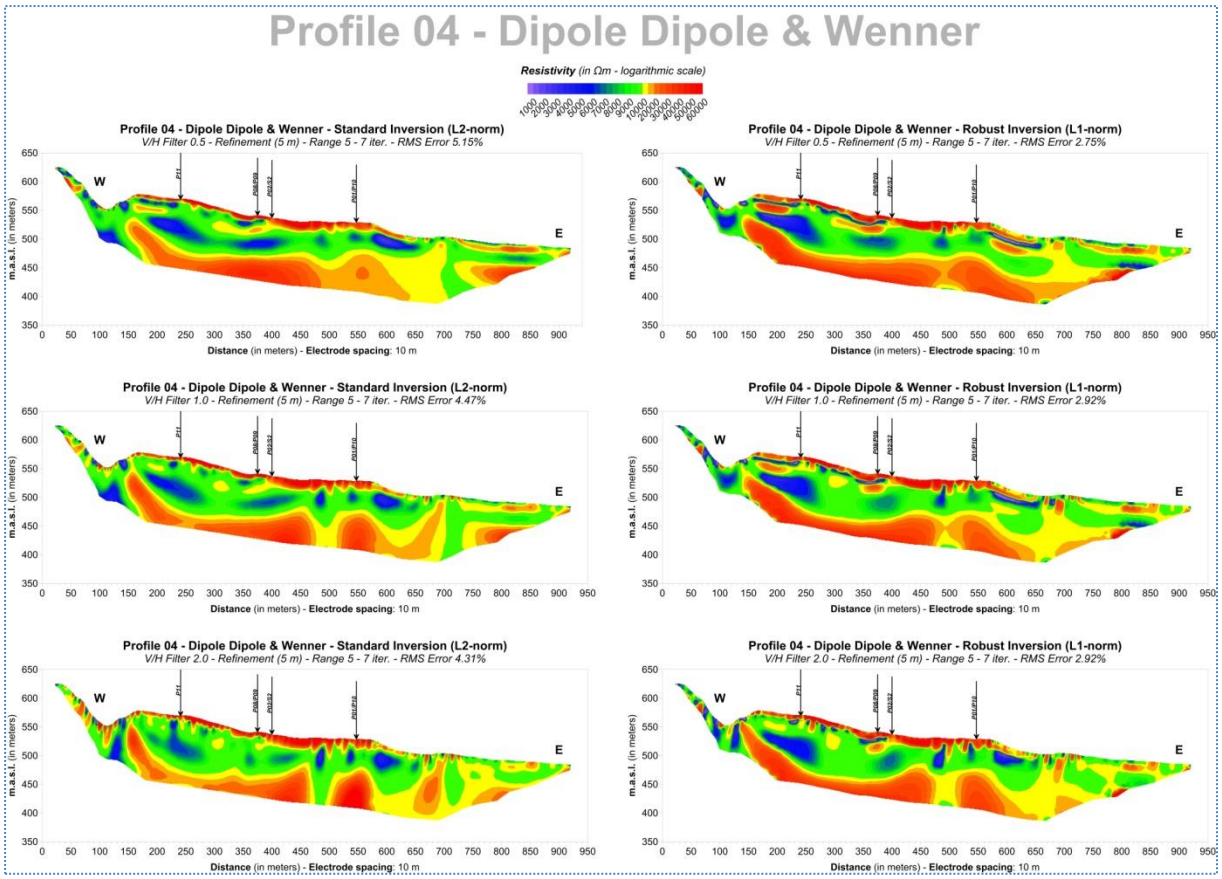

Figure 3.4.5: Reprocessing of **Profile 04** - **Mixed array** using various inversion schemes: Standard or L2-norm (Left) and Robust or L1-norm (Right) inversion with V/H filters equal to 0.5, 1.0 and 2.0 (from top to bottom).

3.5 ERT Profile 05

As seen in **figure 2.1**, Profile 05 is positioned about 250 meters south of Profile 04 and shares both projected (985 meters) and length along topography (1000 meters). It is also following a general West to East trend with a slight shift towards the North near its end while no boreholes or refraction seismic lines are matching its course. As implied by the small deviation between its length along topography and its projected length, the topography is not very dramatic for Profile 05.

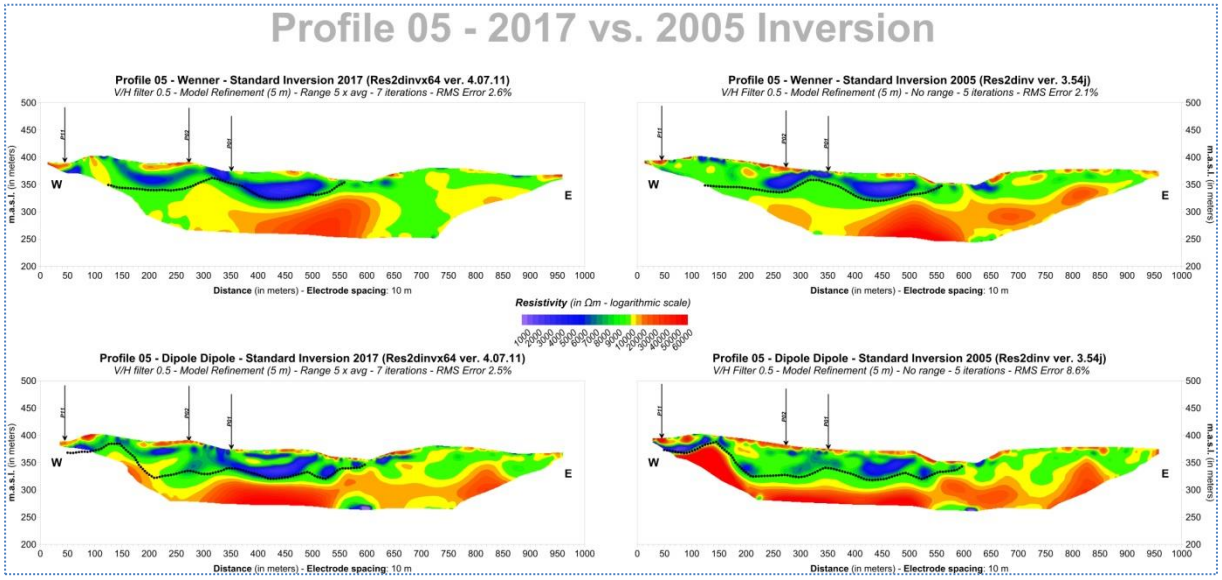

Figure 3.5. 1: Wenner (top) and Dipole-Dipole (bottom) inversion results for **Profile 05** with the use of new (left) and old (right) Res2DInv versions. Black dotted lines represent interpretations based on the old results.

Figure 3.5.1 demonstrates the results after implementing inversion on Wenner and Dipole-Dipole array along Profile 05 in two different times: 2017 and 2005. Focusing on Wenner, we deduce again that new inversion causes different high resistivity arrangement than with the past processing. Resistivities in the eastern flank of the profile are lower but that doesn't change the fact that the distribution of very low resistivities is not much affected and that interpretation for the old processing matches the new one quite well. New inversion on Dipole-Dipole at the same time, presents a more coherent bedrock structuring, but the distribution of very low resistivities is more homogeneous. Ultimately, RMS errors are comparable for Wenner (2.6 % versus 2.1 %) but much improved for Dipole-Dipole (2.5 % versus 8.6 %).

Figure 3.5.2 presents a small statistical analysis of the reprocessing results for Profile 05. These statistics are extracted from six different inversions on 422 Wenner points, 1064 Dipole-Dipole points and 1486 Mixed points. Comparing the outcome of the analysis for Profile 05 with the equivalent analysis for Profile 06, it is evident that there is a further increase in the frequency of very low-resistivity values (blue - 12 % instead of 8 %) and newfound decrease on the percentage of extremely high resistivities (red – 3 % instead of 11 %). This could help quantifying the pattern which registers a less resistive environment as we move towards the fjord.

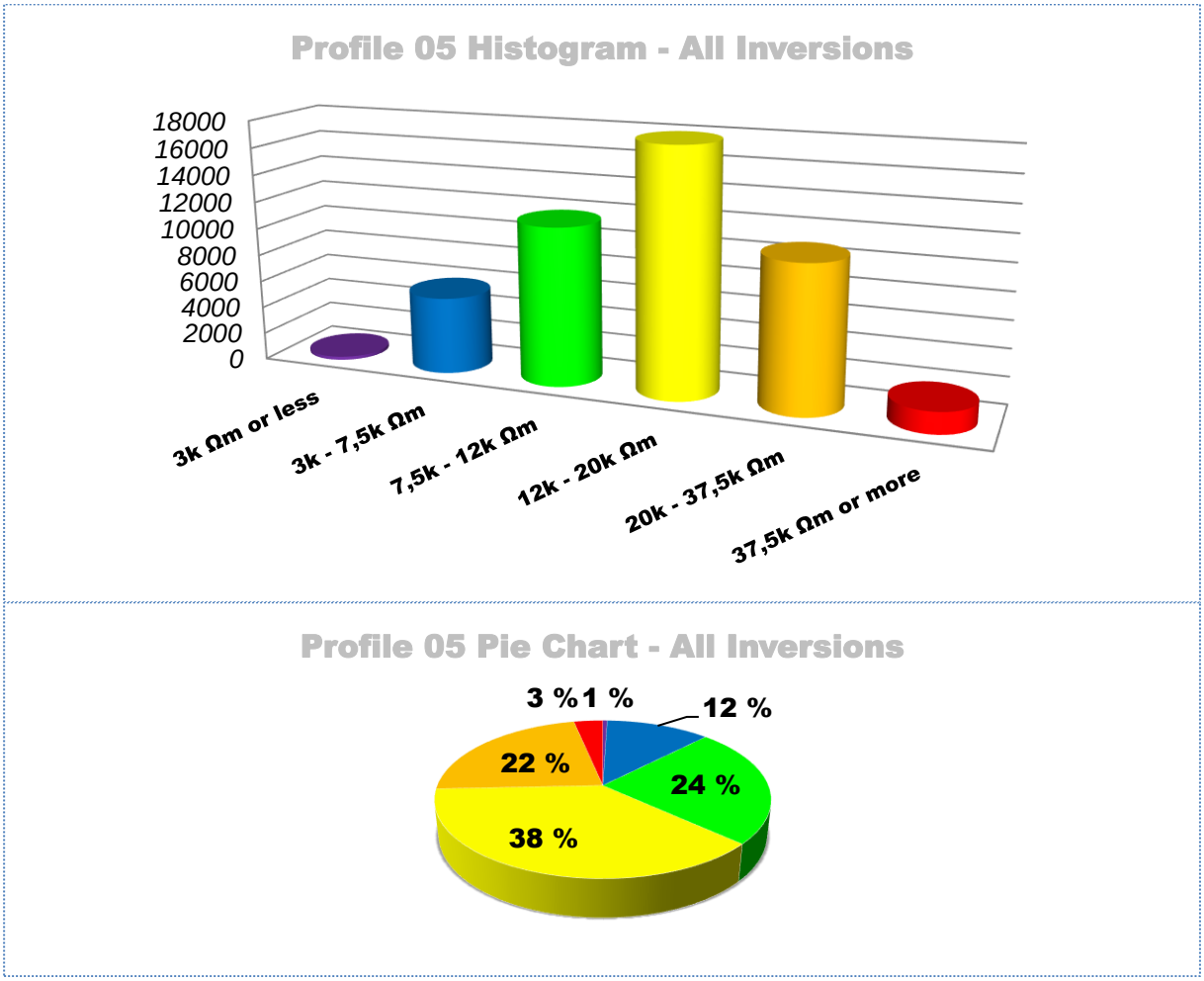

Figure 3.5.2: Top: Histogram depicting the statistical characteristics of all inversion results for **Profile 05**. Bottom: Pie chart depiction of the same data (custom rainbow $\log_{10}$ color scale).

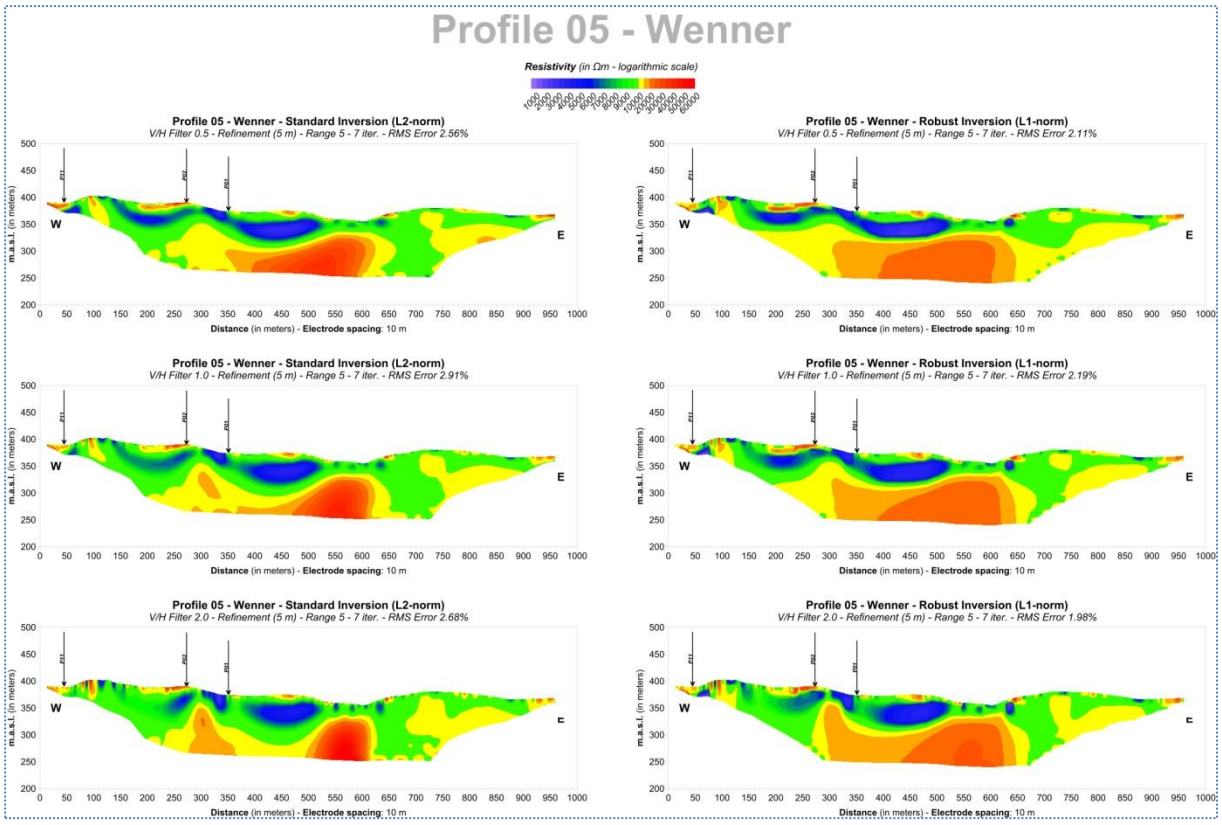

Figure 3.5.3: Reprocessing of **Profile 05** - **Wenner array** using various inversion schemes: Standard or L2-norm (Left) and Robust or L1-norm (Right) inversion with V/H filters equal to 0.5, 1.0 and 2.0 (from top to bottom).

Figure 3.5.3 presenting six different inversion results for Wenner array, does not reveal any significant change in the resistivity distribution. *Robust inversion* (L1-norm) seems to be more consistent in results even with higher V/H filters but the low-resistivity top layer remains relatively uninfluenced by the variety in parameters used. It is also meaningful that the extremely highly resistive top layer representing drained fractured bedrock is less pronounced here than in profiles 03 and 04.

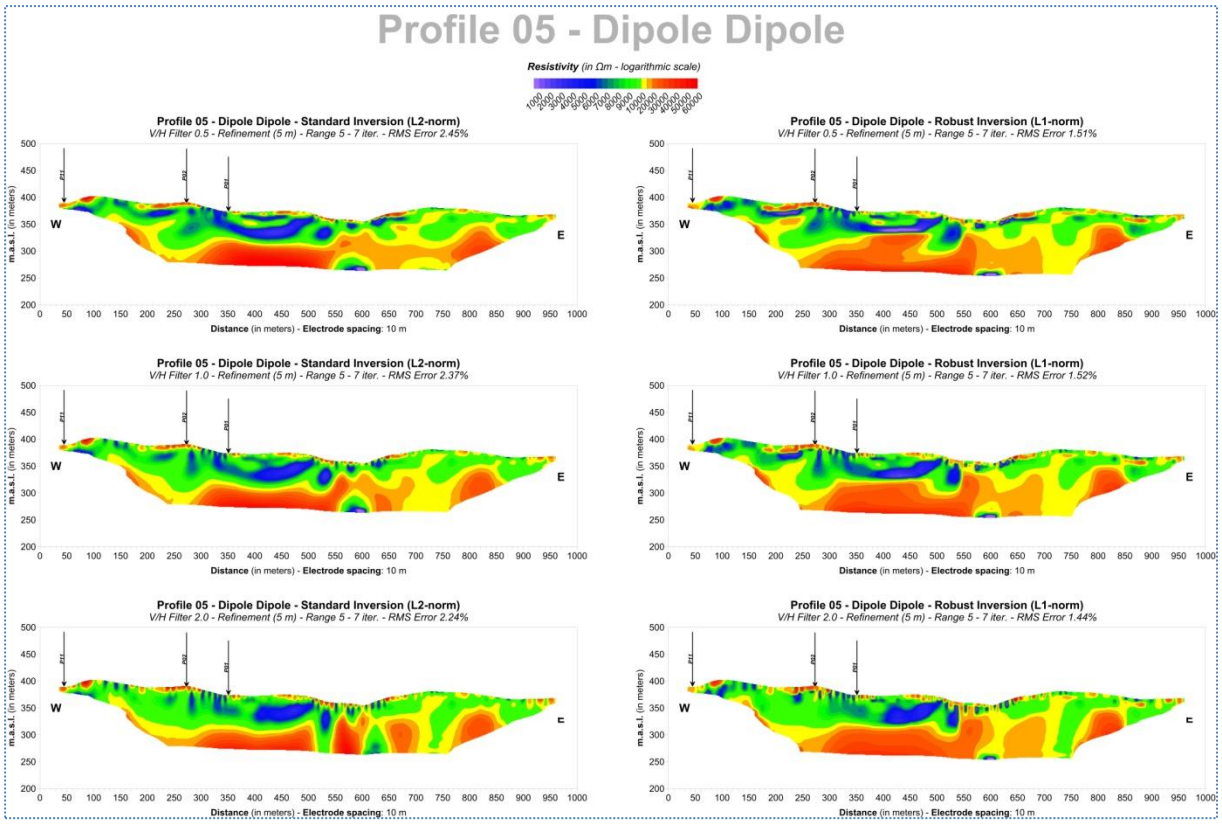

Figure 3.5.4: Reprocessing of **Profile 05** - **Dipole-Dipole array** using various inversion schemes: Standard or L2-norm (Left) and Robust or L1-norm (Right) inversion with V/H filters equal to 0.5, 1.0 and 2.0 (from top to bottom).

Figures 3.5.4 and **3.5.5** holds inversion results for Dipole-Dipole and Mixed array respectively and demonstrates a rather consistent image for Profile 05. Varyingly healthy and unfractured bedrock which is represented by orange-red, appears more consistent on the western half of the profile, underlying a low-resistivity top layer with a higher contrast than in the eastern part of Profile 05. An interesting feature, which is common in all inversion results, is the small low-resistivity concentration appearing in depth at ca. 600 meters distance. This clustering is not continued into shallower depths even when higher V/H filters are employed except for the profile at the bottom left side of **figure 3.5.4** which displays *Standard (L2-norm) inversion* with V/H filter equal to 2.0. In any case, both Dipole-Dipole and Mixed arrays indicate that the area between 550 and 750 meters is more complex than the rest of the profile. Wenner images in this area as being more homogeneous, but it could be the lack of resolution that produces such result. Finally, it is important to note the extremely low RMS errors obtained for *Robust inversion* when Dipole-Dipole and Mixed arrays are inverted. These values vary between 1.44 % and 1.77 % and show an almost perfect match between calculated and measured resistivity values.

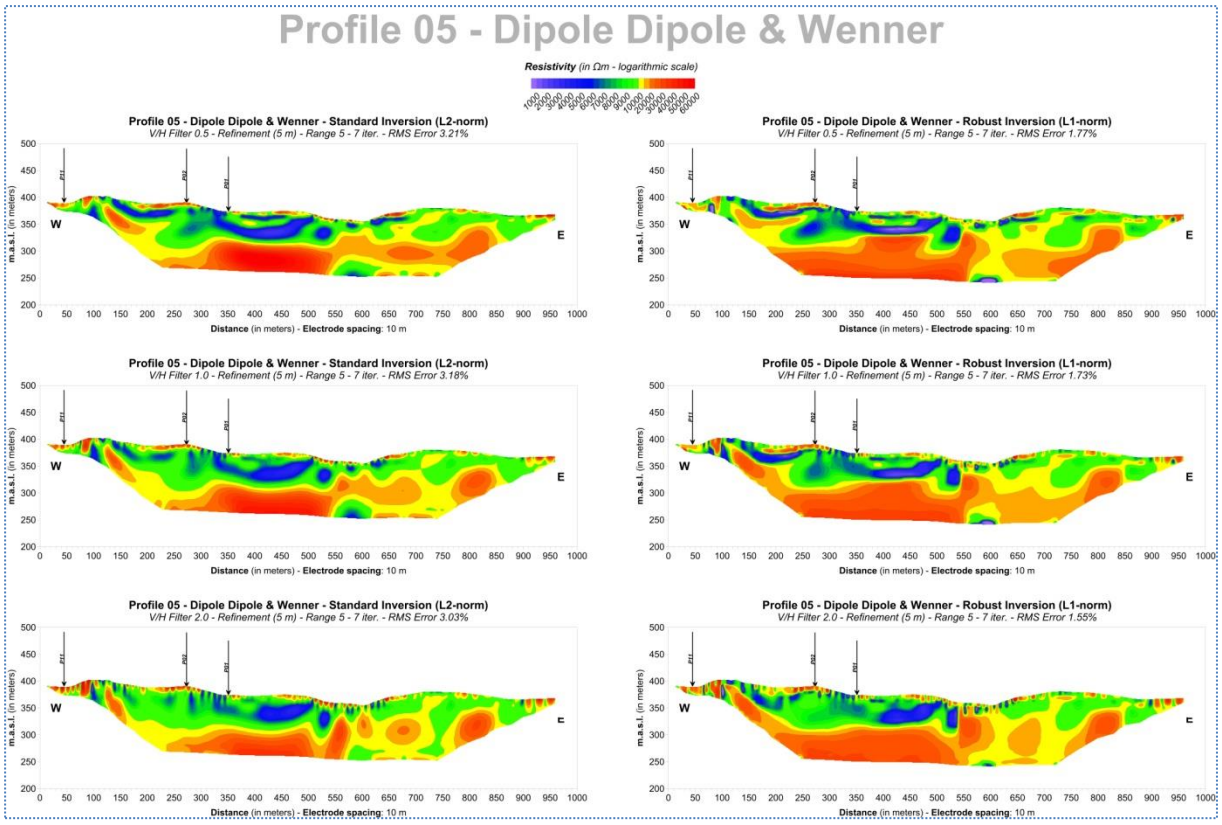

Figure 3.5.5: Reprocessing of **Profile 05** - **Mixed array** using various inversion schemes: Standard or L2-norm (Left) and Robust or L1-norm (Right) inversion with V/H filters equal to 0.5, 1.0 and 2.0 (from top to bottom).

3.6 ERT Profile 06

Profile 06 is not following the southward placement of the previous profiles up until now but can instead be found at the northern end of the survey area, 250 meters north of Profile 03 and at a varying distance north of the back-scarp (20 meters in its beginning and 200 meters at its end - **figure 2.1**). Its total length along topography is a little shorter than the rest of the West-East profiles and is equal to 800 meters which becomes 721 meters of projected horizontal distance due to steep topography (30º for first half and 20º for the second). No additional information is matching its course.

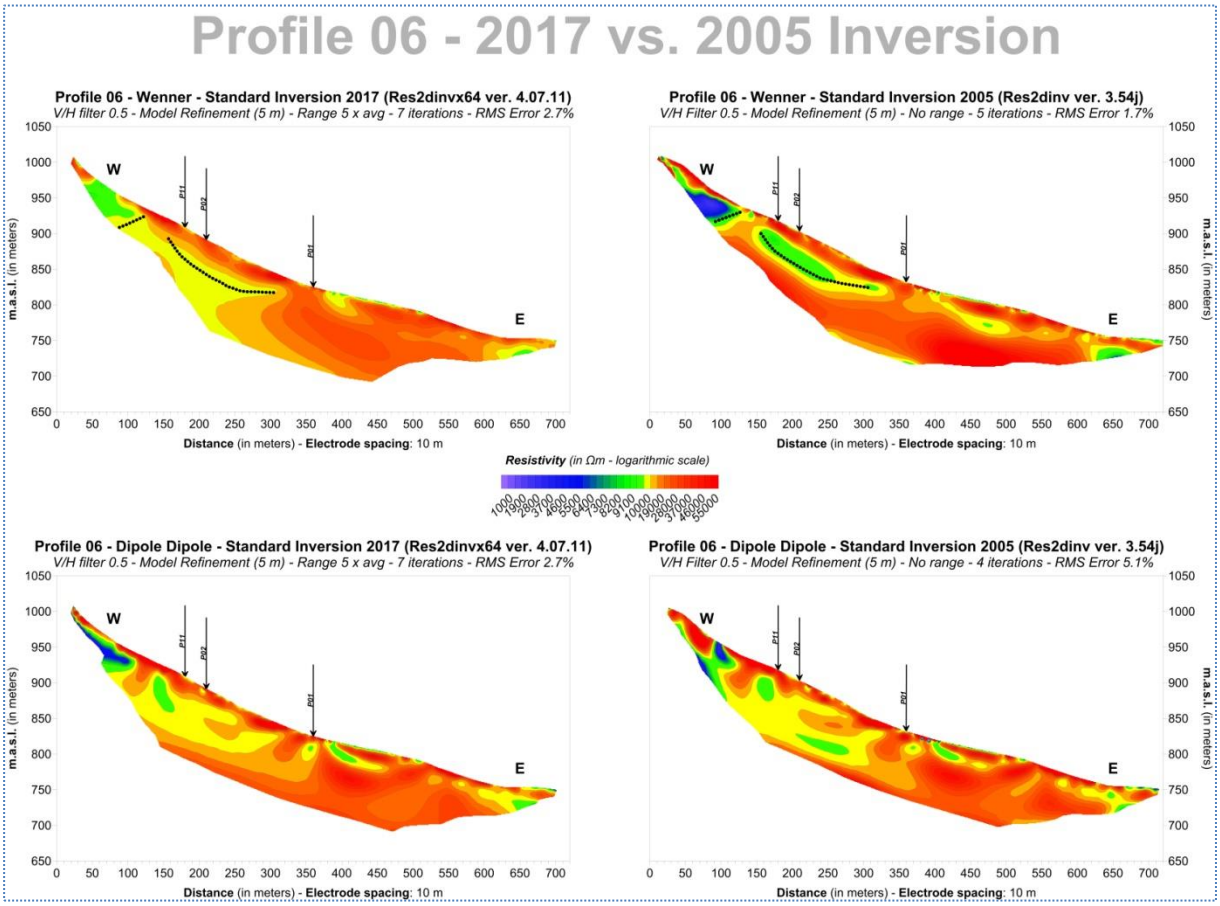

Figure 3.6.1: Wenner (top) and Dipole-Dipole (bottom) inversion results for **Profile 06** with the use of new (left) and old (right) Res2DInv versions. Black dotted lines represent interpretations based on the old results.

Figure 3.6.1, presenting the new inversion juxtaposed with the old one, shows a highly resistive setting with only a slight drop in resistivity in the first half of Profile 06. As already established, the differences are greater when Wenner array is examined and the overall resistivity level lower on the reprocessing result. This means that the relatively lower resistivity concentrations in the western part of the profile are about 1000 Ωm higher with Res2DInv version 4.07.11. The interpretation done in the old result is matching features in the new inversion, however, since the resistivity calculations are different, we wouldn't consider these areas as possible water-saturated highly fractured bedrock, on the contrary fresh bedrock. Dipole-Dipole array on the bottom side of **figure 3.6.1** provides more consistent results, but the qualitative features of both profiles are better matched with the new inversion.

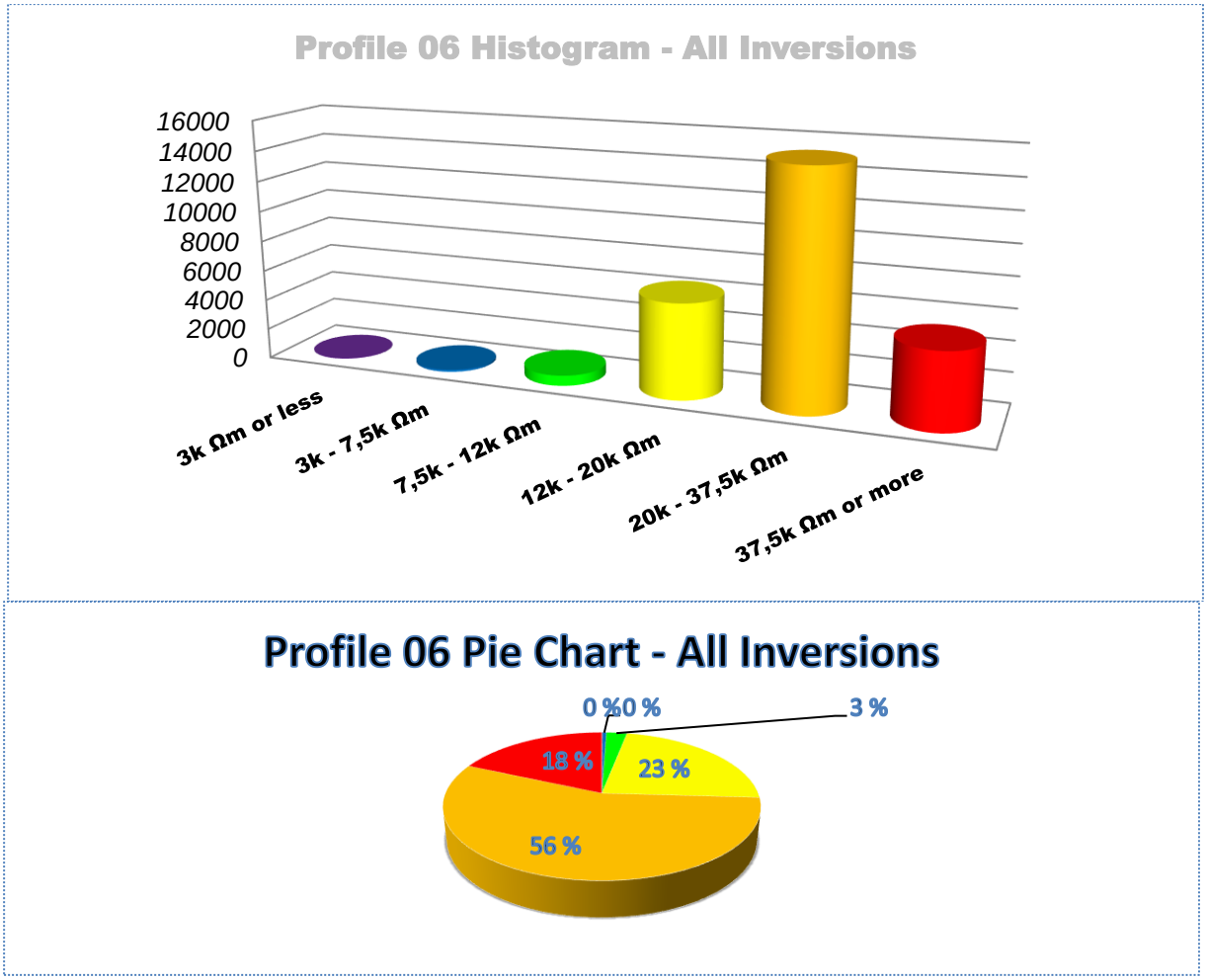

Figure 3.6.2: Top: Histogram depicting the statistical characteristics of all inversion results for **Profile 06**. Bottom: Pie chart depiction of the same data (custom rainbow $\log_{10}$ color scale).

The reprocessing statistics shown in **figure 3.6.2** validates the highly resistive environment along Profile 06 and shows that this is confirmed regardless of array or inversion scheme used. The percentage of generally high resistivity values is 97 %, (18 % being extremely highly resistive drained fractured/low porosity bedrock) which shows that only a handful of the 202, 636 and 838 points for Wenner, Dipole-Dipole and Mixed arrays respectively would qualify as possible water-saturated highly fractured bedrock.

Figures 3.6.3, **3.6.4** and **3.6.5** show the reprocessing results for Wenner, Dipole-Dipole and Mixed arrays and present a negligible variety in resistivity settings which does not add anything towards the interpretation of water-saturated or fractured bedrock. RMS errors are very low in all cases (between 1.87 % and 3.37 %) and the very few low-resistivity vertical structures more vividly seen at the beginning of Dipole-Dipole and Mixed array, do not constitute a noteworthy feature.

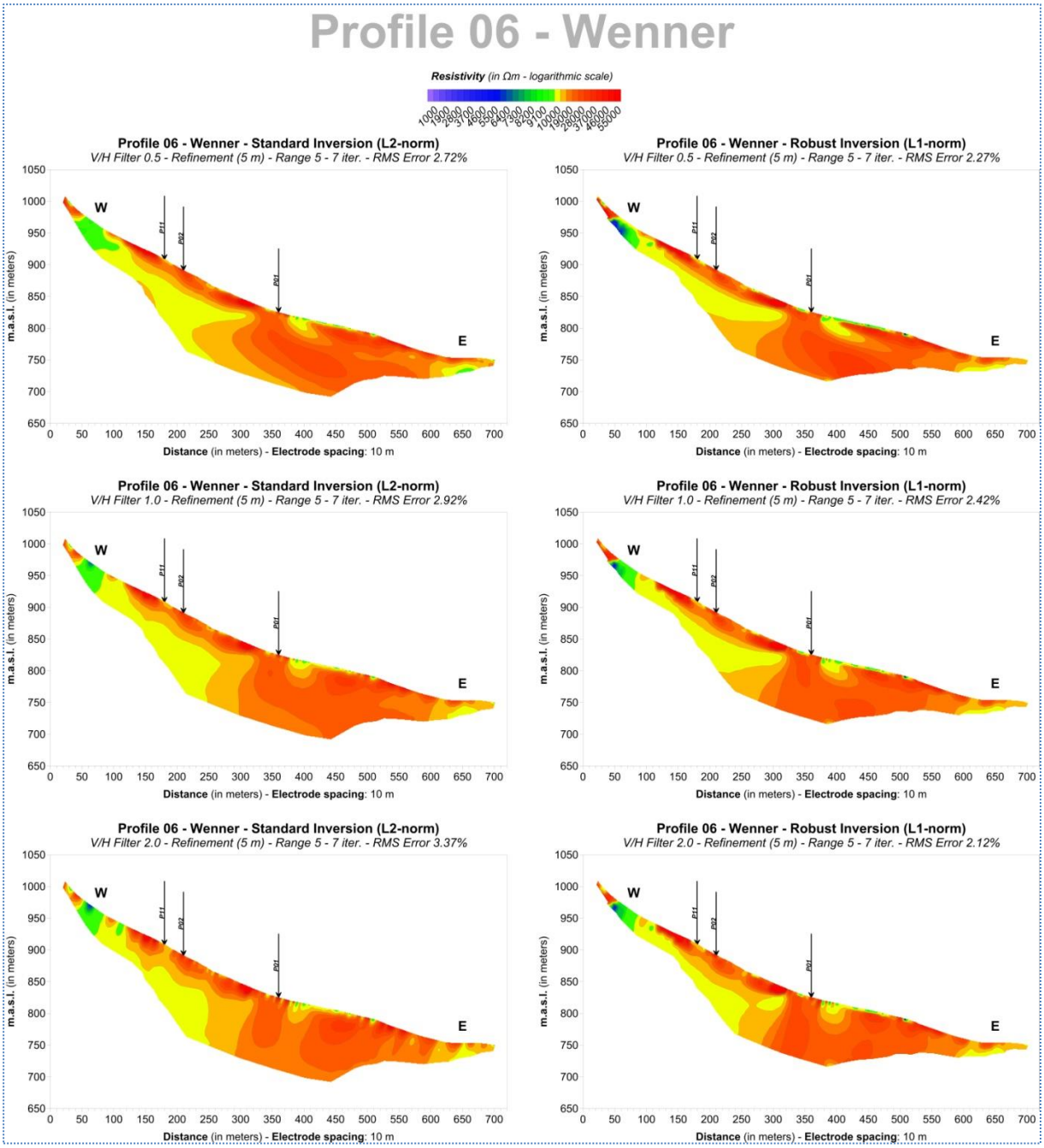

Figure 3.6.3: Reprocessing of **Profile 06** - **Wenner array** using various inversion schemes: Standard or L2-norm (Left) and Robust or L1-norm (Right) inversion with V/H filters equal to 0.5, 1.0 and 2.0 (from top to bottom).

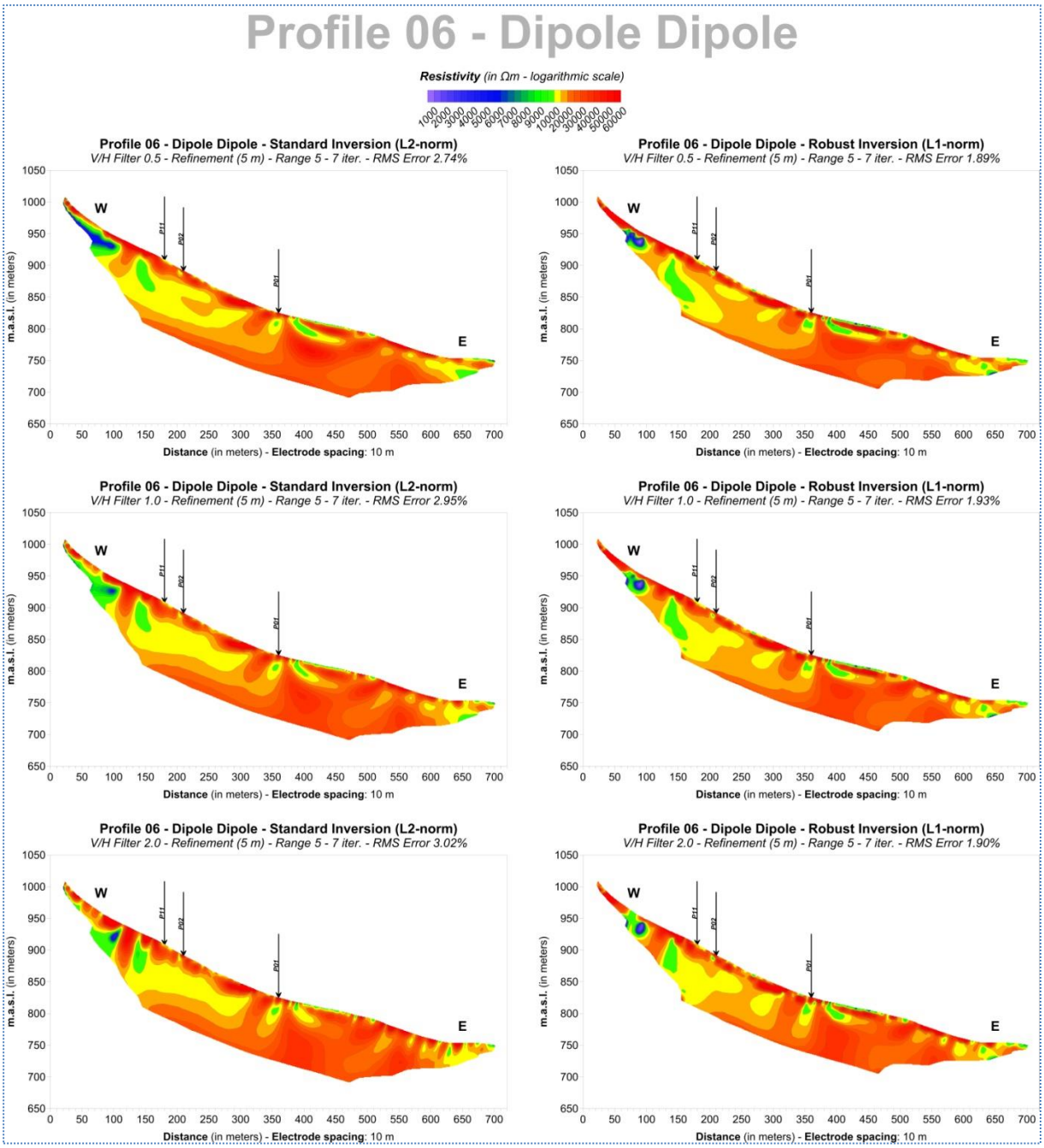

Figure 3.6. 4: Reprocessing of **Profile 06** - **Dipole-Dipole array** using various inversion schemes: Standard or L2-norm (Left) and Robust or L1-norm (Right) inversion with V/H filters equal to 0.5, 1.0 and 2.0 (from top to bottom).

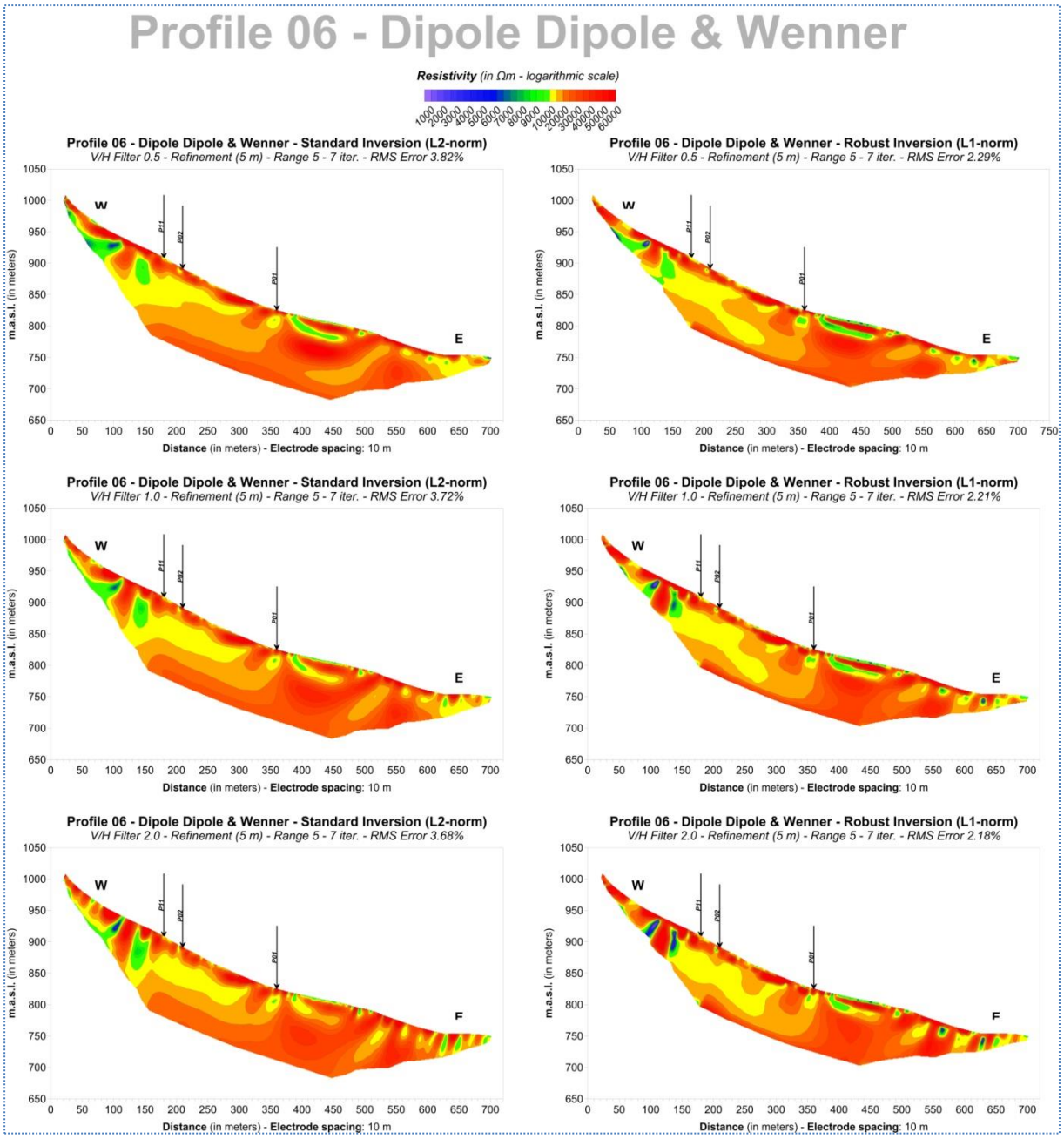

Figure 3.6.5: Reprocessing of **Profile 06** - **Mixed array** using various inversion schemes: Standard or L2-norm (Left) and Robust or L1-norm (Right) inversion with V/H filters equal to 0.5, 1.0 and 2.0 (from top to bottom).

3.7 ERT Profile 07

Profile 07 is the southernmost profile in Åknes. It is positioned 400 meters south of Profile 05 at its beginning and 150 meters at its end, it is 800 meters long along topography and 754 meters when projected on a map like the one in **figure 2.1**. Bh-03 (see **figure 2.1**) is positioned just 15 meters away to the south of the profile but no additional information matches the profile's path.

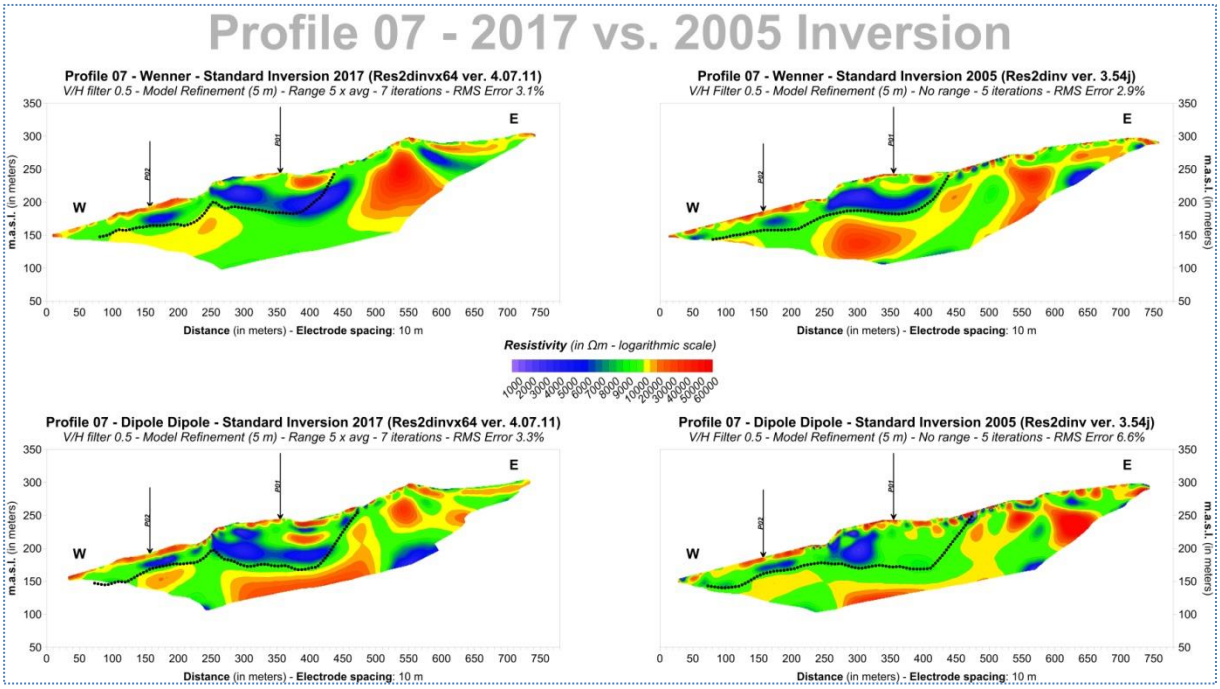

Figure 3.7.1: Wenner (top) and Dipole-Dipole (bottom) inversion results for **Profile 07** with the use of new (left) and old (right) Res2DInv versions. Black dotted lines represent interpretations based on the old results.

Figure 3.7.1 exposes some noticeable differences in both Wenner and Dipole-Dipole inversion results using Res2DInv in 2017 and 2005. Wenner array presents a different distribution of low-resistivity values, highlighted by the mismatch with the black dotted line which represents the old interpretation. There are also differences concerning bedrock below this low-resistivity layer but generally, we are talking about two very different results even though RMS errors are comparable (3.1 % versus 2.9 %). The Dipole-Dipole reprocessing outcome on the other hand is again more consistent regardless of Res2DInv version used but the difference in low-resistivity distribution is obvious. Finally, the dominance of low-resistivity values is evident in all results, old and new.

Figure 3.7.2 depicts low-resistivity dominant stats for Profile 07 (Wenner: 417 points, Dipole-Dipole: 691 points, Mixed: 1108 points), as was already established for the southern part of the survey area with Profile 05. Comparing these stats with those of Profile 05 more specifically, we deduce that the statistics are almost identical when it comes to low-resistivity values (green-blue-purple). This part of the data represents 35 % of the total in Profile 07, while the same group represents 36 % of the total in Profile 05. This essentially means that the overall conditions in Profile 07, are as less resistive as in Profile 05.

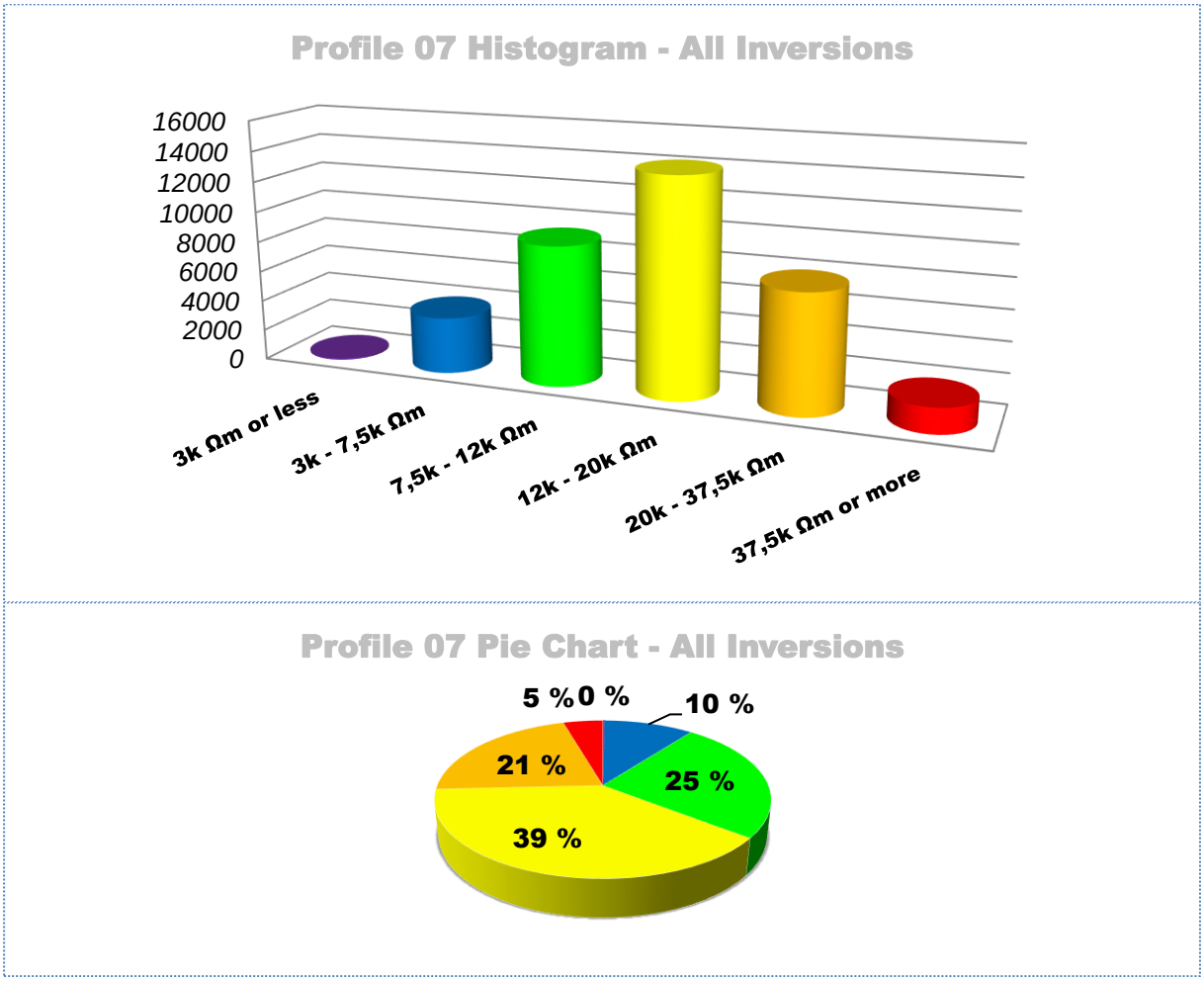

Figure 3.7.2: Top: Histogram depicting the statistical characteristics of all inversion results for **Profile 07**. Bottom: Pie chart depiction of the same data (custom rainbow $\log_{10}$ color scale).

Figure 3.7.3 shows a variety of obtained results for Wenner, depending on the inversion scheme utilized. The common feature in all results is that the middle part of the profile is characterized by low resistivities. However, it is unclear how low these resistivities are and how they are distributed. *Standard* and *Robust inversion* with V/H filter equal to 0.5 and *Robust inversion* with V/H filter equal to 1.0 present the highest compatibility with the lowest RMS errors obtained with *Robust inversion* (2.31 % and 2.50 % for V/H filter 0.5 and 1.0 respectively). Higher V/H filters in *Standard inversion* cause the low-resistivity area to expand in depth in an unreliable manner. **Figures 3.7.4** and **3.7.5** on the other hand show cases much more coherent reprocessing results for Dipole-Dipole and Mixed arrays. The projected thickness of the low-resistivity central part of Profile 07, remains relatively uninfluenced by the change in

inversion parameters but its distribution is becoming more fragmented as the V/H filter value increases. This possible water-saturated or fractured bedrock is delimited by healthier bedrock appearing in depth between distances 250 and 550 meters, seems to be horizontal especially when low V/H filter values are used and is split between 350 and 450 meters by a high resistivity wedge. Fracture zones could be interpreted at the edges of this formation but the indications are not strong enough. Finally, RMS errors in *Robust inversion* are around 2 % whereas for *Standard inversion* they are around 3.5 %.

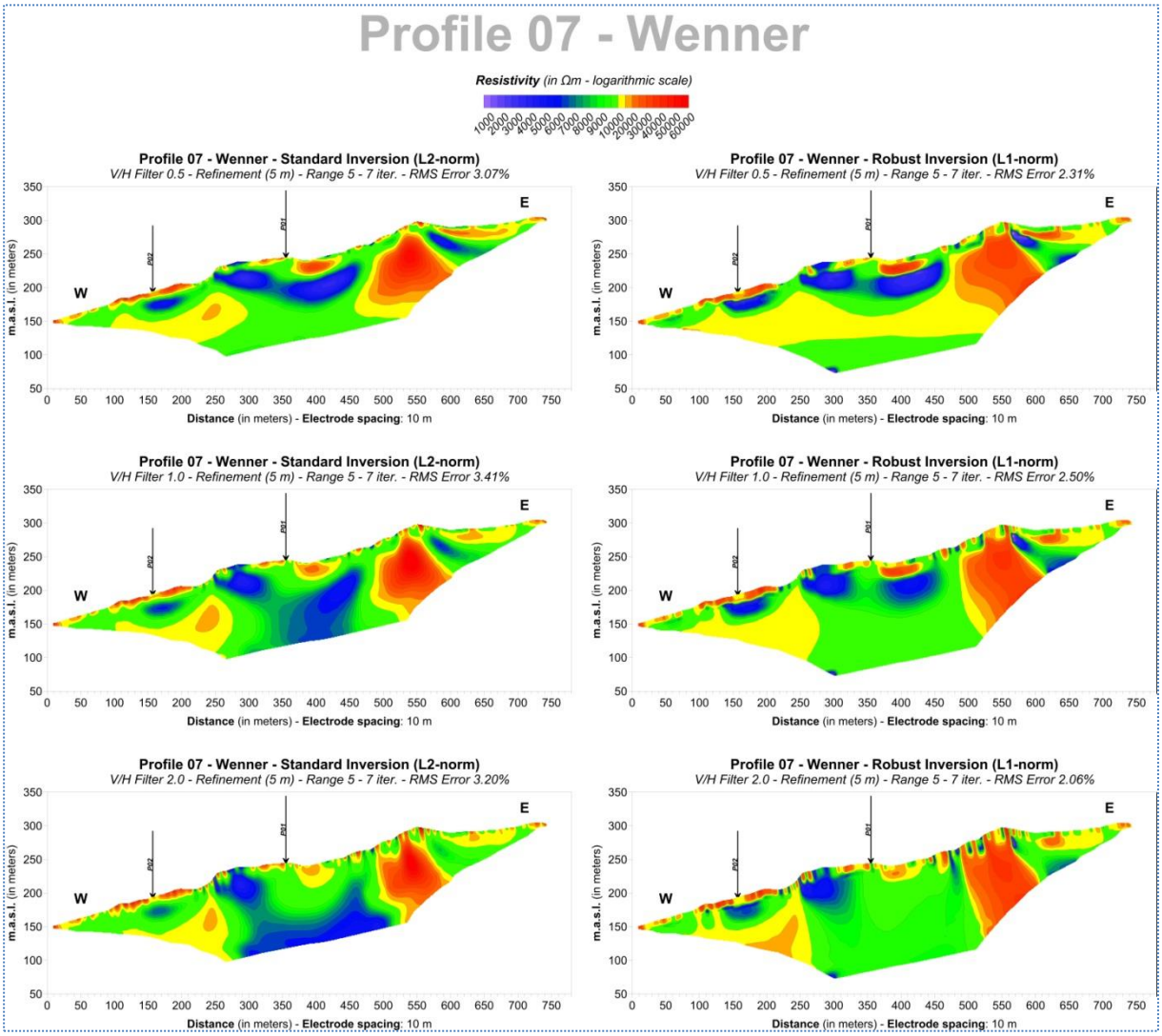

Figure 3.7.3: Reprocessing of **Profile 07** - **Wenner array** using various inversion schemes: Standard or L2-norm (Left) and Robust or L1-norm (Right) inversion with V/H filters equal to 0.5, 1.0 and 2.0 (from top to bottom).

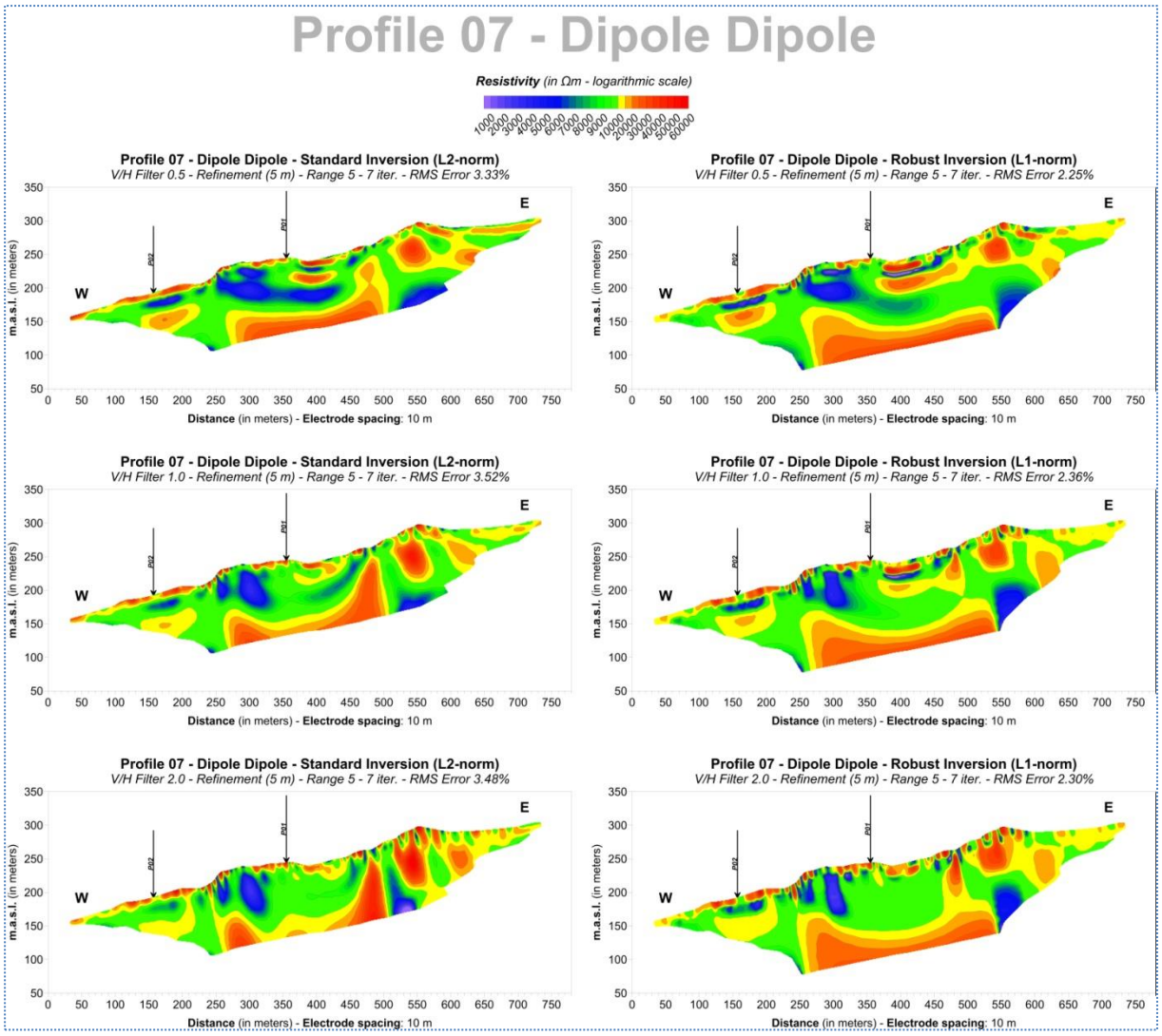

Figure 3.7.4: Reprocessing of **Profile 07** - **Dipole-Dipole array** using various inversion schemes: Standard or L2-norm (Left) and Robust or L1-norm (Right) inversion with V/H filters equal to 0.5, 1.0 and 2.0 (from top to bottom).

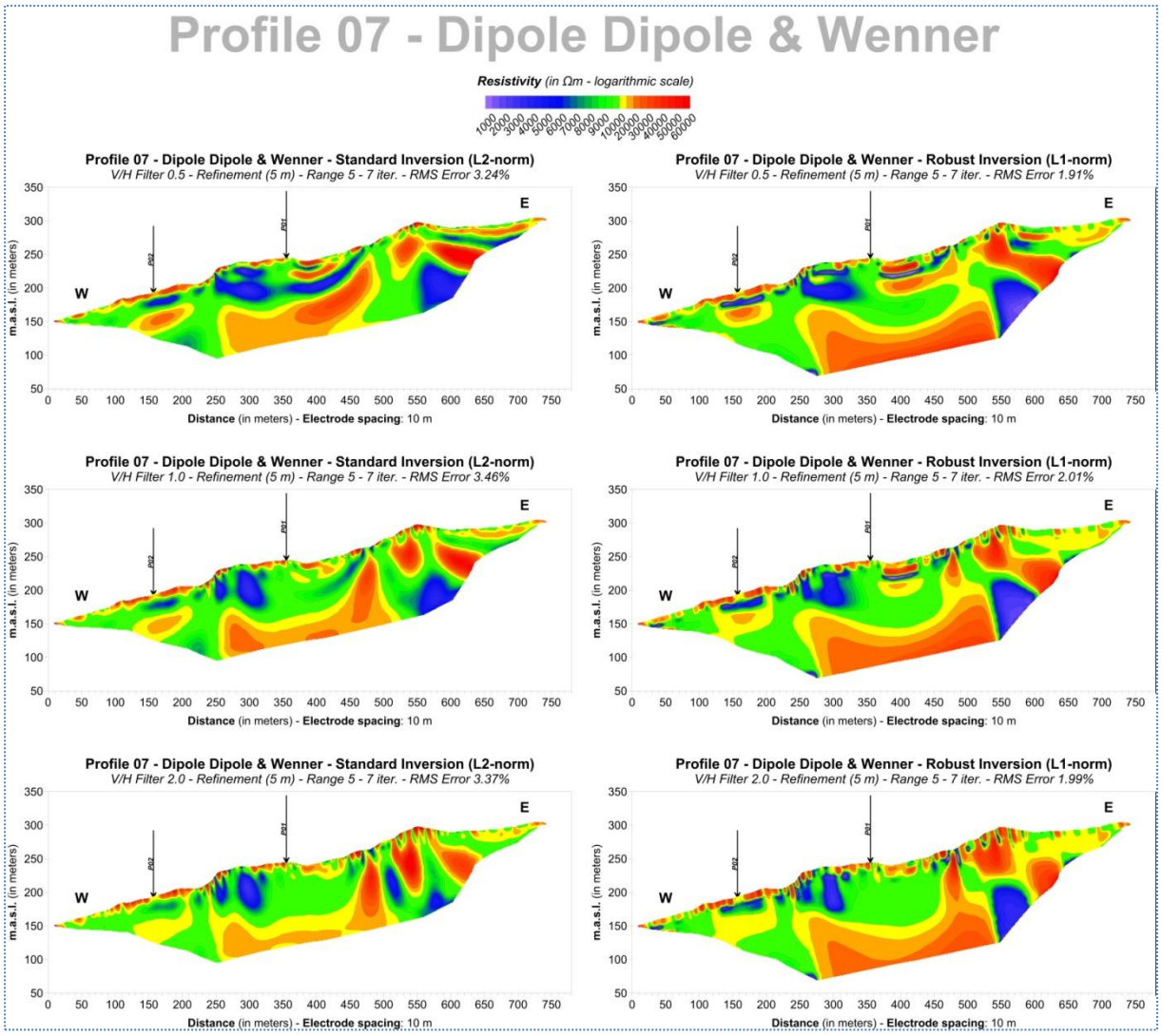

Figure 3.7.5: Reprocessing of **Profile 07** - **Mixed array** using various inversion schemes: Standard or L2-norm (Left) and Robust or L1-norm (Right) inversion with V/H filters equal to 0.5, 1.0 and 2.0 (from top to bottom).

3.8 ERT Profile 08

Profile 08, as seen in **figure 2.1,** is running the survey area diagonally, starting about 85 meters after the end of Profile 06 (Northeast) and ending about 75 meters north of the beginning of Profile 05 (Southwest). Its projected length is 950 meters (101 electrodes with 10 m spacing) and its middle part between 410 and 790 meters is matching Profile 09 which will be presented in the next section. Some boreholes are in neighboring positions like Bh-1 (35 meters to its Southeast) but none is strictly matching the course of the profile.

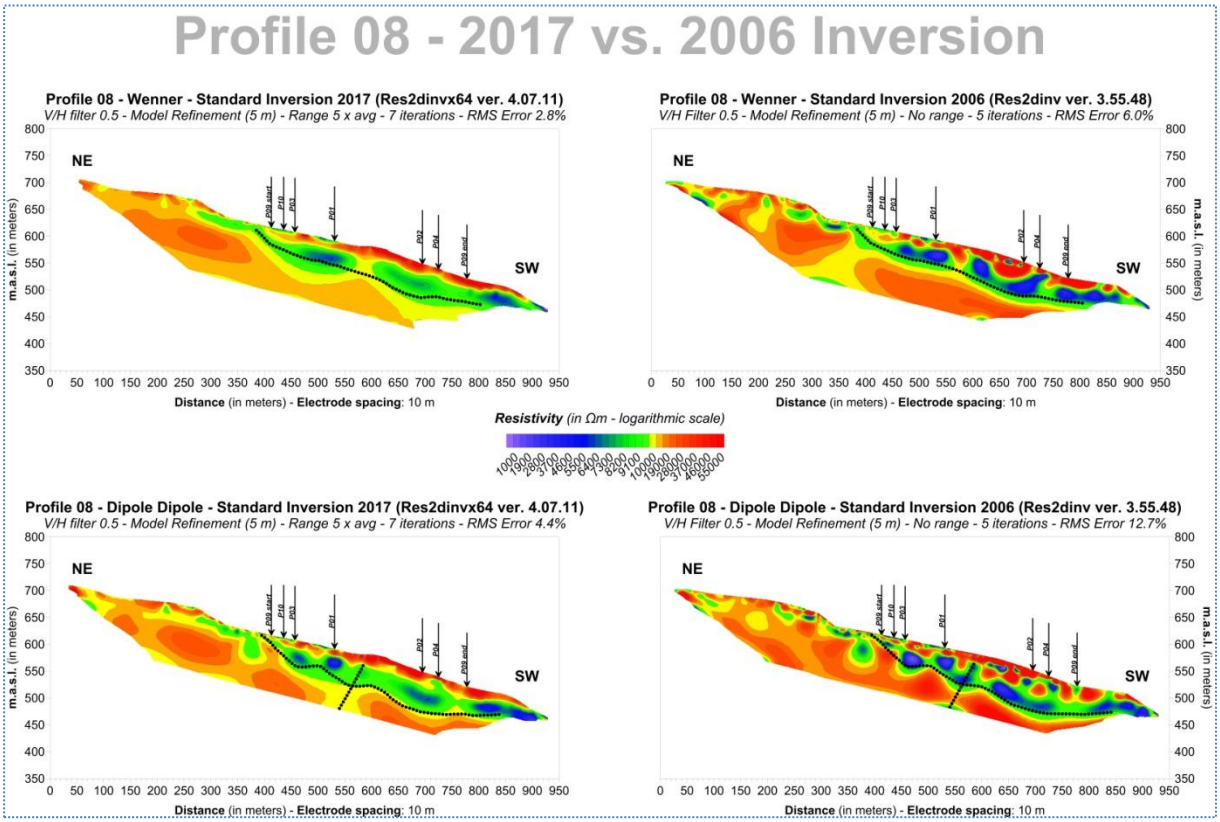

Figure 3.8.1: Wenner (top) and Dipole-Dipole (bottom) inversion results for **Profile 08** with the use of new (left) and old (right) Res2DInv versions. Black dotted lines represent interpretations based on the old results.

Figure 3.8.1 exhibits how the old inversion code has yielded results with higher resistivity contrast than the new one. It should be noted that the old inversions from this profile are done in 2006 with Res2DInv version 3.55.48 instead of 3.54j which was used for Profiles 01 to 07. Quantitatively, both Wenner and Dipole-Dipole results present the same geoelectrical structure i.e. a higher resistivity environment on the northeastern part of Profile 08 which transforms into a gradually deepening low-resistivity layer towards the Southwest. However, the difference in resistivity levels is obvious and that also affects the validity of an interpretation of a fracture zone in the old result which is not as strong in the new Dipole-Dipole inversion result. Nonetheless, RMS errors are at least halved when using Res2DInv version 4.07.11 and the overall lower resistivity levels are matching the reprocessing results for all other intersecting profiles better.

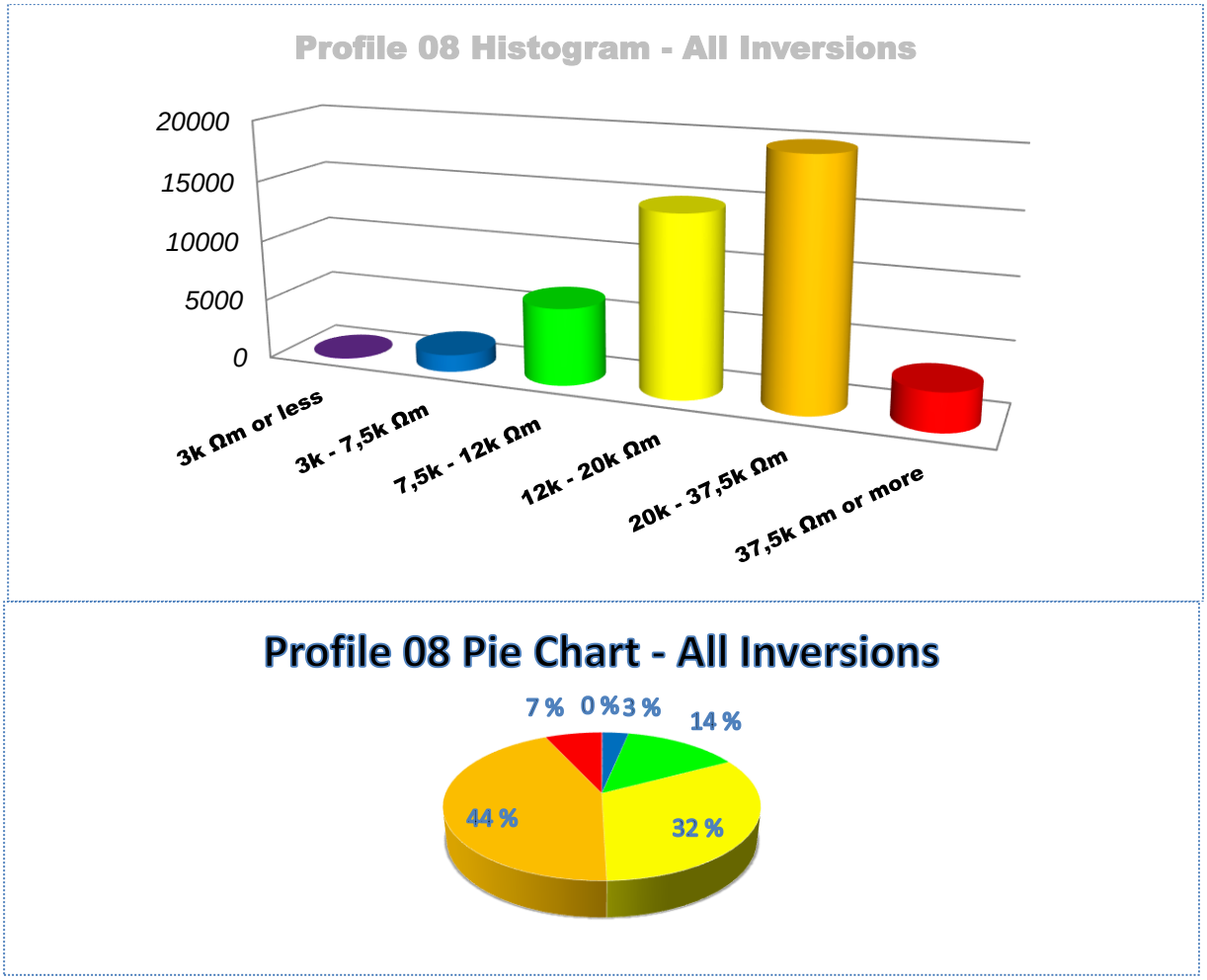

Figure 3.8.2: Top: Histogram depicting the statistical characteristics of all inversion results for **Profile 08**. Bottom: Pie chart depiction of the same data (custom rainbow $\log_{10}$ color scale).

Statistics based on all inversion results for Profile 08 shown in **figure 3.8.2** display relatively resistive conditions with varyingly healthy bedrock (yellow and orange) representing 76 % of the data. This resistivity value distribution is comparable in values to that of Profile 03 which is intersecting Profile 08 halfway. However, Profile 08 is uniquely designed to connect the results from other profiles therefore its collective statistics are also unique and cannot be compared to any other profile in Åknes. Therefore, it is more beneficial to examine each inversion result separately. For each resulting profile presented in **figures 3.8.3**, **3.8.4** and **3.8.5,** 443 Wenner, 1037 Dipole-Dipole and 1480 Mixed array points were used.

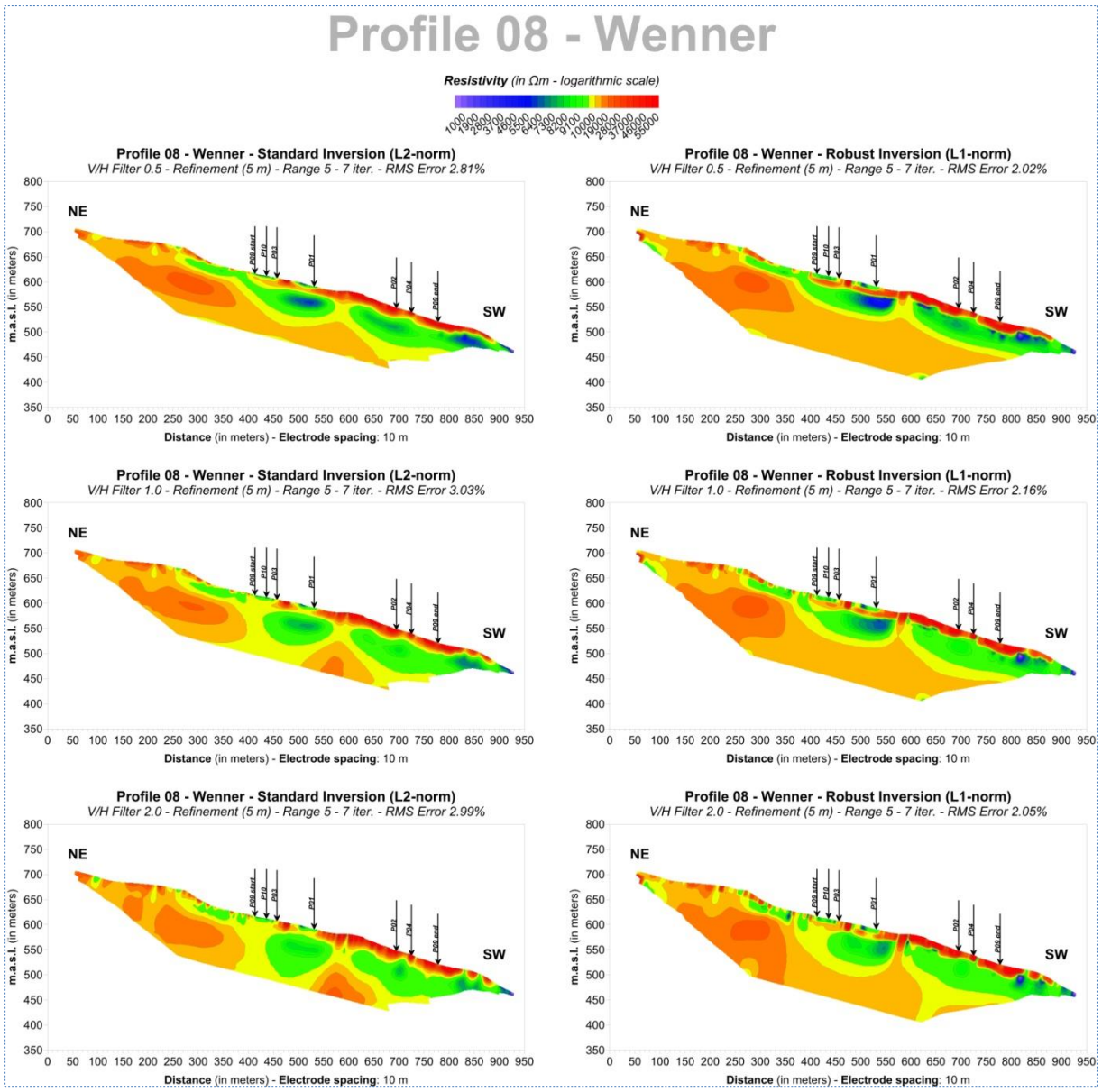

Figure 3.8.3: Reprocessing of **Profile 08** - **Wenner array** using various inversion schemes: Standard or L2-norm (Left) and Robust or L1-norm (Right) inversion with V/H filters equal to 0.5, 1.0 and 2.0 (from top to bottom).

Figure 3.8.3 displays how Wenner array is responding to the use of *Standard* (L2-norm) or *Robust* (L1-norm) *inversion* with various V/H filters. Generally, the low-resistivity body is consistently increasing in thickness towards the Southwest but higher V/H filter values seem to position a high resistivity barrier at 625 meters which divides it into two parts. This effect is more pronounced with the use of *Robust inversion* - which also yields half the RMS error percentages - and this is validated in **figures 3.8.4** and **3.8.5** where Dipole-Dipole and Mixed array results are presented. Regardless, the low-resistivity formation is still in place with relatively lower resistivities than in Wenner while no possible vertical structures are standing out in any of the resulting profiles.

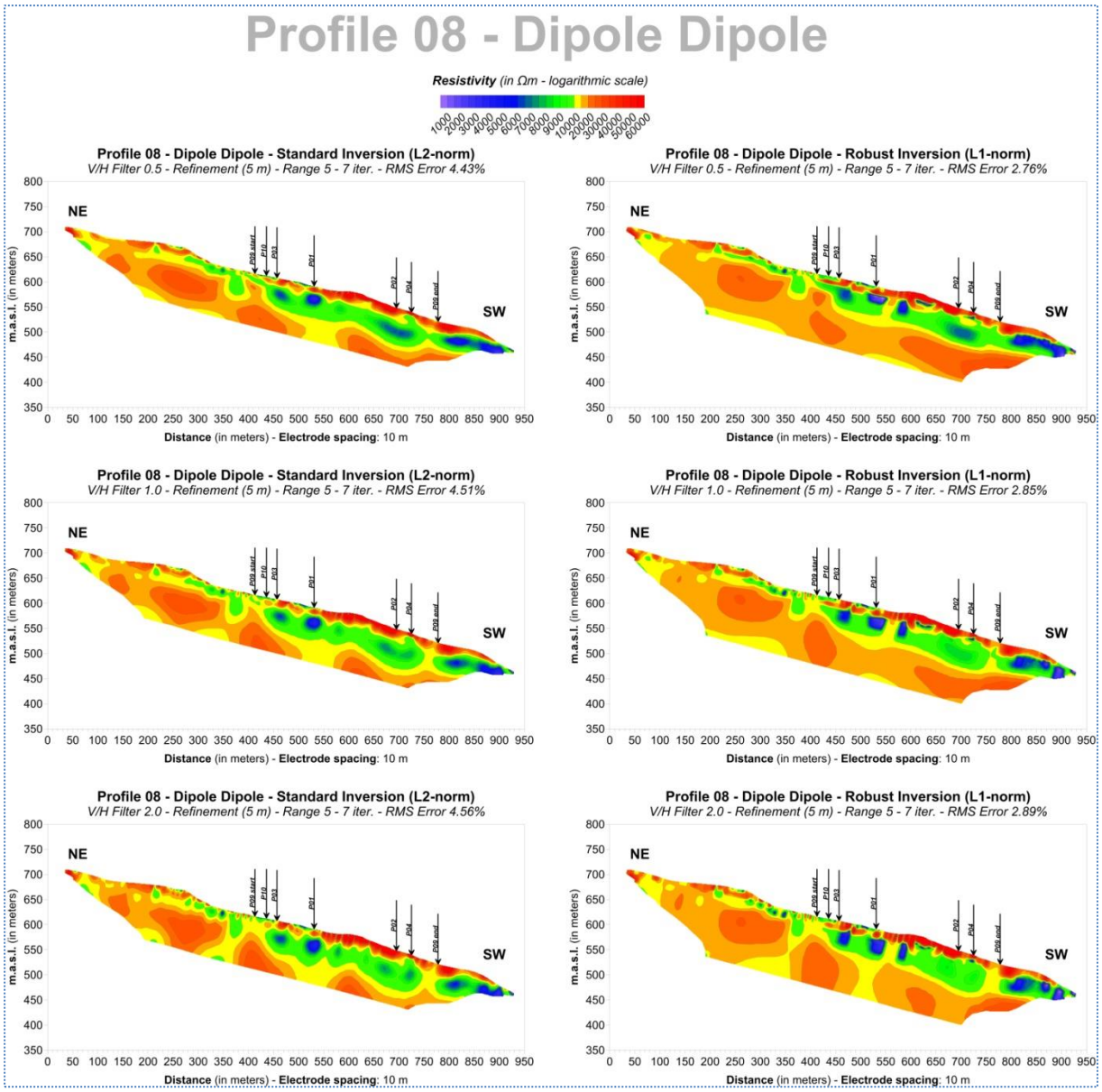

Figure 3.8.4: Reprocessing of **Profile 08** - **Dipole-Dipole array** using various inversion schemes: Standard or L2-norm (Left) and Robust or L1-norm (Right) inversion with V/H filters equal to 0.5, 1.0 and 2.0 (from top to bottom).

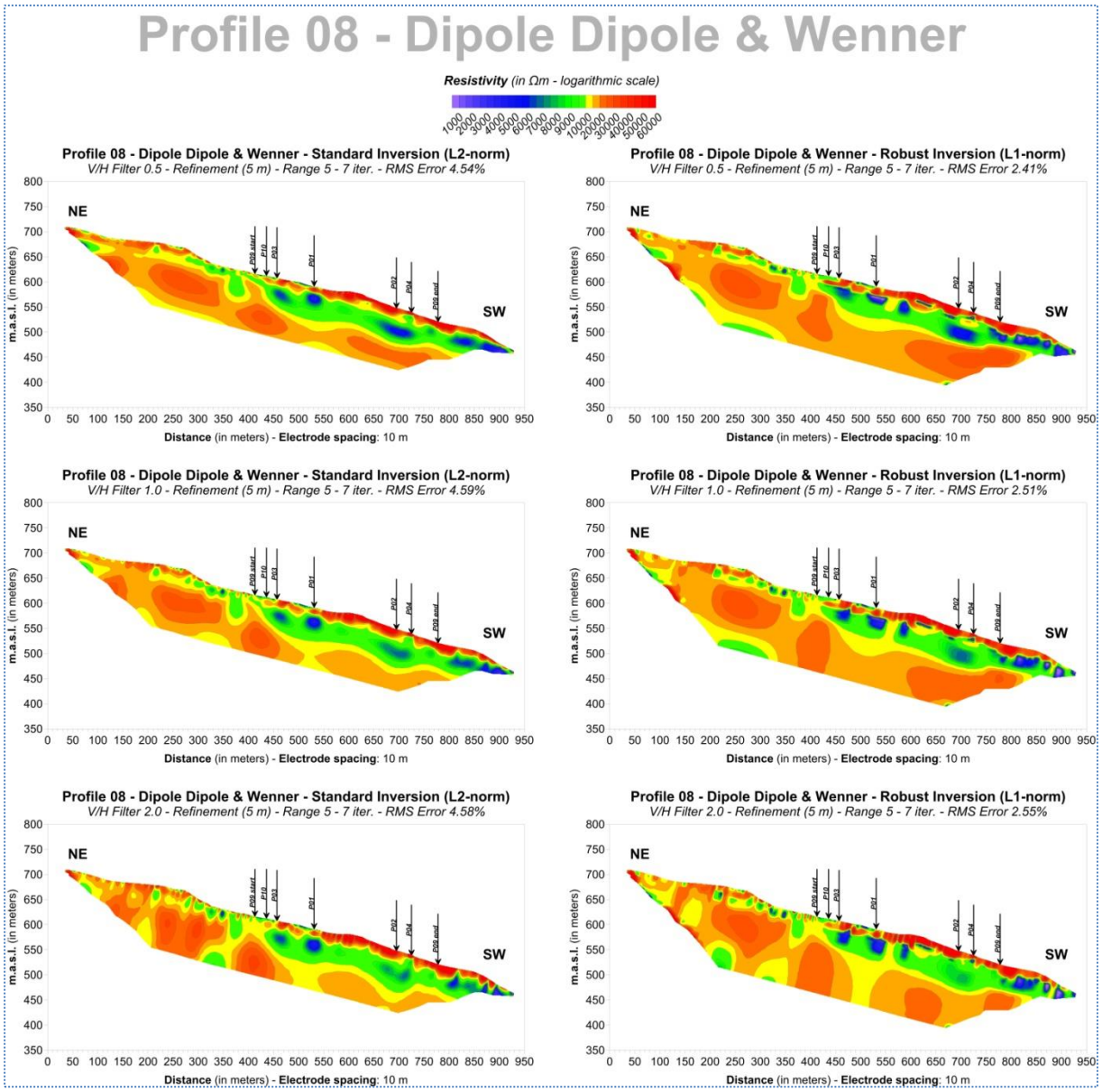

Figure 3.8.5: Reprocessing of **Profile 08** - **Mixed array** using various inversion schemes: Standard or L2-norm (Left) and Robust or L1-norm (Right) inversion with V/H filters equal to 0.5, 1.0 and 2.0 (from top to bottom).

3.9 ERT Profile 09

Profile 09 is one out of two profiles conducted with a 5 m electrode spacing, and it is covering the middle part of Profile 08 in higher detail. Its total length is 383 meters (81 electrodes with **5 m spacing**) and its depth coverage is of course half the one of Profile 08.

Figure 3.9.1 shows results concerning inversions performed in 2017 and 2006 for Wenner and Dipole-Dipole array. First and foremost, we should point out how the new inversion results for both arrays are more consistent than the results obtained with the old Res2DInv version. Then, it is interesting to see how this high resistivity barrier dividing the low-resistivity body seen in **figure 3.8.3** is mapped with denser electrode spacing both with Wenner and Dipole-Dipole arrays. Wenner array is failing to map this barrier whereas the new inversion clearly positions it at 160 meters (600 meters in Profile 08) but with a probably artificial widening with depth. When it comes to Dipole-Dipole array, old and new results are again more similar, but the resistivity values in the southwestern half of the profile are not as low as in 2006. Lastly, the interpretation of fracture zones is probably not very accurate when included in the new inversion result.

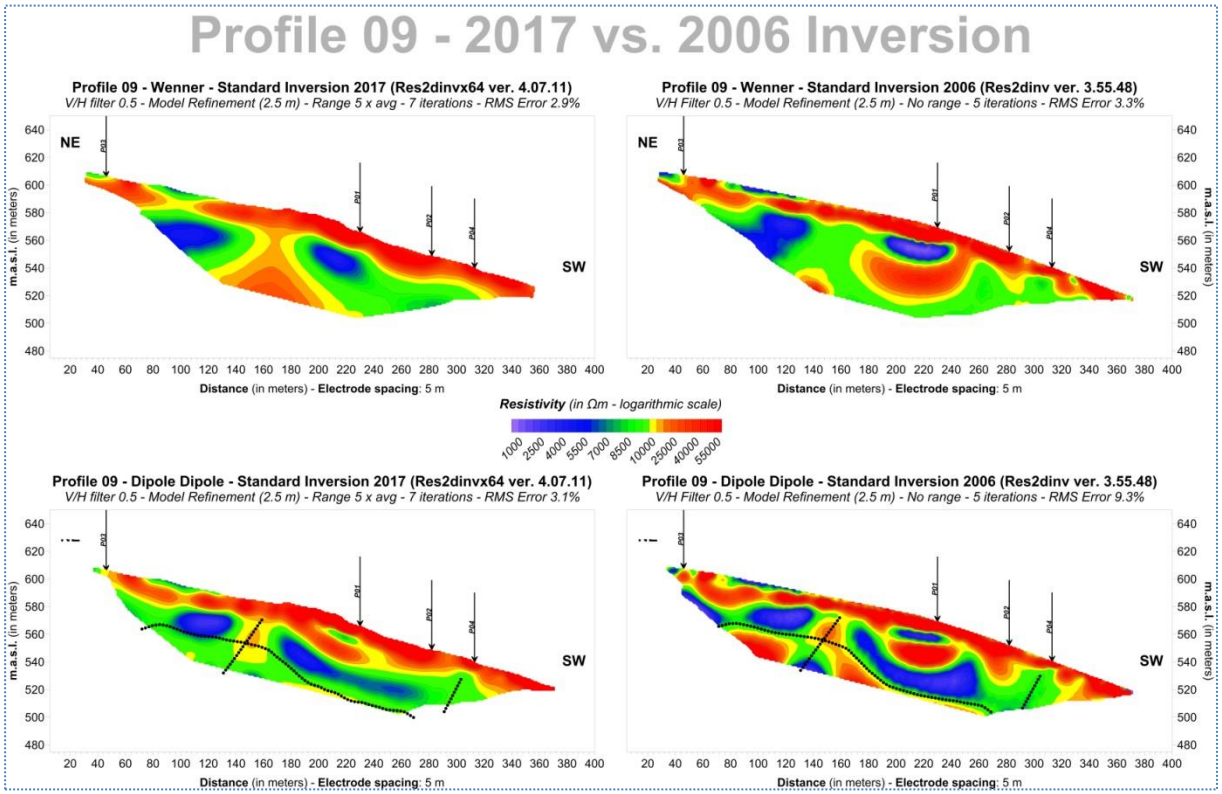

Figure 3.9.1: Wenner (top) and Dipole-Dipole (bottom) inversion results for **Profile 09** with the use of new (left) and old (right) Res2DInv versions. Black dotted lines represent interpretations based on the old results.

The statistic shown in **figure 3.9.2** reveal a low-resistivity environment for Profile 09 which is not a surprise since this profile is focusing on an equally low-resistive area within Profile 08. For Profile 09 or in other words, for this particular slice of Profile 08, 29 % of the values represent water-saturated fractured bedrock and 27 % represent highly fractured drained bedrock. The number of values contributing to this statistical analysis for Wenner, Dipole-Dipole and Mixed array are 279, 672 and 951 points respectively.

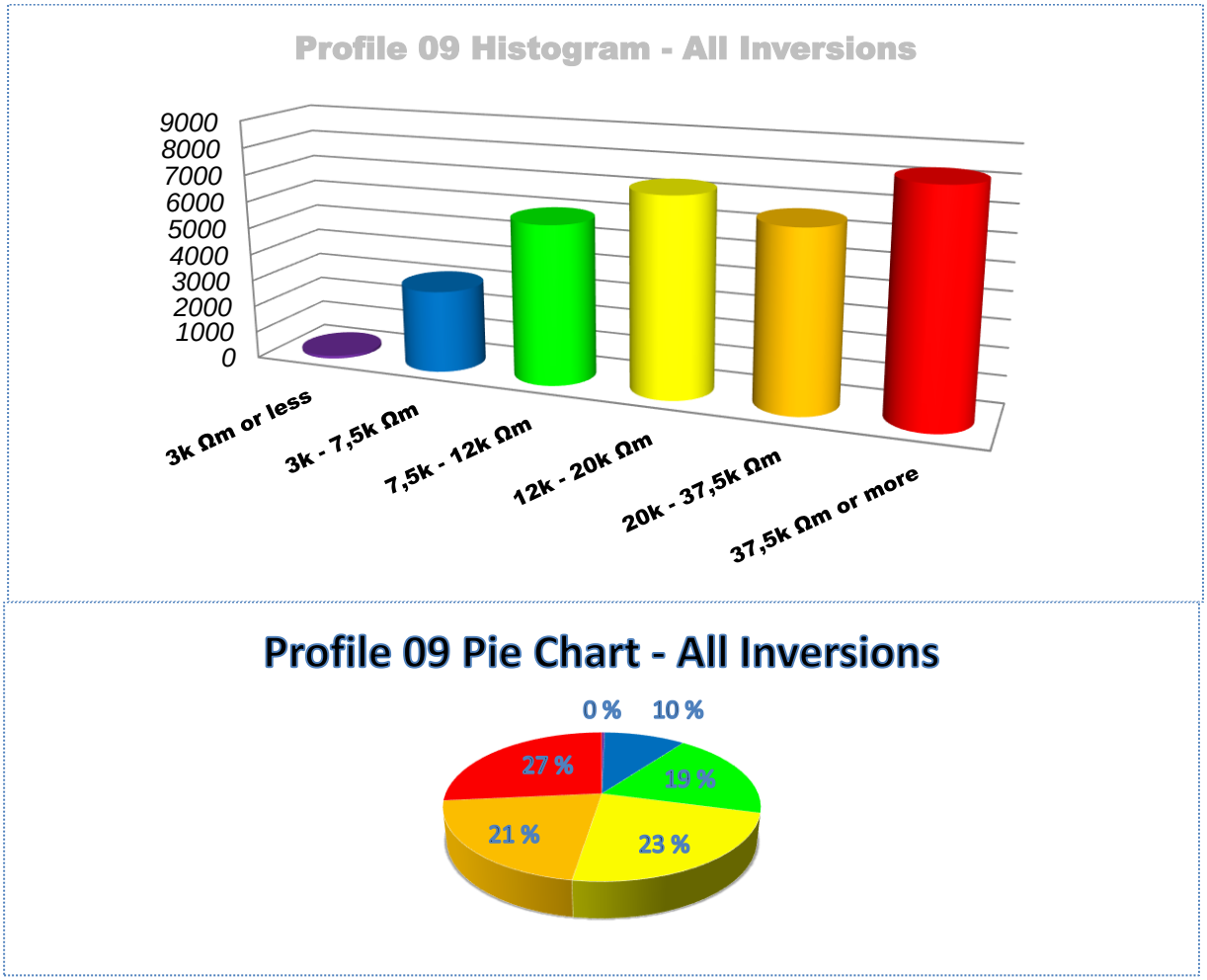

Figure 3.9.2: Top: Histogram depicting the statistical characteristics of all inversion results for **Profile 09**. Bottom: Pie chart depiction of the same data (custom rainbow $\log_{10}$ color scale).

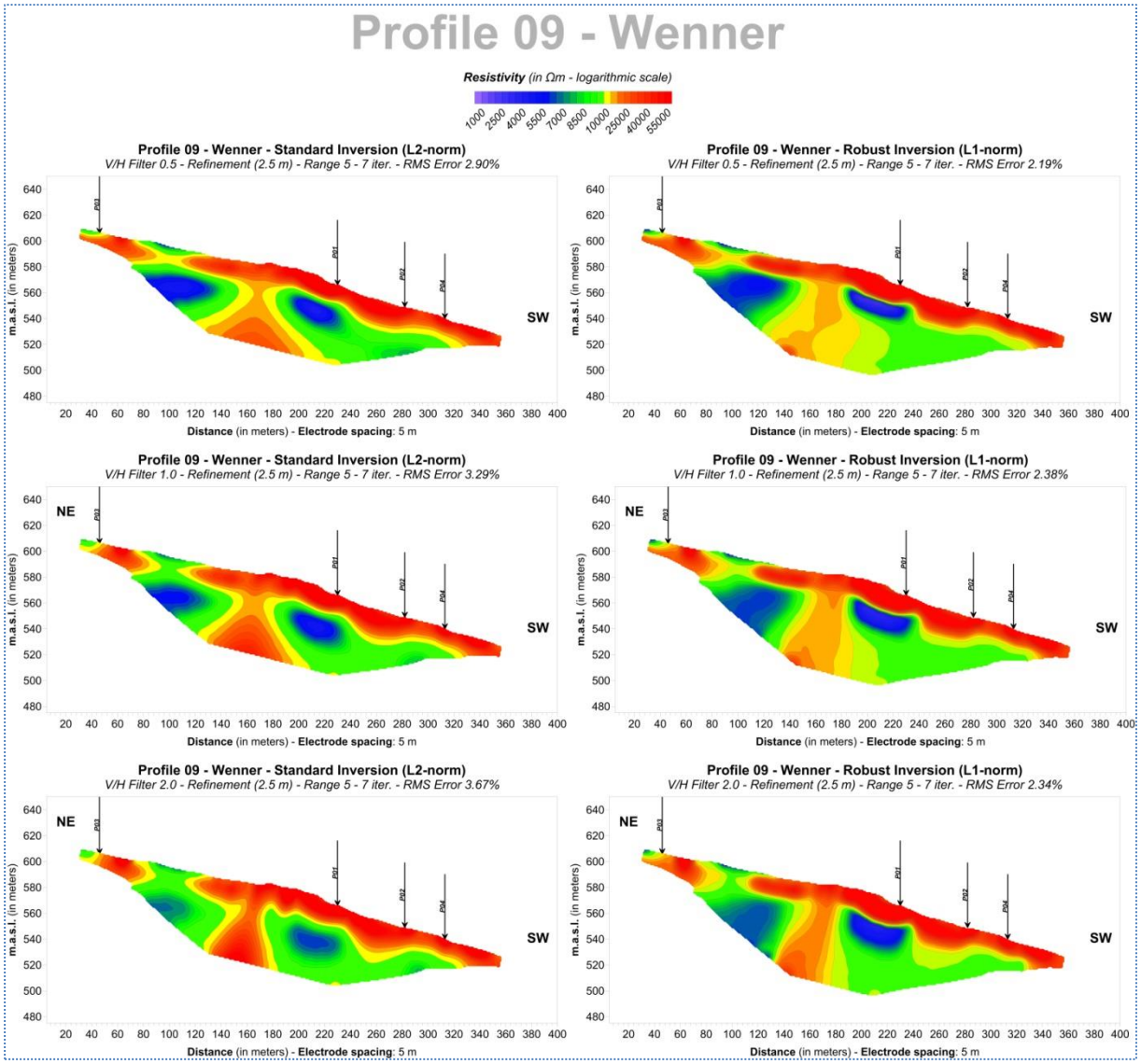

Figure 3.9.3: Reprocessing of **Profile 09** - **Wenner array** using various inversion schemes: Standard or L2-norm (Left) and Robust or L1-norm (Right) inversion with V/H filters equal to 0.5, 1.0 and 2.0 (from top to bottom).

Figure 3.9.3 shows that this high resistivity barrier at 160 meters is detectable regardless of inversion scheme used. However, when *Robust (L1-norm) inversion* is utilized, the widening in depth seen in *Standard (L2-norm) inversion* results is eliminated while the RMS errors are 1 % lower on average (2 % versus 3 %). The same setting for the aforementioned barrier is confirmed in **figures 3.9.4** and **3.9.5** where Dipole-Dipole and Mixed array results are shown. Higher V/H filters formulate it better in depth and push it to acquire a more vertical shape. Moreover, all inversion results show that it is framed by very low resistivities, which could be an artificial effect. The low-resistivity environment on either side of the barrier is beyond any doubt.

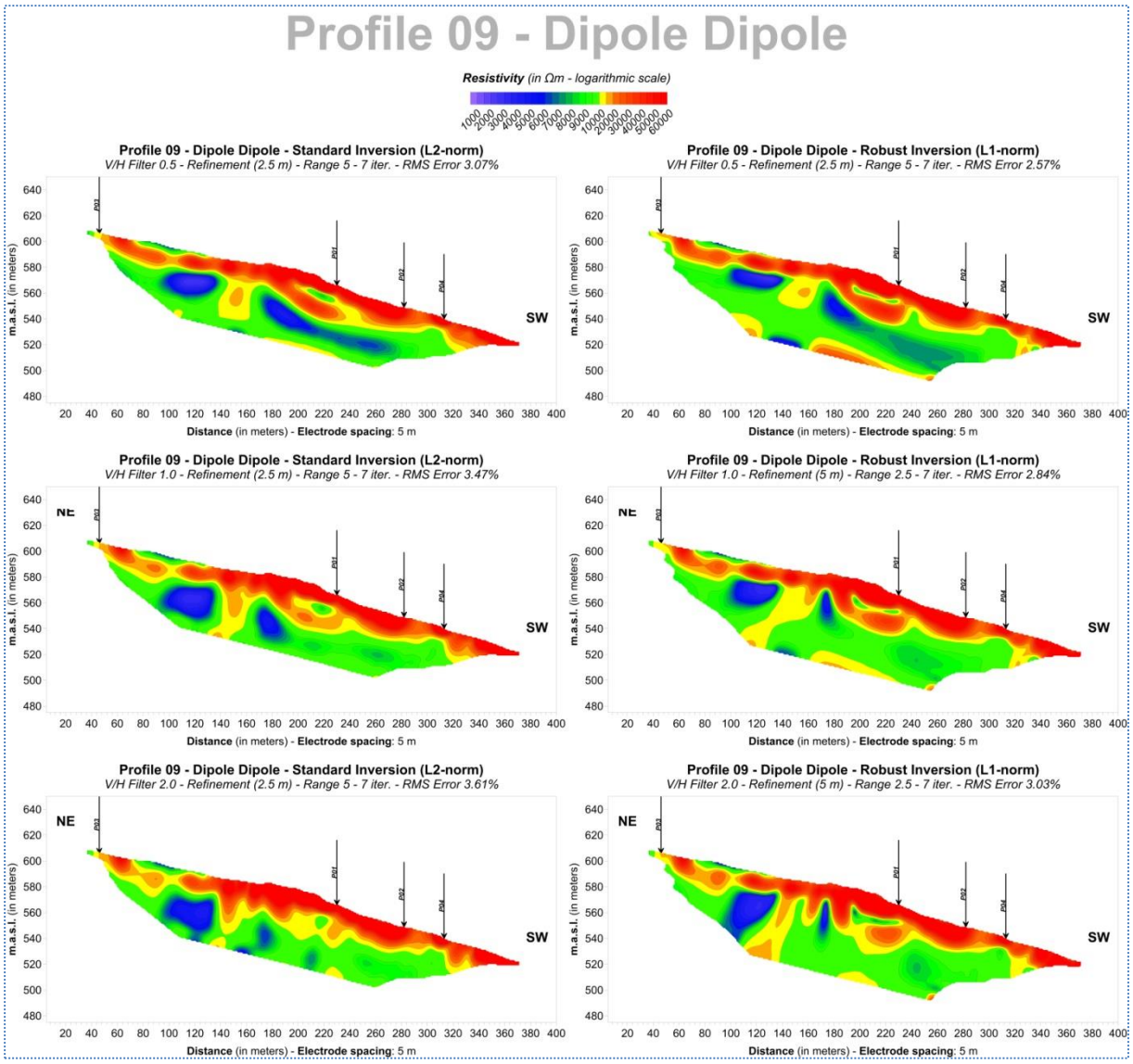

Figure 3.9.4: Reprocessing of **Profile 09** - **Dipole-Dipole array** using various inversion schemes: Standard or L2-norm (Left) and Robust or L1-norm (Right) inversion with V/H filters equal to 0.5, 1.0 and 2.0 (from top to bottom).

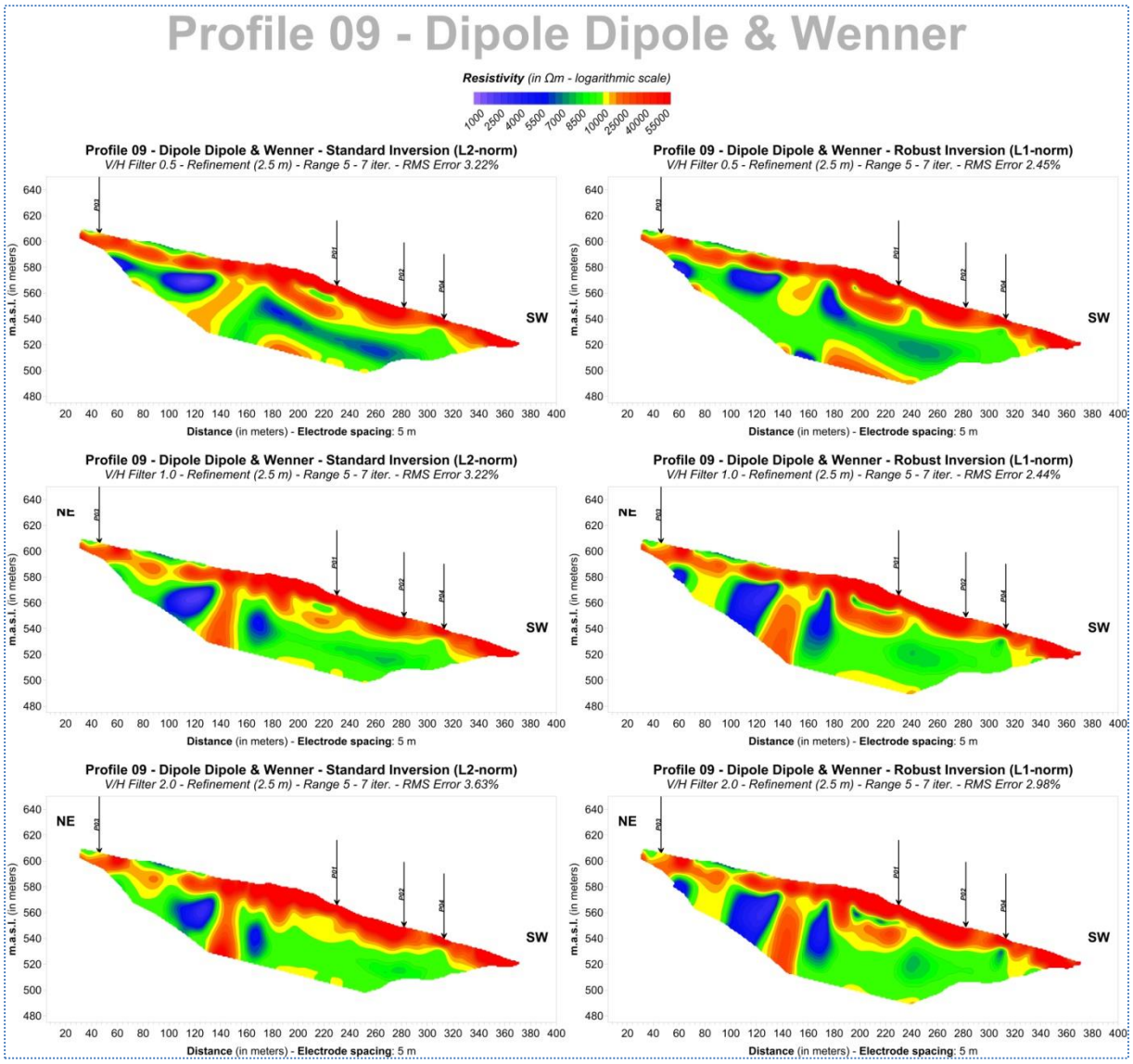

Figure 3.9.5: Reprocessing of **Profile 09** - **Mixed array** using various inversion schemes: Standard or L2-norm (Left) and Robust or L1-norm (Right) inversion with V/H filters equal to 0.5, 1.0 and 2.0 (from top to bottom).

3.10 ERT Profile 10

Figure 2.1 shows the position of Profile 10 which is a profile aligned at an almost pure North to South trend. This profile is the second one conducted in Åknes with a denser electrode spacing i.e. 5 m but unlike Profile 09, it is not matching any of the 10 m electrode spacing profiles. Its last 100 m is almost common with Profile 01, but the remaining length out of its 345 meters in total is deviating from that course. Borehole Bh-01-17 is accurately matching its course at 250 meters, a point where Profile 01, 04 and 10 all intersect each other.

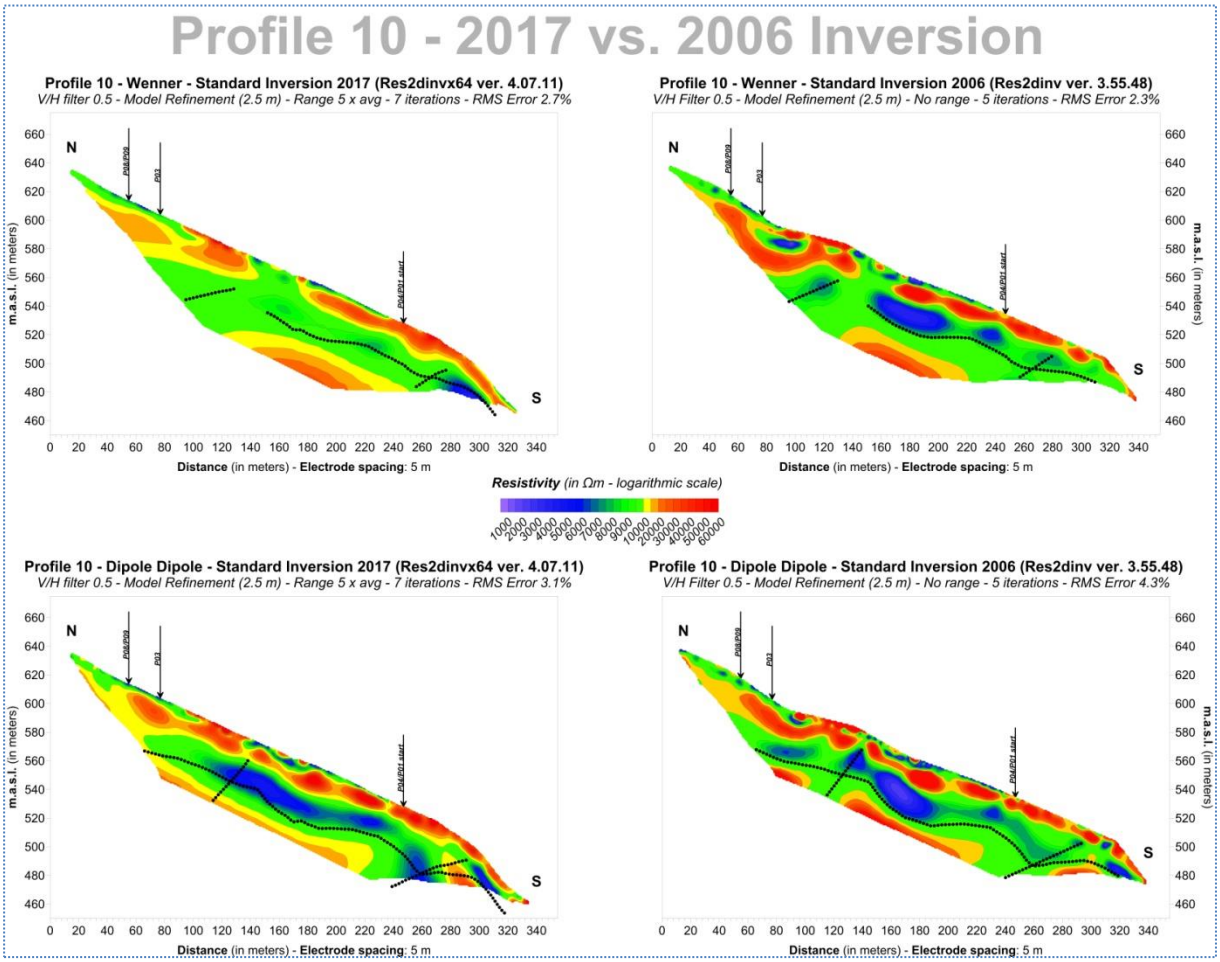

Figure 3.10.1: Wenner (top) and Dipole-Dipole (bottom) inversion results for **Profile 10** with the use of new (left) and old (right) Res2DInv versions. Black dotted lines represent interpretations based on the old results.

Figure 3.10.1 displays the same regime seen in Profile 09 i.e. smaller resistivity contrasts when new inversion is implemented compared to the old module and low-resistivity overall setting which is expanding throughout the profile length framed by a top and bottom high resistivity layer. Generally, high resistivities are higher in the inversion results from 2006, but the Dipole-Dipole outcomes appear to be more similar than the Wenner ones. Reprocessing of Wenner array yields higher values for the low-resistivity area which is not in good agreement with the Dipole-Dipole reprocessing result but matches the respective results for Profile 01 and 04 well. Finally, the old interpretations shown with black dotted lines are accurately matching the horizontal layering but we cannot say the same for the vertical structures.

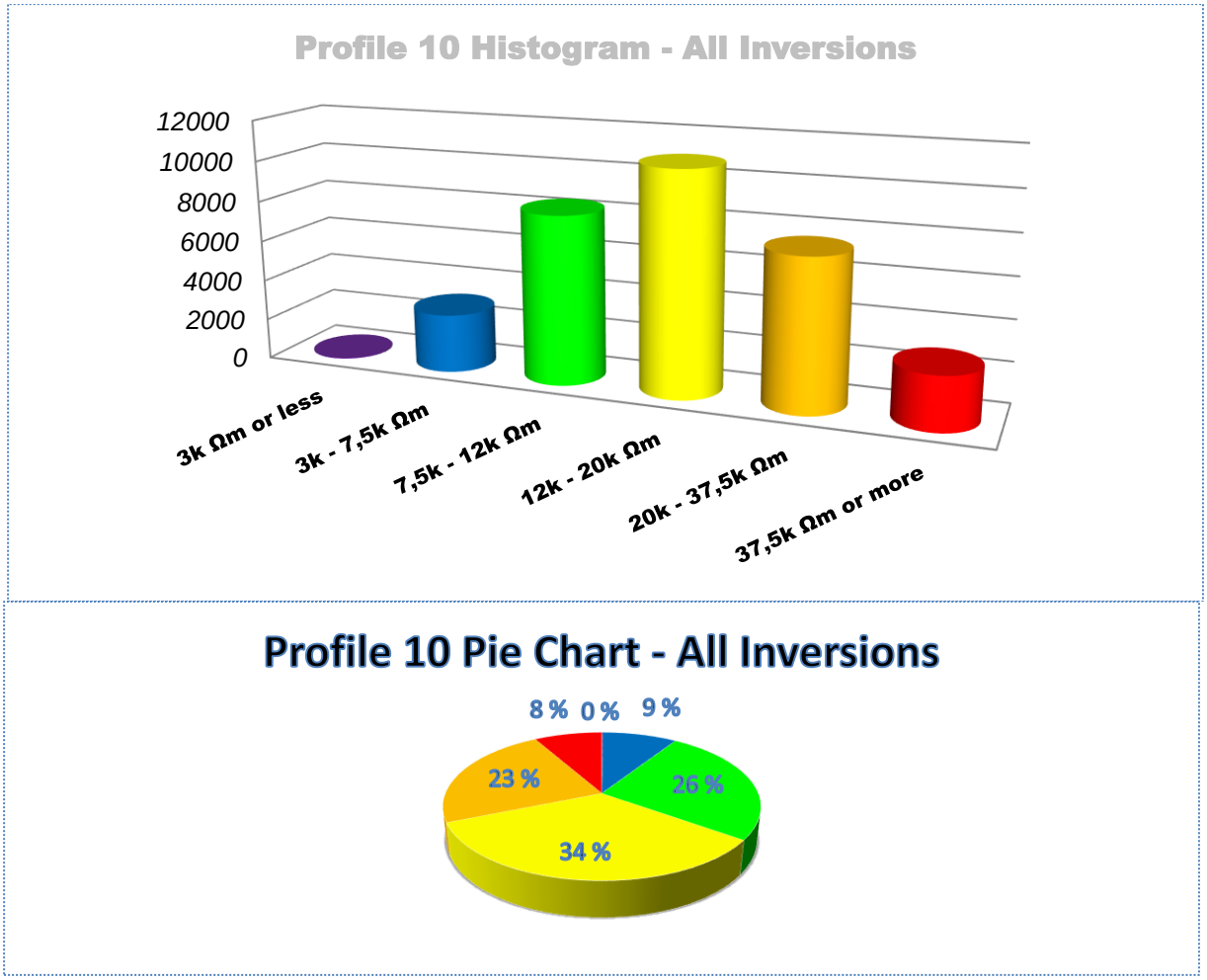

Figure 3.10.2: Top: Histogram depicting the statistical characteristics of all inversion results for **Profile 10**. Bottom: Pie chart depiction of the same data (custom rainbow $\log_{10}$ color scale).

Statistics for Profile 10 presented in **figure 3.10.2** are obtained after the implementation of six inversion schemes on 295 points for Wenner, 699 points for Dipole-Dipole and 994 points for Mixed array. The value distribution is only showing a slightly low-resistivity fraction increase (green – 26 % instead of 19 %) but also a big drop in drained fractured bedrock (red – 8 % instead of 27 %). The most dominant value group for Profile 10 when all inversions are taken into consideration is the varyingly healthy bedrock shown in yellow and orange colors.

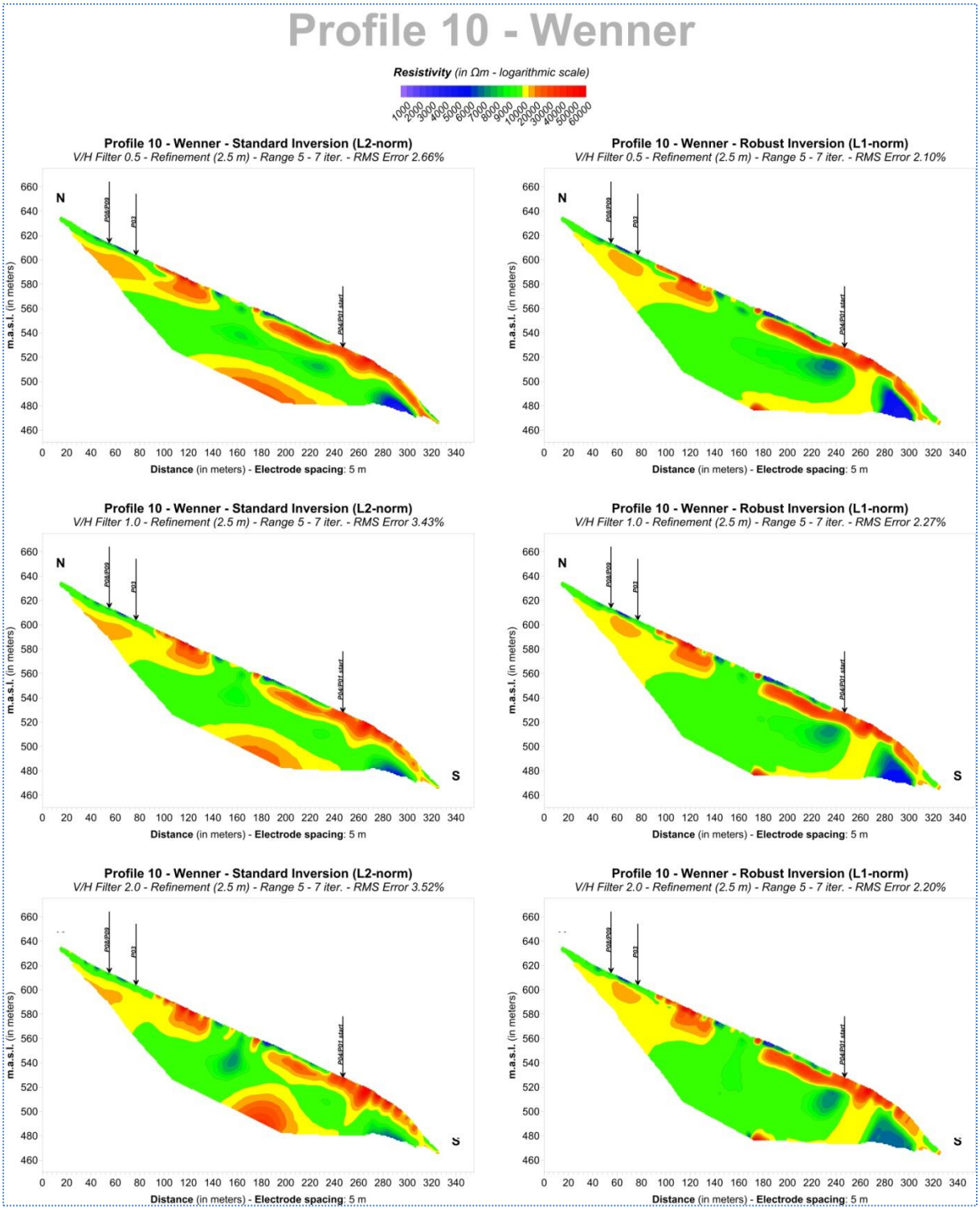

Figure 3.10.3: Reprocessing of **Profile 10** - **Wenner array** using various inversion schemes: Standard or L2-norm (Left) and Robust or L1-norm (Right) inversion with V/H filters equal to 0.5, 1.0 and 2.0 (from top to bottom).

Figure 3.10.3 showing the reprocessing results for Wenner does not offer much variation in information given. The profile is dominated by low-resistivity values and the change in relatively higher resistivities does not alter the obtained results. However, the highly resistive top layer representing drained fractured bedrock can be seen in the southern half of the profile with a thickness of about 10 meters.

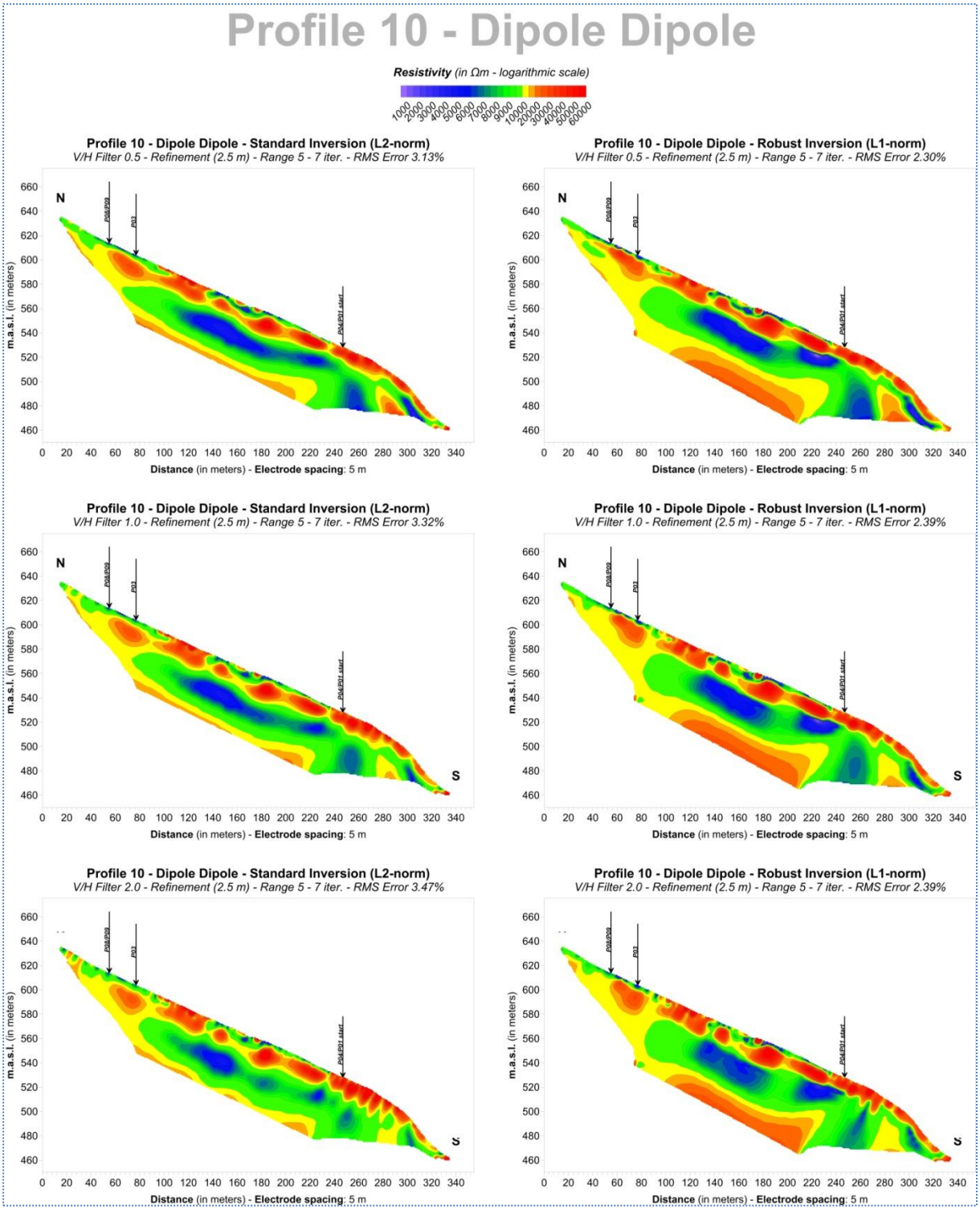

Figure 3.10.4: Reprocessing of **Profile 10** - **Dipole-Dipole array** using various inversion schemes: Standard or L2-norm (Left) and Robust or L1-norm (Right) inversion with V/H filters equal to 0.5, 1.0 and 2.0 (from top to bottom).

Figures 3.10.4 and **3.10.5** present more detailed images with a similar distribution of low versus high resistivities but with higher contrasts. Both Dipole-Dipole and Mixed array show a relatively homogeneous low-resistivity layer which is taking up almost the entire length and finishes at 260 meters where a fracture zone could be interpreted. This possible fracture zone may acquire several different shapes with the increase of V/H filters, but it remains apparent regardless of inversion scheme applied. Higher V/H

filters combined mainly with Standard inversion also split bedrock at 160 meters, but it is dubious whether a fracture zone could be there or not. Again, the top layer representing the drained fractured bedrock is still apparent but this time more continuous throughout the length of the profile with similar thickness to Wenner inversion result (10 meters).

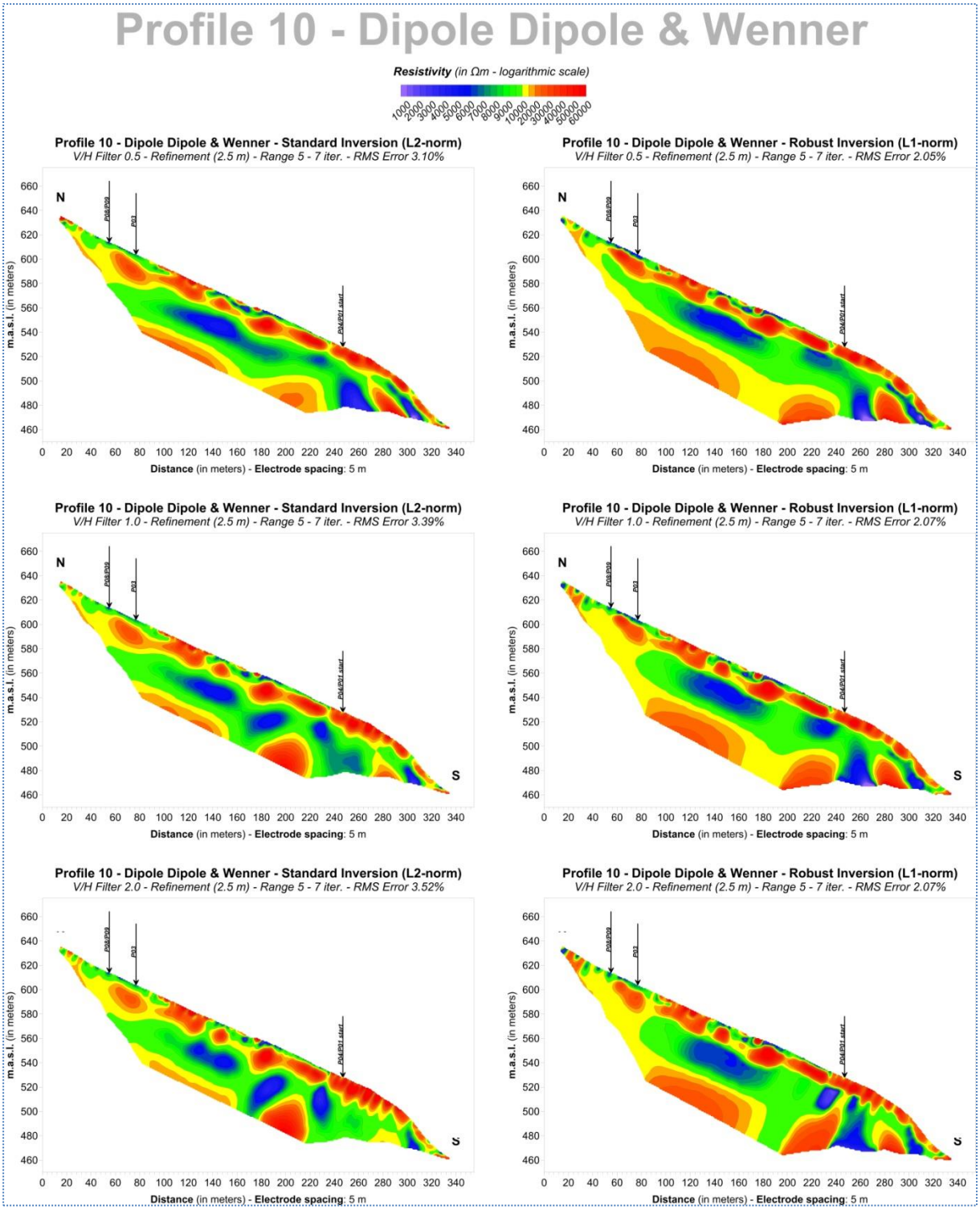

Figure 3.10.5: Reprocessing of **Profile 10** - **Mixed array** using various inversion schemes: Standard or L2-norm (Left) and Robust or L1-norm (Right) inversion with V/H filters equal to 0.5, 1.0 and 2.0 (from top to bottom).

3.11 ERT Profile 11

Profile 11 was conducted in 2017 by E. Dalsegg and its purpose was to better frame the survey area on its western flank. As can be seen in **figure 2.1**, Profile 11 is starting about 100 meters to the Southwest of Profile 02 and then follows a converging course until intersecting it at 215 meters (255 meters within Profile 02). From that point on, Profile 11 follows a rough North to South trend which gradually distances it from Profile 02 towards the West until the gap between them becomes 200 meters at the point where Profile 02 ends. The reason for this irregular profile pattern is due to the extreme topography in the area and the possibility of establishing a profile.

Like Profiles 01 and 02, which follow the same North-South trend, Profile 11 is characterized by equally steep topography (35^{o} inclination) which amounts to a projected length of 981 meters (121 electrodes with 10 m spacing). In addition to Wenner and Dipole-Dipole which were the standard arrays used in the old measurements, Profile 11 was also measured using Gradient Plus which has become the NGU guideline array in the years to follow the Åknes survey. In principle, the Gradient Plus array should be comparable to the Mixed array which represents the joint Wenner and Dipole-Dipole file. However, the Mixed array for this case will also include the Gradient Plus points rendering it the most populous point file in the whole survey. Finally, Profile 11 does not cross any boreholes along its path, but KH-08 and Bh-2 (see **figure 2.1**) can be found 15 and 35 meters, respectively to its East.

It is easily understood that no old inversion is done for Profile 11 therefore, we will be presenting the only processing results available for this profile obtained from Res2DInv version 4.07.11. **Figure 3.11.1** shows the statistics for the profile at hand which are directly comparable to those for Profile 01 and 02 and can help identify patterns along the East to Westtrend. The number of points included in this statistical analysis are 567 for Wenner, 1946 for Dipole-Dipole, 1572 for Gradient Plus and 4045 for Mixed array.

Profile 11 contains 63 % of relatively higher resistivities (yellow / orange) which is similar but also slightly higher than 59 % found for both Profile 02 and 01 to its East. Proportionally, the percentage for low to very low resistivity values is slightly lower for Profile 11 (24 %) as opposed to Profile 02 (26 %) and Profile 01 (29 %). However, the possible water-saturated and fractured bedrock percentage for Profile 11 presents a ratio which is more comparable to Profile 01 i.e. very low resistivities represent 9 % (10 % in Profile 01) of the grouping while the respective percentage for Profile 02 is 6 %. Finally, extremely high resistivities representing drained fractured bedrock consist 15 % of Profile 11 which is identical to Profile 02 (also 15 %) and higher than Profile 01 (11 %).

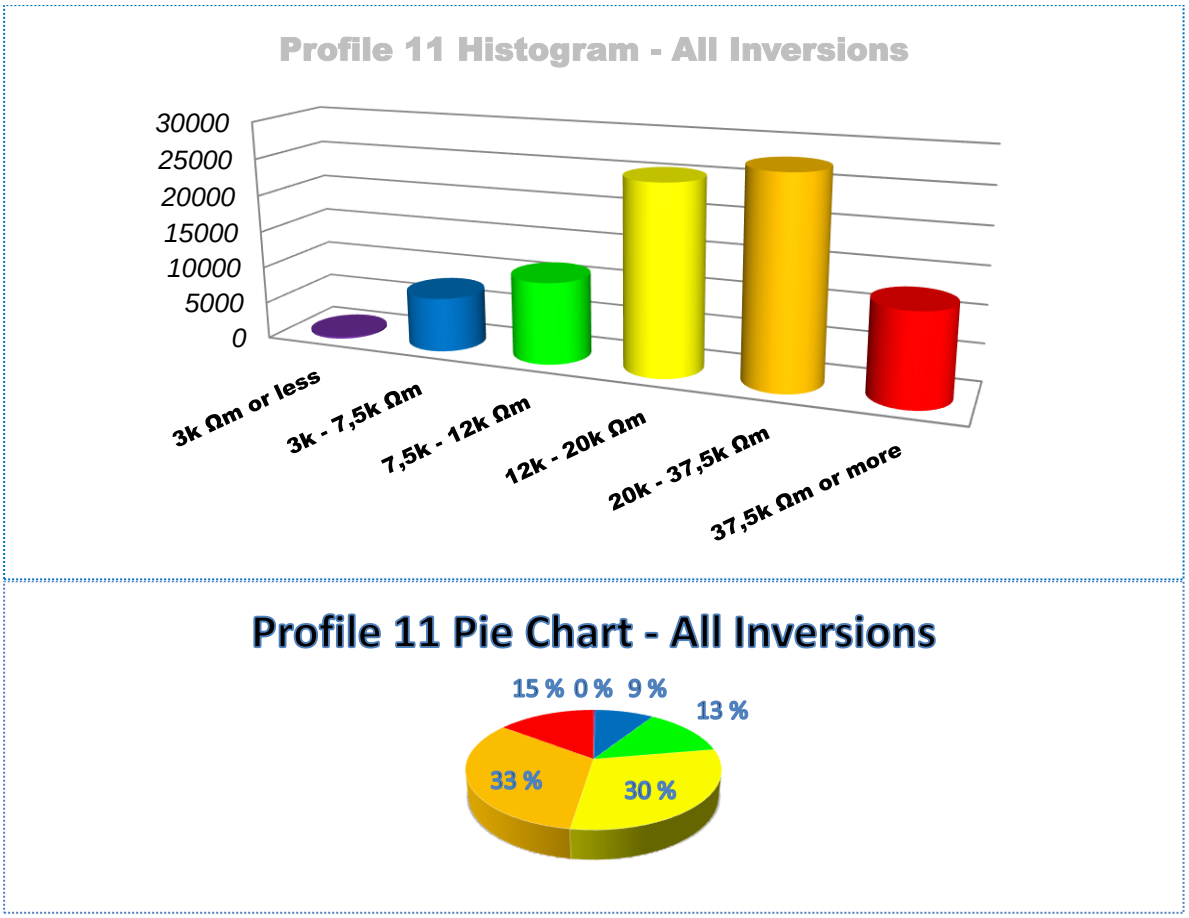

Figure 3.11.1: Top: Histogram depicting the statistical characteristics of all inversion results for **Profile 11**. Bottom: Pie chart depiction of the same data (custom rainbow $\log_{10}$ color scale).

Profile 11 processing results shown in all figures that follow, present a qualitative setting which is very similar to the one seen in Profile 01 and 02 i.e. an environment which is characterized by a gradual decrease of resistivity towards the fjord, a clear fracture zone indication below the superficial fracture and a generally less resistive bedrock in the middle of the profile with regard to its edges. Processing for Wenner and Gradient Plus arrays shown in **figures 3.11.2** and **3.11.4** respectively, present similar results which appear to be consistent regardless of inversion parameters used. All resulting profiles start off with a low-resistivity basin-shaped layer overlaying a highly resistive block which then turns into a possible fracture zone whose verticality is strengthened with the increase of the V/H filter value. This fracture zone appears to be framed by high resistive bodies (higher towards the north) but as we move southwards, bedrock resistivity drops down and a low-resistivity layer appears at about 500 meters distance. This layer becomes thicker the closer we get to the fjord but bedrock lying beneath it also increases in resistivity near the south end of the profile. RMS errors are comparable between *Standard* (L2-norm) and *Robust (L1-norm) inversion* for both Wenner and Gradient Plus, but when the latter is used, the percentages are roughly 1.5 % lower on average.

Figures 3.11.3 and **3.11.5** present the results for Dipole-Dipole and Mixed arrays and don't change the general geoelectrical regime that Wenner and Gradient Plus have established. The only major difference found in these results is the fact that below the back-scarp, the beginning of the low-resistivity layer is starting at an earlier stage i.e.

at around 400 meters distance. Dipole-Dipole array is detecting a possible fracture zone at about 650 meters which is vertical to topography but is not fully formulated. Naturally, higher V/H filters are accentuating the low-resistivity area and give it a higher contrast. However, the zone does not become unified even with the use of a V/H filter equal to 2.0 but remains subdivided into a dubious upper part and a clearer lower one. The effect is even weaker with Mixed array but in this case, the majority of points that consist it is not Dipole-Dipole anymore, therefore the influence of Wenner and Gradient Plus array points is possibly masking this feature. Nonetheless, the implementation of Robust inversion besides returning almost 2 % lower RMS errors, it still calculates a very low-resistivity concentration at the base of the profile at 600 meters. It should be noted though, that Profile 04 which is intersecting Profile 11 in the neighborhood of this point, indicates a strong low-resistivity presence which could lead interpretation towards positioning a possible fracture zone there.

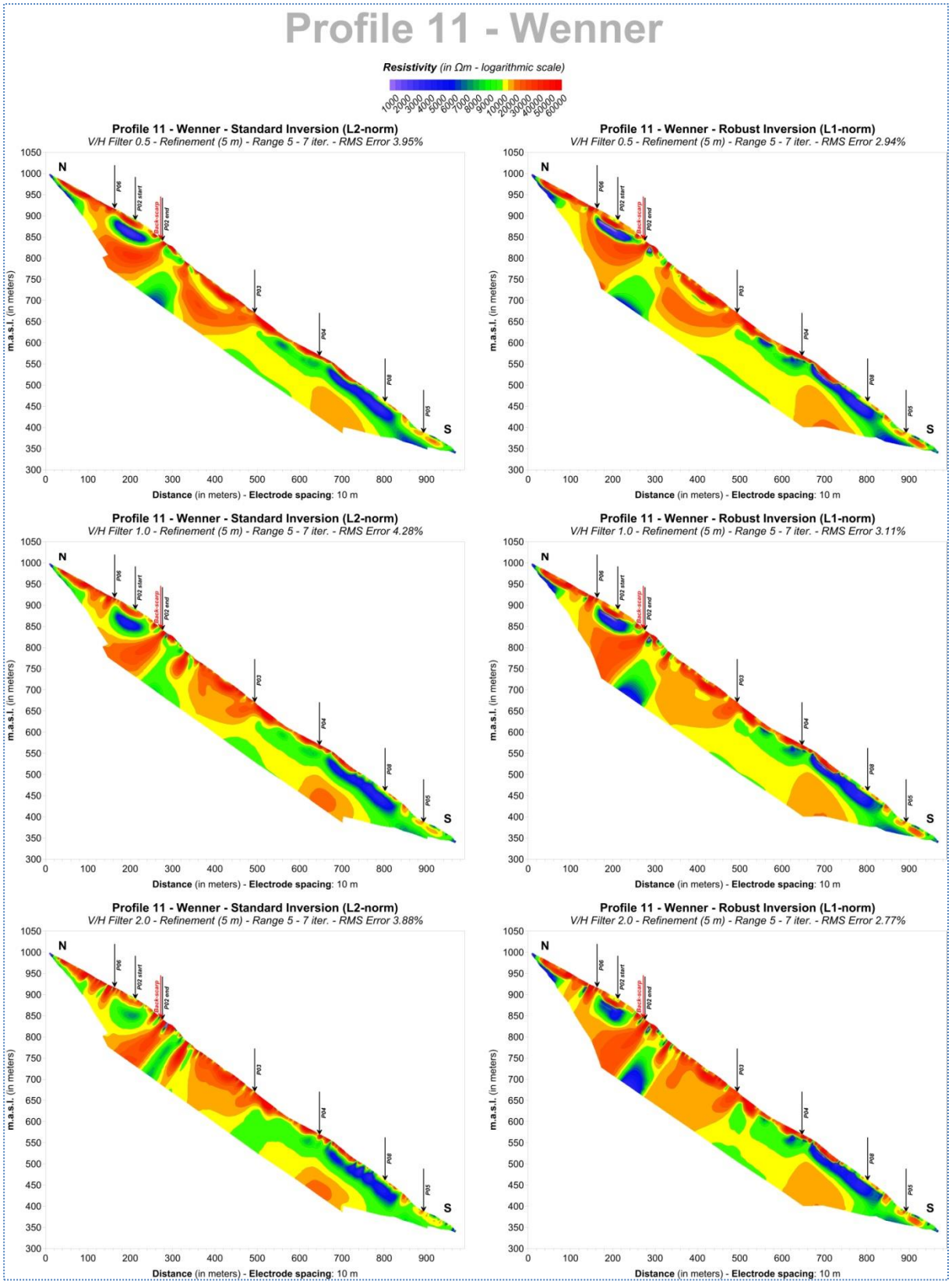

Figure 3.11.2: Processing of **Profile 11** - **Wenner array** using various inversion schemes: Standard or L2-norm (Left) and Robust or L1-norm (Right) inversion with V/H filters equal to 0.5, 1.0 and 2.0 (from top to bottom).

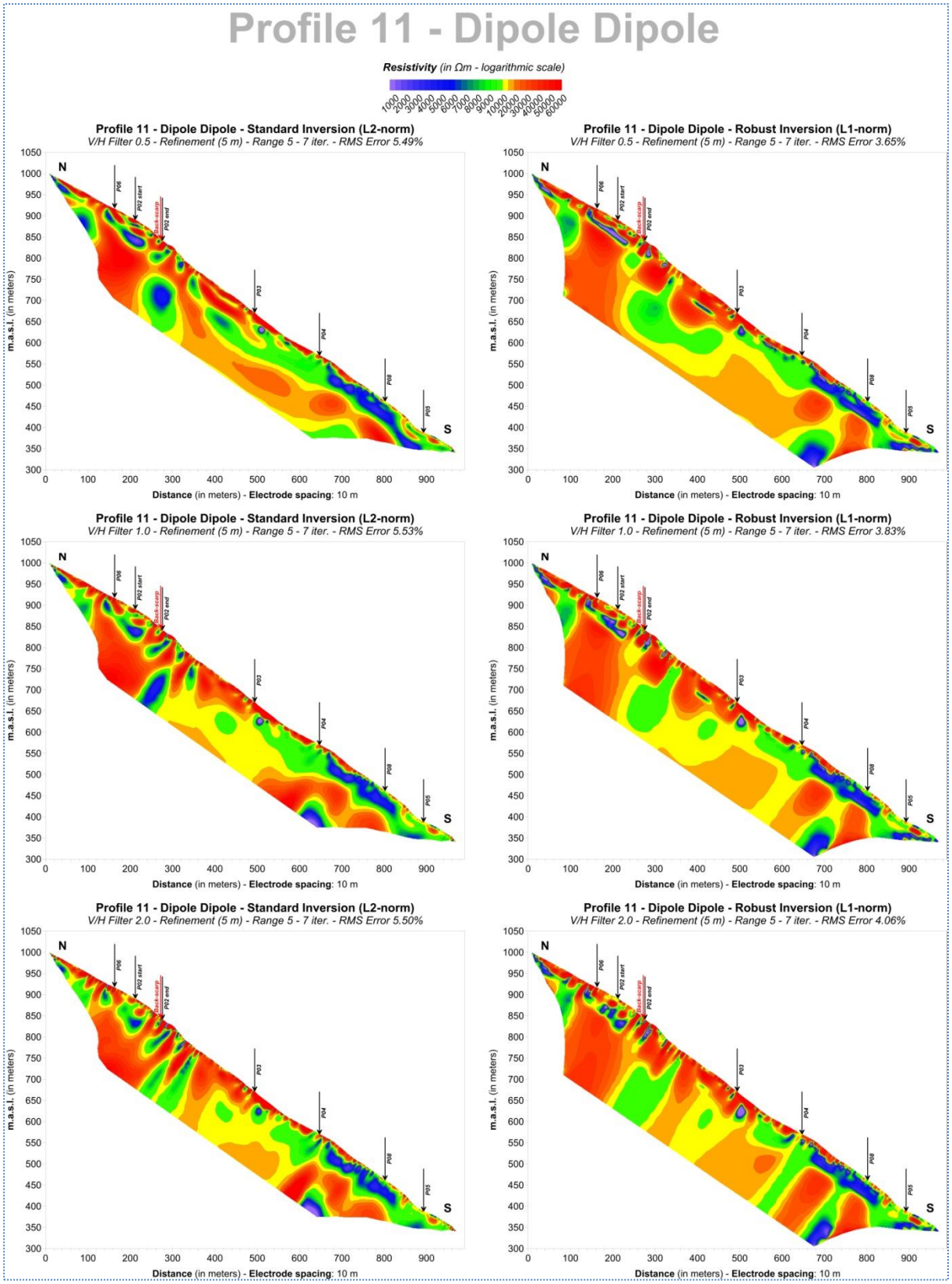

Figure 3.11.3: Processing of **Profile 11** - **Dipole-Dipole array** using various inversion schemes: Standard or L2-norm (Left) and Robust or L1-norm (Right) inversion with V/H filters equal to 0.5, 1.0 and 2.0 (from top to bottom).

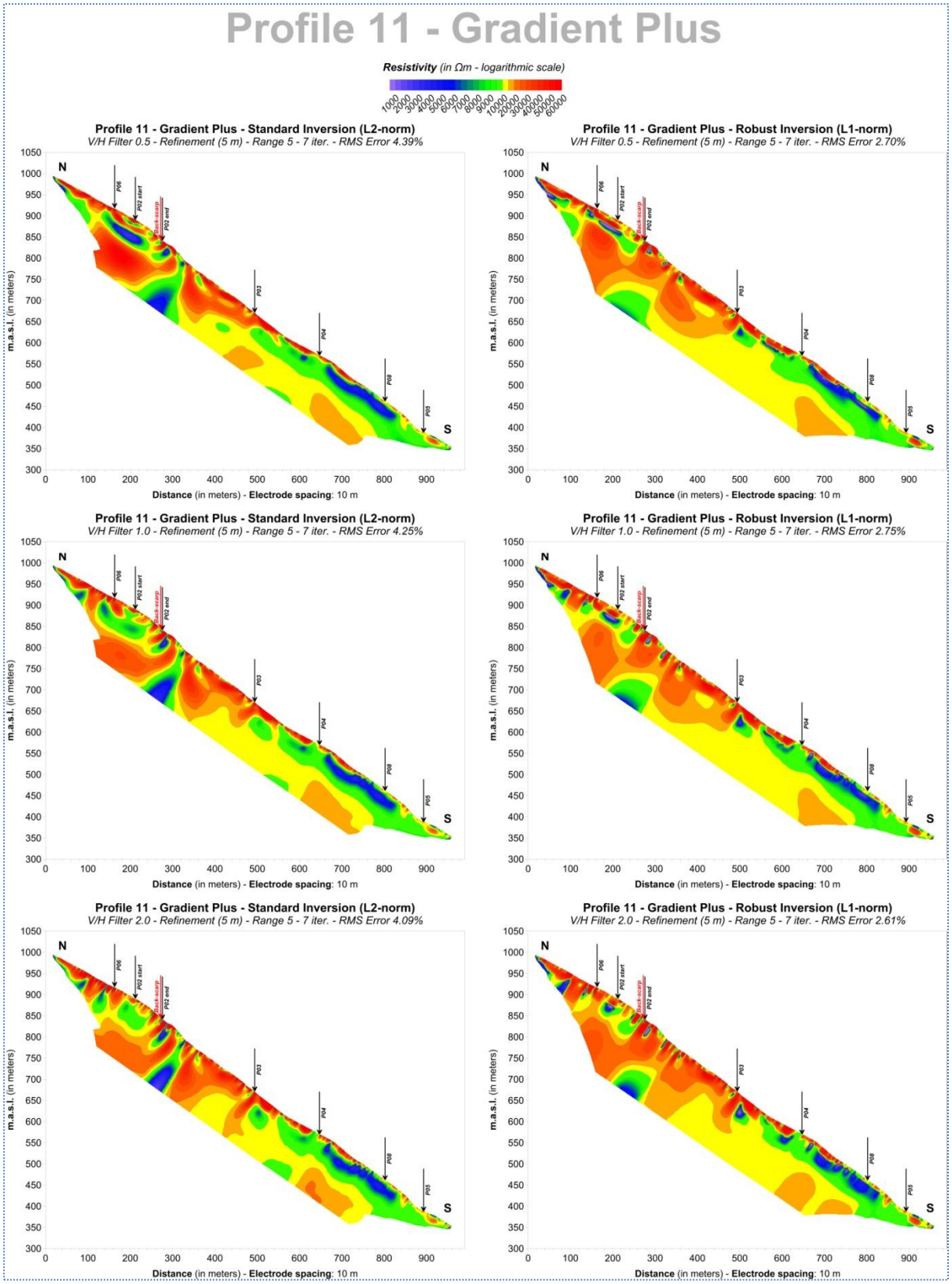

Figure 3.11.4: Processing of **Profile 11** - **Gradient Plus array** using various inversion schemes: Standard or L2-norm (Left) and Robust or L1-norm (Right) inversion with V/H filters equal to 0.5, 1.0 and 2.0 (from top to bottom).

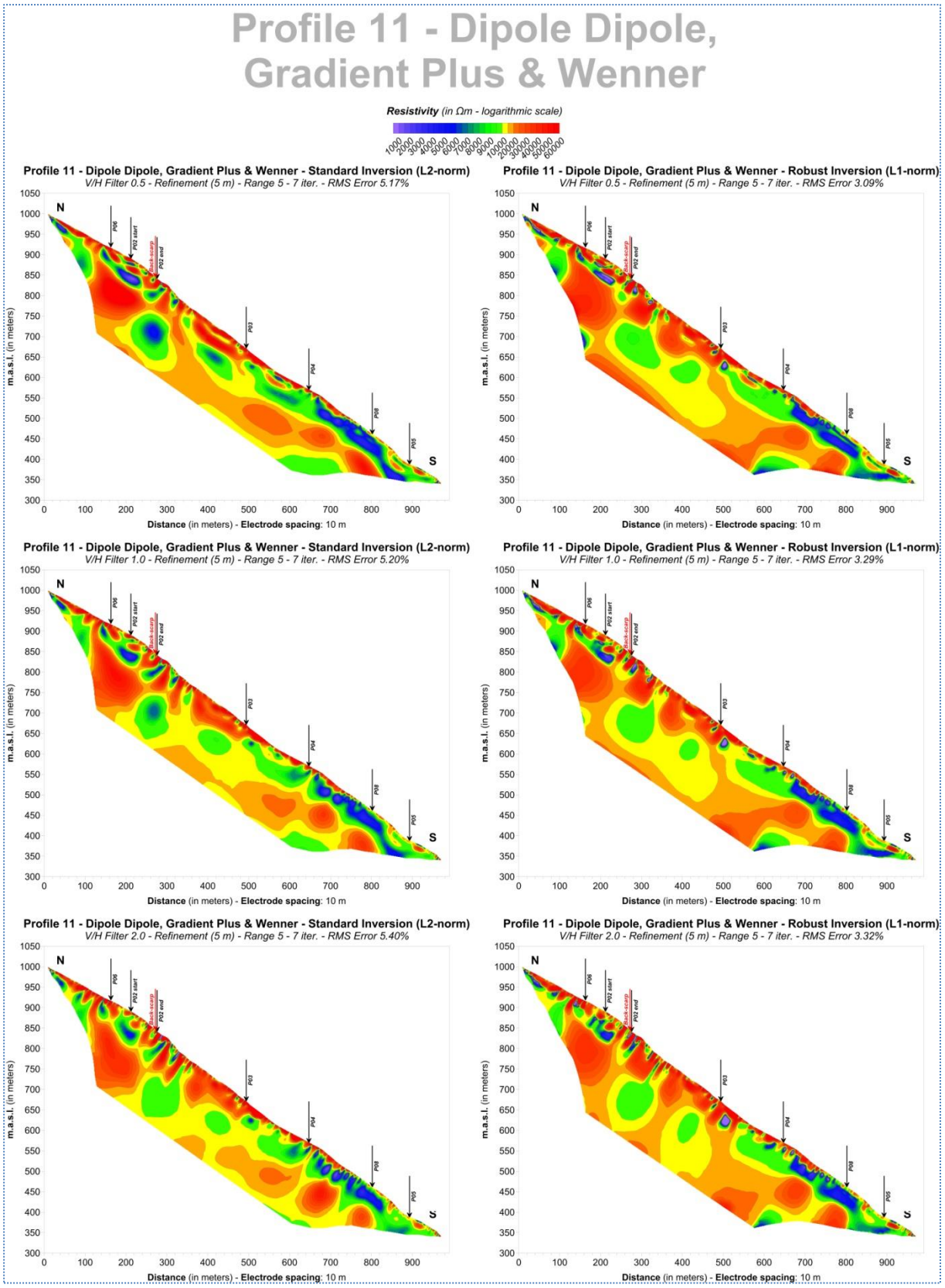

Figure 3.11.5: Processing of **Profile 11** - **Mixed array** using various inversion schemes: Standard or L2-norm (Left) and Robust or L1-norm (Right) inversion with V/H filters equal to 0.5, 1.0 and 2.0 (from top to bottom).

3.12 3D Presentation of Results

In the figures shown in the previous sections, crisscross points between profiles are marked with arrows but the reader must browse between pages to evaluate how good the match is. This can only give a generic impression of the pairing between profiles but when plotting in 3D space, this problem is redeemed. We have converted our reprocessing results into section grids readable by Geosoft Oasis Montaj software (version 9.3.2) and arranged them in 3D space and this is the best possible way for assessing the agreement between inversion results. **Figure 3.12.1** shows a view of the 3D cube containing all profiles. The profiles shown here are the ones for Mixed array inverted with *Standard inversion* (L2-norm) module and V/H filter equal to 0.5. Ideally, this demonstration can be exported in a 3D pdf file which the user can spin, revolve and zoom in and out to check every crisscross point and discern the agreement separately for each pair of profiles. In the printed version of this report though, we may only describe the general level of compatibility.

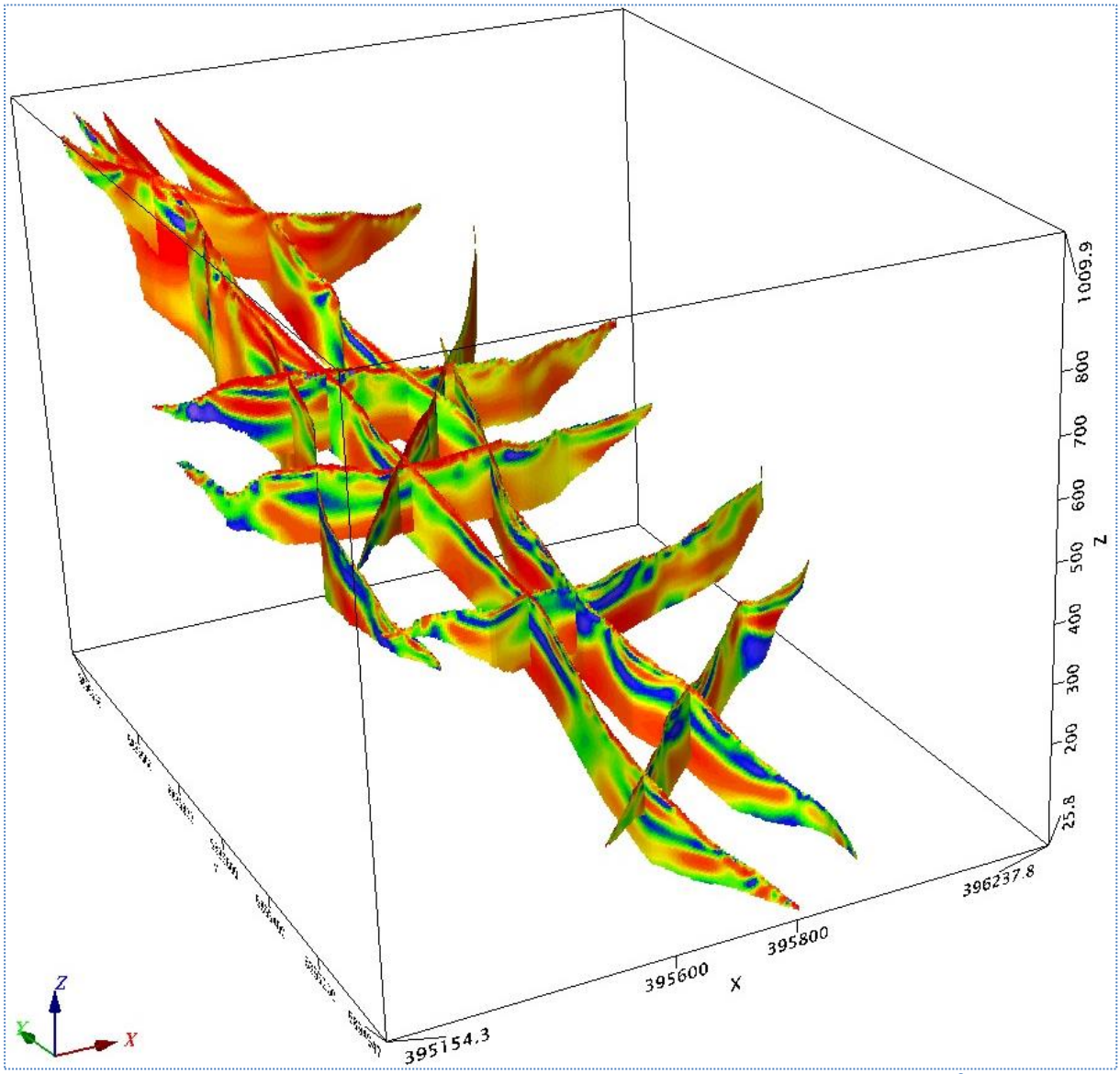

Figure 3.12.1: 3D presentation of the reprocessed ERT profiles from Åknes in Geosoft Oasis Montaj version 9.3.2. Coordinates in UTM zone 32 North and x, y, z axes in meters (View inclination: 24º, Azimuth: 30º).

Speaking from a qualitative standpoint, the reprocessing results present a very satisfying compatibility, i.e. relatively low-resistivity areas match with each other and relatively high-resistivity areas do too. Some profiles fit better than others but there's also areas where mismatch can be seen. This mismatch is due to two main points. First and foremost, the positioning is imperfect both in general terms and in relation with the electrode distribution within each profile. Besides that, anisotropy and 3D effects could also be a reason for observed discrepancy and essentially, mismatch is expected even with perfect positioning.

4. INTERPRETATION

A variety of interpretations has been presented in Rønning et al. (2006; 2007) which are based on the intuitive interpretation of horizontal layers on each 2D profile by E. Dalsegg except for Profile 11. A structural model of undulating unstable bedrock masses was then founded on these interpretations for the whole Åknes region (Ganerød et al. 2007, Ganerød 2008; Ganerød et al. 2008, Nøttveit et al. 2008) with projected thickness of 40 to 60 meters and high inhomogeneity. These old interpretations have been digitized, modified and incorporated in our results to be used for comparative reasons. In this report, we will be using a different qualitative approach for interpreting the unstable bedrock which will be based on the actual resistivity values obtained and the classification we have established. Additionally, possible fracture zones will also be delineated with the use of more favorable inversion schemes than the one used in 2006 and 2007 (*Standard* or L2-norm *inversion* with V/H filter = 0.5).

4.1 Statistics

For this interpretation, we will try to highlight changes in geoelectrical conditions by using profiles positioned in a row along the North-South and East-West direction and by plotting their statistics for each resistivity grouping the new color scale has. More specifically, we will be using Profiles 06, 03, 04, 05 and 07 along the North-South trend and Profiles 11, 02 and 01 along the West-East to identify possible resistivity patterns. **Figures 4.1.1** and **4.1.3** show the statistical results referring to the North-South and East-West direction respectively and **figures 4.1.2** and **4.1.4** a 3D view of some of the resulting profiles, upon which these interpretations were built (Mixed array - L2-norm - V/H filter = 0.5).

Figure 4.1.1 displays a quite clear pattern along the North-South trend. The distances shown at the bottom of the figure refer to mean distances between the profiles utilized along the slope and towards the fjord (the route of Profile 02 in approximation). The yellow, blue and red curves are supplementary (adding up to 100 % for every point) and describe the overall geoelectrical conditions if we decide to split the resistivity content in three parts i.e. 12,000 Ωm or less, 12,000 - 37,500 Ωm and 37,500 Ωm or more. The blue curve expresses the water-saturated fractured bedrock content variation and we can easily detect a clear increase of this percentage towards the southern part of the mountainside. This increase appears to be more rapid over the first 700 meters starting off at 3 % and rising to 33 % (30 % boost) over this distance but then it becomes relatively stabilized just over 35 % (37 and 35 % respectively). Subsequently, the percentages representing drained fractured and varyingly healthy bedrock present a decrease towards the South, with the area around 700 meters to

appear as an area where overall changes in the geoelectrical environment occur, shifting from rapidly decreasing resistivities in the northern half of the study area to more stable but generally less resistive environment near the fjord.

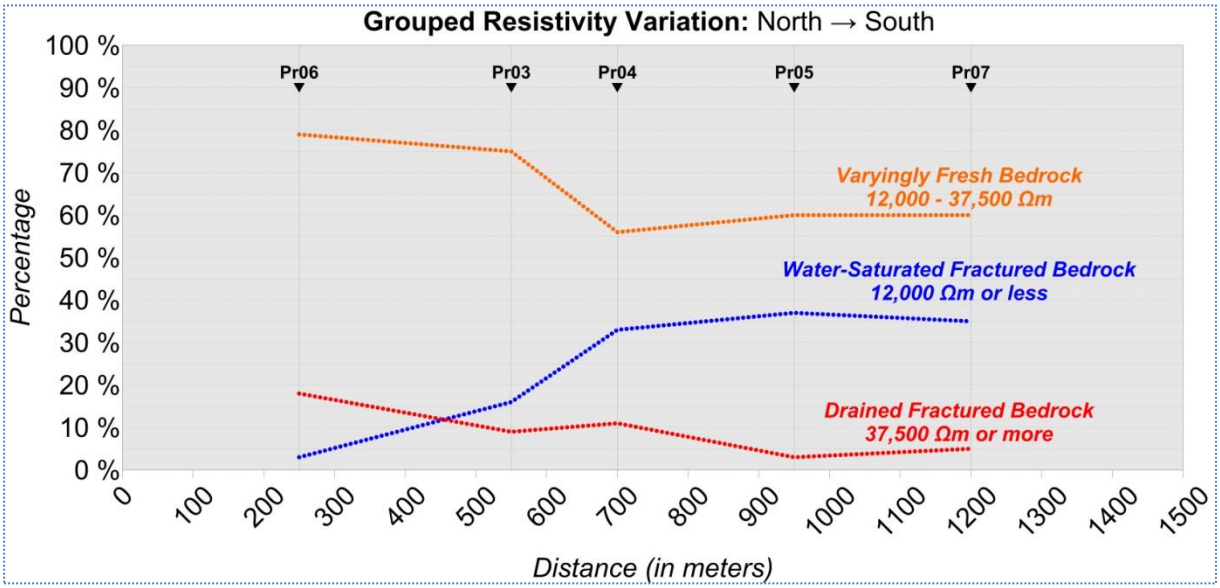

Figure 4.1.1: Variation in resistivity classes from North to South.

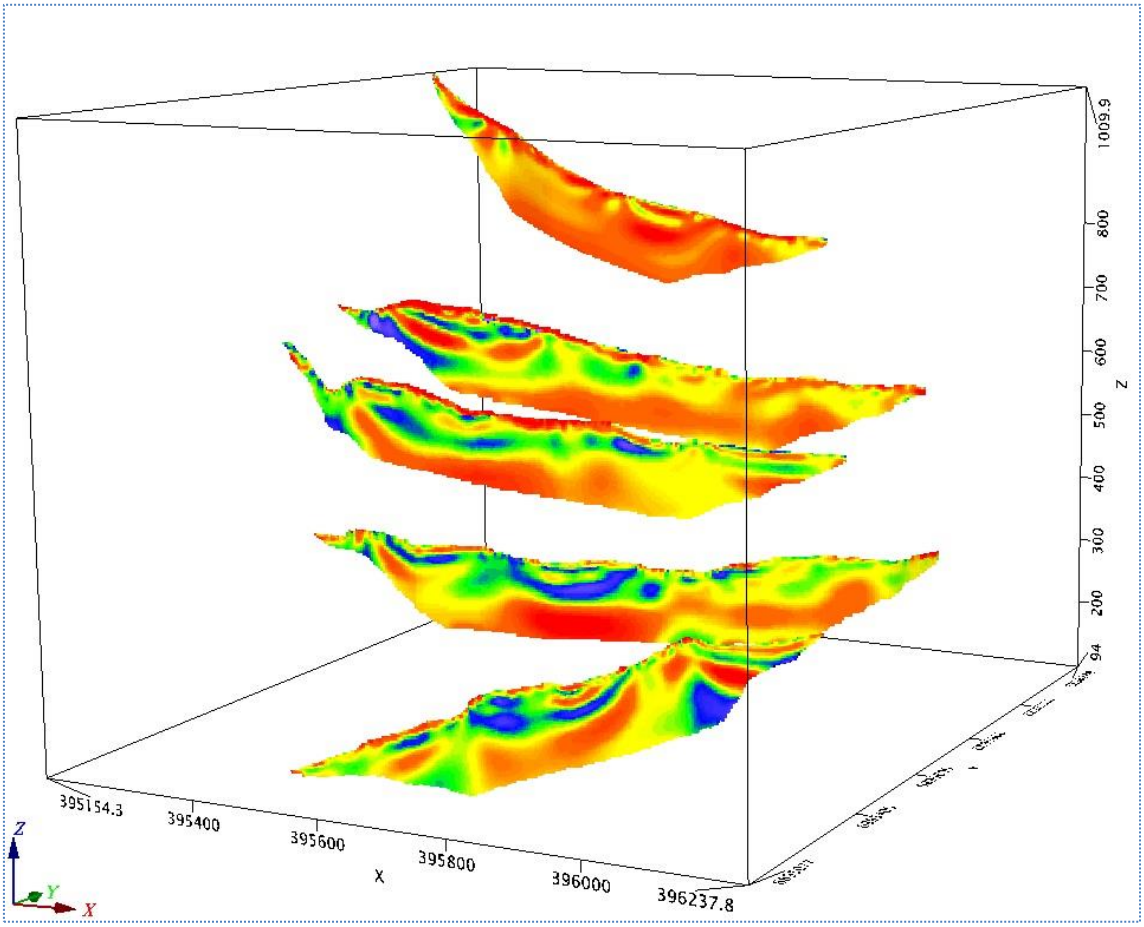

Figure 4.1.2: 3D view of Profiles 06, 03, 04, 05 and 07 from North to South (View inclination: 10º, Azimuth: 335º).

Figure 4.1.3 presents the same type of statistical interpretation but this time along the East-West trend over a distance of c. 300 meters. In this case, the regime appears to be more constant, but we can identify an increase in the percentage of water-saturated fractured bedrock (blue curve) towards the East which is slightly less than 10 % (from 20 to 30 % roughly). As expected, the percentages for varyingly healthy and drained fractured bedrock are dropping towards the East by 5 % each. Still, we need to remember that Profile 11 is not as long as Profiles 01 and 02.

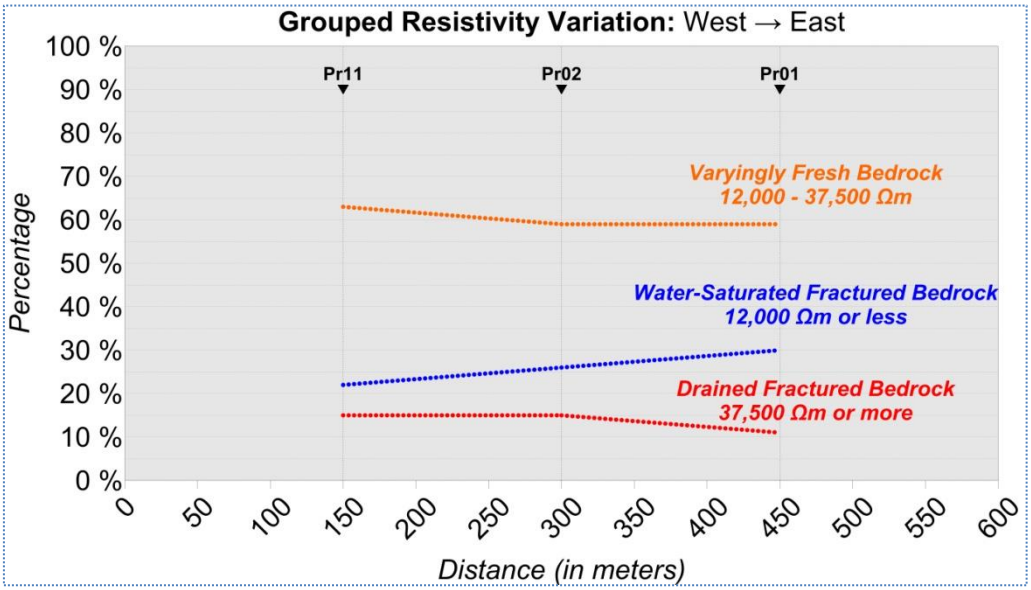

Figure 4.1.3: Variation in resistivity classes from West to East.

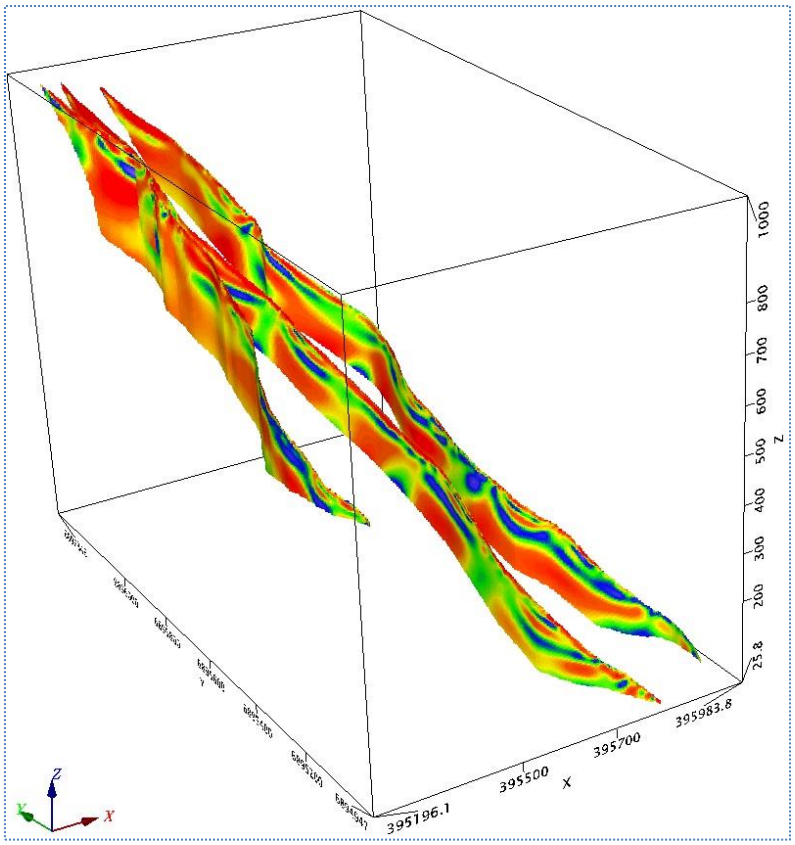

Figure 4.1.4: 3D view of Profiles 11, 02 and 01 from East to West (View inclination: 25º, Azimuth: 35º).

4.2 Water-Saturated vs. Drained Fractured Bedrock

In this section, we will present a quantitative interpretation for the unstable masses in Åknes based on the reprocessing results we have obtained from the use of the new Res2DInv inversion software. To do so, it was necessary to create point clouds which are denser than the inversion export product i.e. denser than half the electrode spacing. This was achieved by gridding all inverted resistivity values with a 1 m point spacing and then extracting these grids into simple text files containing these points. This does not increase the resolution but makes the resistivity sections more homogenous and easier to handle. Thus, the gridding procedure was done under full control from our part and the inversion results presented in previous sections can now be presented as point clouds or class post maps. By classed post maps we refer to the plotting of individual point values in 2D or 3D space as dots which are colored after the inverted resistivity value they carry. The word "class" is used since we are no longer displaying the reprocessing results in gradually changing colored contours but as single colored entities which represent a span of values. Therefore, we may classify the inversion results in a way that would highlight water-saturated or fractured bedrock but also accurately isolate unstable masses from healthier bedrock in a pure numerical way.

As already seen, we have elected 12,000 Ωm to be the highest possible resistivity that water-saturated fractured bedrock can have in Åknes while the unstable masses overlaying this layer are consisting of unreasonably high resistivities which mark heavily fractured bedrock which can be drained. It would also be useful to further classify the water-saturated bedrock by splitting it in two classes at 7,500 Ωm. Essentially, we have formed three classes that distinguish what we generally refer to as highly water-saturated fractured bedrock (7,500 Ωm or less) water-saturated fractured bedrock (7,500 - 12,000 Ωm) and extremely drained and fractured bedrock (37,500 Ωm or more). The lower resistivity limit for drained and extremely fractured bedrock was raised to 50,000 Ωm to focus on those extremely high resistivities found on the top layers of the majority of our inversion results. **Figures 4.2.1**, **4.2.2** and **4.2.3** present point clouds or classed post maps based on the aforementioned classification along with the old interpretations for demonstrative purposes.

Figure 4.2.1 shows classed posts for unstable masses and water-saturated areas along the North-South trend using Profiles 06, 03, 04, 05 and 07. We have chosen to present two different versions of results: one based on the Wenner array (favorable for horizontal structures) as was done in the old reports and another based on the Mixed array (most detailed). Both interpretations are based on *Standard* (L2-norm) *inversion* with V/H filter equal to 0.5 which is more favorable when horizontal layering is surveyed. The second interpretation is given to utilize the most populous inversion result in our possession i.e. the Mixed array which contains more data points and thus richer information than Wenner alone. Additionally, the Mixed array also contains Dipole-Dipole array points that can help inversion detect lateral inhomogeneities concluded for the unstable masses in the old reports. It should finally be noted that the interpretations incorporated in the Mixed array profiles are practically the old Dipole-Dipole ones. Since the majority of points contained in Mixed array is indeed Dipole-Dipole, these interpretations should match each other quite well.

We have established that there is an increasing volume of possible water-saturated fractured bedrock as we move southwards towards the fjord and this was supported

by the graph shown in **figure 4.1.1**. **Figure 4.1.2** validates this claim and indicates that unstable masses in the form of extremely highly resistive drained fractured bedrock are mainly found in the northern part of the study area. As far as the old interpretation goes, there is a good general agreement but the new inversion and the point cloud imaging method provides much more detailed results which highlight just how inhomogeneous this layer is. Bedrock masses prone to movement over the water-saturated fractured bedrock appear to be more abundant in the North and West than in the South and East where the water-saturated body is not overlain by such an extremely resistive top-layer. In any case, the morphology of the layers of interest are quite consistent regardless of array used. Water-saturated fractured bedrock is commonly framed by drained fractured bedrock above and varyingly healthy bedrock below. Its thickness can reach 60 meters, as calculated in the old reports, while the extremely resistive top-layer can reach a depth of maximum 20 meters from the surface even though drilling has shown that it can exceed such thickness.

Figure 4.2.2 presents the classed post expressions for Profiles 11, 02 and 01 along the West-East trend in the exact same manner as in **figure 4.2.1**. Statistics along this trend presented in **figure 4.1.3** have revealed a slight increase in water-saturated fractured bedrock towards the East but this is not easily discernible in **figure 4.2.1**. However, what can be seen in the figure is a quite detailed distribution of water saturated fractured bedrock possibly unstable masses over water-saturated unfractured bedrock, as well as some possible fracture zones which are going to be investigated in the following section. Again, Wenner seems to be producing more fragmented and arch-shaped low-resistivity concentrations whereas the point cloud from the Mixed array results is more condensed. The dimensions of the water-saturated fractured bedrock are comparable to what we've seen along the North-South direction and the highly resistive top-layer is still apparent throughout all three profiles. However, extremely high resistivity concentrations can also be found in depth in several localities and not only superficially. Those calculation can be attributed to inversion algorithms and we do not consider them as drained fractured bedrock in depth where the reliability of inverted resistivity is lesser. However, their presence affects the statistical interpretation presented in **figure 4.1.3** and increases the possible unstable mass percentage. **Figure 4.2.2** on the other hand, clearly **shows that drained fractured bedrock is more voluminous at the northern and western parts of the study area.**

Figure 4.2.3 concludes the presentation of the remaining classed post interpretations i.e. for Profiles 08 (10 m electrode spacing), 09 and 10 (5 m electrode spacing). An interesting feature here is related to the fact that profile 09 is investigating a fraction of the Profile 08 with a 5 m electrode spacing. Wenner array shows a fragmented low-resistivity layer and this is verified in both Wenner and Mixed inversion results for Profile 09. Mixed array on the other hand, doesn't detect this high resistivity barrier and shows the unstable bedrock uninterrupted. However, all Profile 08 and 09 results calculate a consistent 30 m thickness for water-saturated fractured and a 15 m resistive overburden on top of it (drained bedrock). Lastly, similar are the results for Profile 10 which is neighboring to the two aforementioned ones.

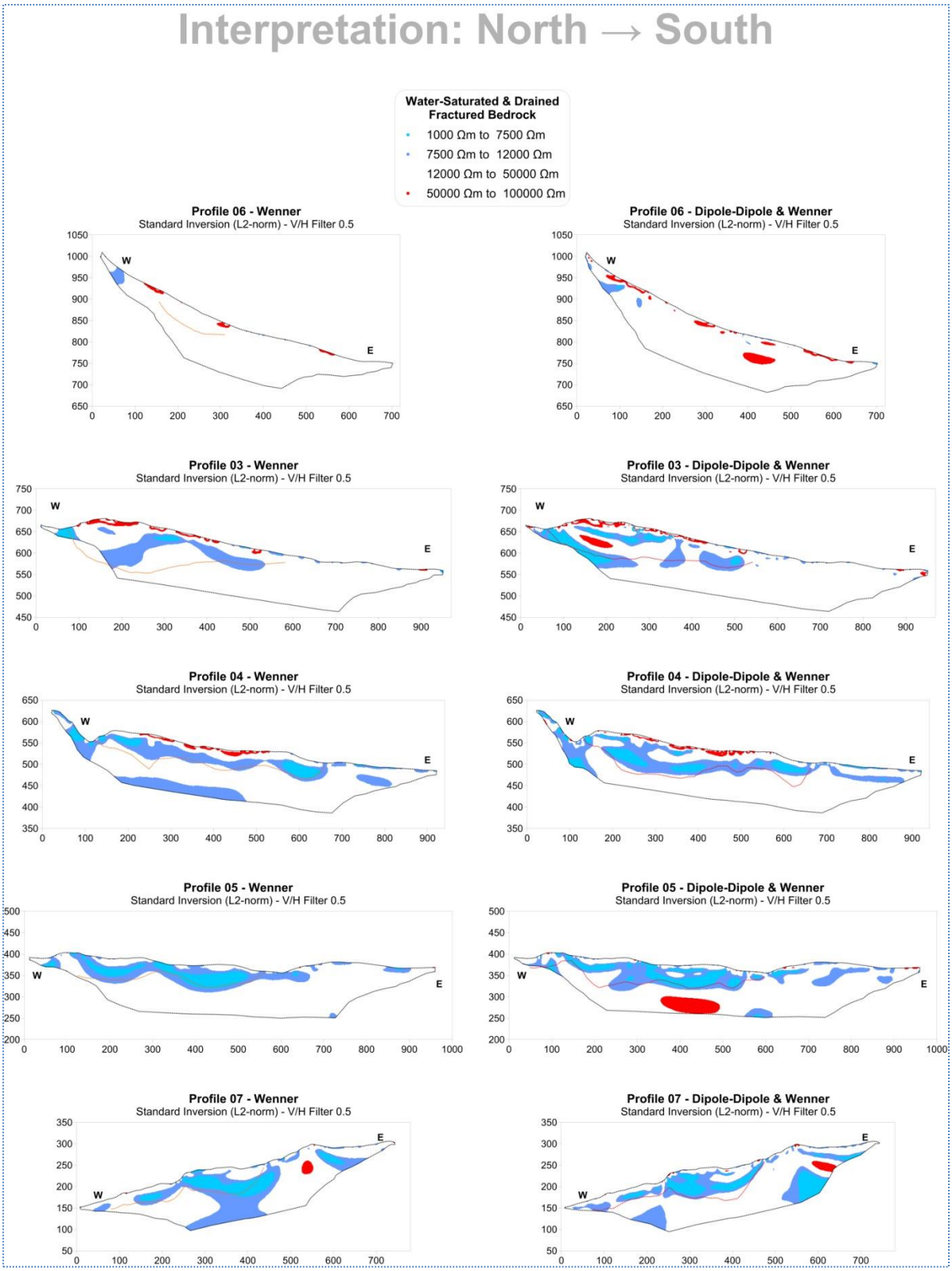

Figure 4.2.1: Point cloud or classed post map representing possible water-saturated (blue and cyan) and drained (red) fractured bedrock along the North-South trending profiles based on results obtained with Standard inversion and V/H filter equal to 0.5 for Wenner (left) and Mixed (right) array. Orange and red dotted lines represent old interpretations made on Wenner and Dipole-Dipole arrays respectively (Rønning et al. 2006; Rønning et al. 2007).

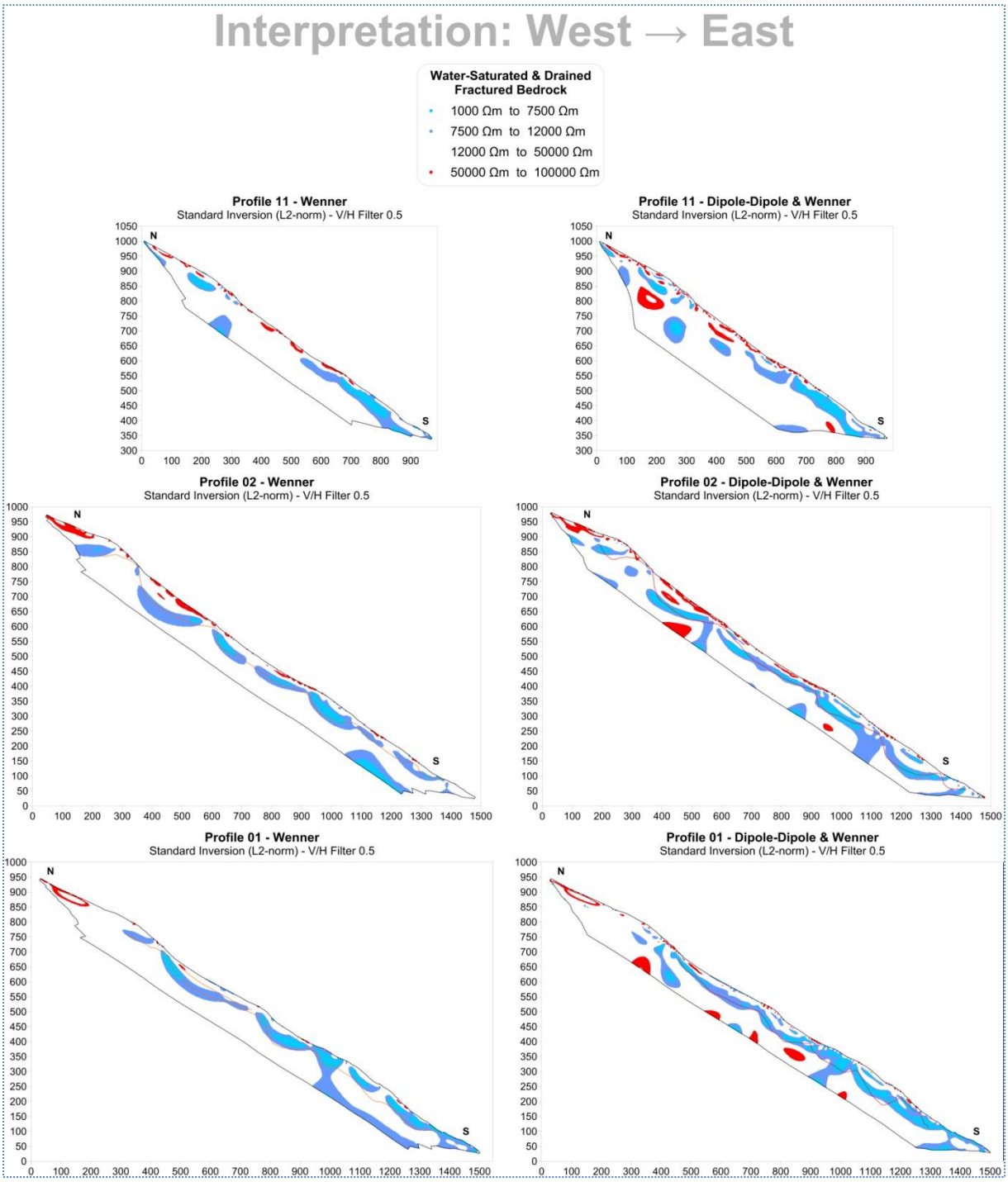

Figure 4.2.2: Point cloud or classed post map representing possible water-saturated (blue and cyan) and drained (red) fractured bedrock along the West-East trending profiles based on results obtained with Standard inversion and V/H filter equal to 0.5 for Wenner (left) and Mixed (right) array. Orange and red dotted lines represent old interpretations made on Wenner and Dipole-Dipole arrays respectively (Rønning et al. 2006; Rønning et al. 2007).

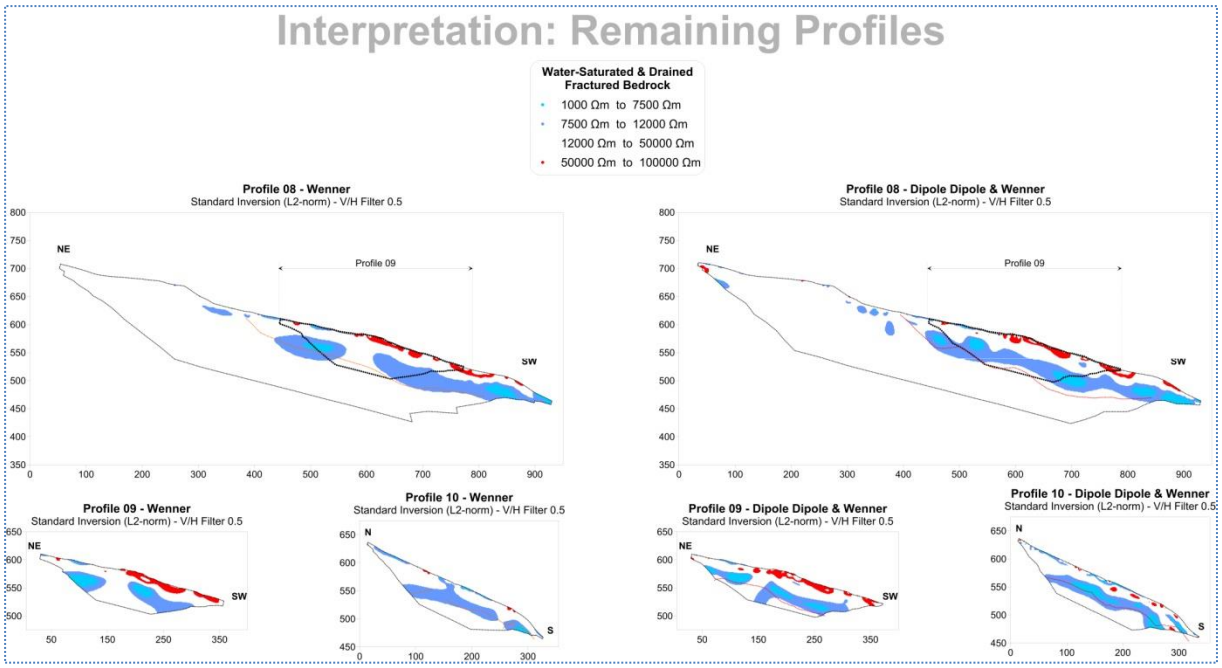

Figure 4.2.3: Point cloud or classed post map representing possible water-saturated (blue and cyan) and drained (red) fractured bedrock along the remaining Profiles 08, 09 and 10 based on results obtained with Standard inversion and V/H filter equal to 0.5 for Wenner (left) and Mixed (right) array. Orange and red dotted lines represent old interpretations made on Wenner and Dipole-Dipole arrays respectively (Rønning et al. 2006; Rønning et al. 2007).

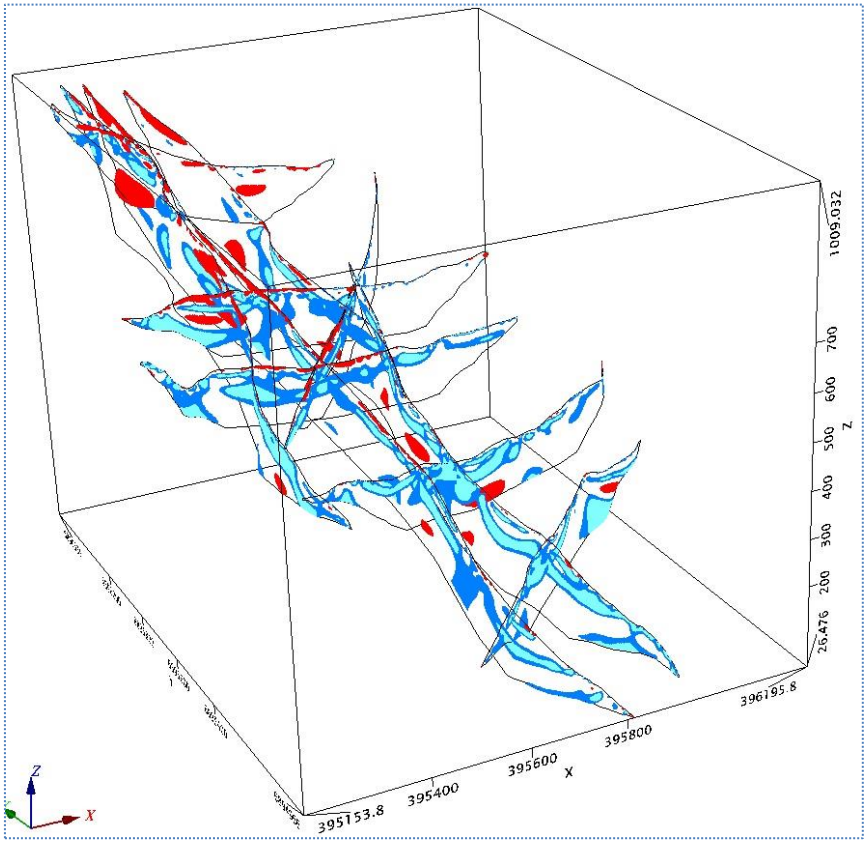

Figure 4.2.4: 3D presentation of all point cloud or classed post interpretations for possible water-saturated (blue and cyan) and drained (red) fractured bedrock - Mixed array (View inclination: 24º, Azimuth: 30º).

Figure 4.2.4 displays a 3D view of all the classed post interpretations based on the Mixed array combined in georeferenced cube. These interpretations match each other very well, and by arranging them in 3D space, it is made possible to get a general idea of the distribution of water-saturated fractured bedrock in Åknes as a whole.

4.3 Possible Fracture Zones

In this section, we will be interpreting lateral variations intuitively (vertical structures) based on favorable ERT reprocessing results. By favorable results, we are referring to the ones obtained with the use of both *Standard* and *Robust inversion* for V/H filters greater than 0.5. This interpretation is established on the notion that the most probable fracture zones should be at least present in some capacity in the majority of inversion results. It is expected that higher V/H filter values would further highlight zones or make vertical structures manifest in new places, but we will only be focusing on those features that can be traced even when inversion schemes are less advantageous for such interpretations. Nonetheless, our efforts will be focalized on the Dipole-Dipole and Mixed array results since Wenner is insensitive to vertical structures by default.

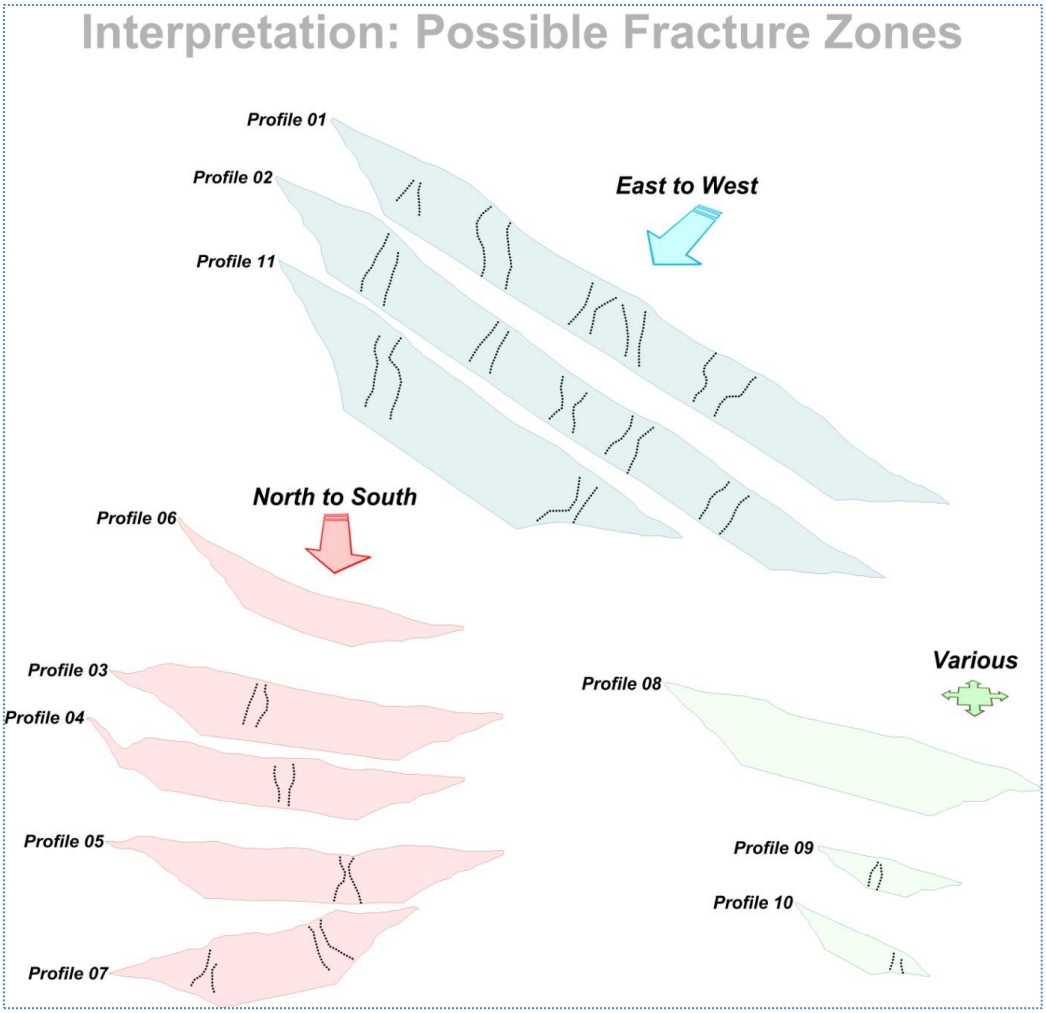

Figure 4.3.1: Interpreted fracture zones along profiles marked with black dotted lines and arranged according to East-West (top), North-South (bottom left) and remaining various (bottom right) directions.

All vertical low-resistivity concentrations in relation with their surroundings (resistivity contrast > 30 %, possibly fractured zones) are shown collectively in a pseudo-3D format in **figure 4.3.1**. It should be noted that not all possible fracture zones were extracted from the same array or inversion scheme. Essentially, all Dipole-Dipole and Mixed array results were examined for both Standard and Robust inversion but for V/H filters equal to 1.0 and 2.0 (0.5 was not taken into consideration). Interpretations are presented using the same outlook as before i.e. along the East-West, North-South and all remaining directions to identify systematic zone appearances. In this way, we may conclude that possible fracture zones in Åknes can vary both in width and shape but the average width for these structures ranges between 20-50 meters.

Another meaningful way of presenting fracture zone interpretations especially when trying to correlate interpretations is by projecting their limits to the surface and then plotting them in maps such as the one shown in **figure 4.3.2**. In a case like the one where five fracture zones are marked both in Profile 01 and 02, correlation is self-evident since we are talking about profiles comparable in length and almost parallel to each other. But in the case of Profile 11 which contains two possible fracture zones located at the beginning and end of the profile, identification of any possible correlation requires the projection of the locations of these zones on a map. **Figure 4.3.2** shows that the first vertical structure marked in Profile 11, is in fact representing the back-scarp mentioned in previous paragraphs and can be correlated to the first possible fracture zones registered in Profiles 01 and 02 which are also matching the back-scarp's general direction.

As we move southwards, the interpreted fracture zones that are marked second, third, fourth and fifth in both Profile 01 and 02 seem to all be in line indicating a possible sub-parallel fracture system oriented along the East-West direction. The third weak zone marked in Profile 11 could be correlated with either the third or fourth vertical structure marked in Profiles 01 and 02. However, things become very interesting when the interpretations made along the profiles oriented in East-West direction come into perspective. Profiles 03, 04 and 07 contain a possible fracture zone in the middle of the distance between the points where they all intersect Profiles 01 and 02 as seen in **figure 4.3.2** but they are also aligned with possible fracture zones marked in Profiles 01 and 02. Considering the fact that Profile 05 does not contain any possible weak zones, we may assess that these fracture zones are imprints of the same potential systematic East-West fracturing.

Generally, the central part of the study area seems to be quite ruptured and that there possibly are smaller zones present in this subarea, too, like the ones found with Profiles 09 and 10 which have a higher resolution (5 m electrode spacing). It should be noted that no possible fractures were marked within Profile 08, which means that the fracture zone seen in Profile 09 is not continued in depth but is instead a part of the low-resistivity layer mapped with Profile 08. The zone found in Profile 10 on the other hand, is matching zones found in all neighboring profiles and therefore is more reliable. Lastly, the southeastern flank of the study area encloses a possible North-South lineament which manifests after connecting the relevant vertical structures found in Profiles 05 and 07. What is interesting about this lineament is that it matches a depression seen in LiDAR topography and this can also be said for the fracture concentration seen in the southernmost parts of Profiles 01 and 02. In conclusion, based on the presented results from ERT profiling, a joint interpretation with additional data observation from refraction seismic profiling, boreholes logging and LiDAR data

a first order 3D fracture pattern can be evolved. A hint of how such a combined interpretation would look like is also shown in **figure 4.3.2** where the results of structural mapping published by Ganerød (2008) are plotted alongside ERT interpretations to reveal a very high correlation between the fracture zone interpretation based on resistivity and foliation joints, fractures and joints mapped in Åknes.

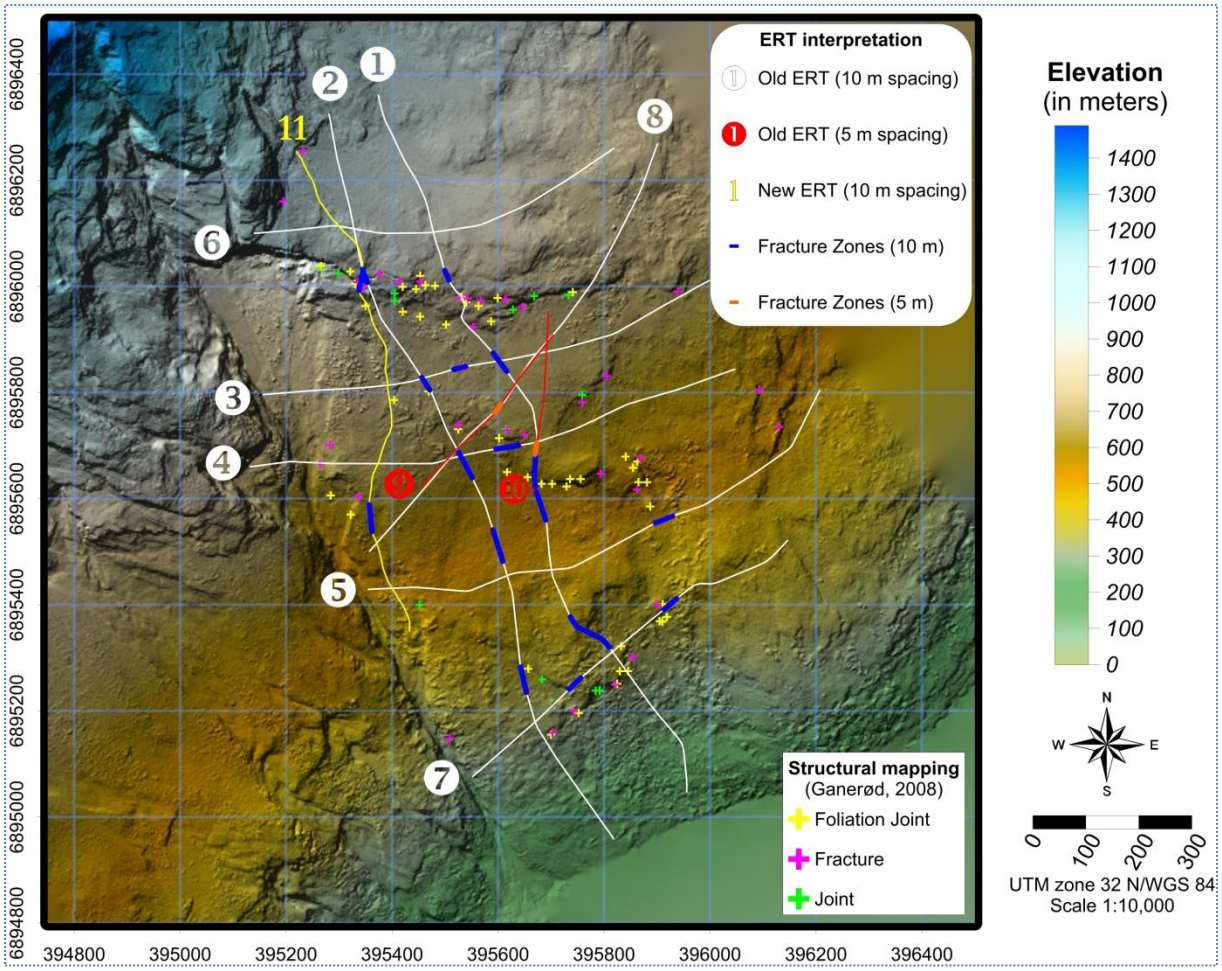

Figure 4.3.2: Positioning for all ERT profiles conducted in Åknes along with interpreted fracture zones shown in colored boxes. LiDAR elevation relief.

5. DISCUSSION - CONCLUSIONS

We may conclude that there is merit in reprocessing geophysical data collected in past years. In the case of ERT measurements, designated software Res2DInv development between 2005 and 2017 has yielded newer codes (versions 3.54j and 3.55.48 evolved into version 4.07.11) which have improved and hastened the inversion procedure. It has been shown that the general outcome is not much different with the use of different program versions but there are qualitative and quantitative differences which could affect results and subsequently interpretation.

Another aspect of newer inversion codes is the ability to produce more results in shorter times, aided by the simultaneous development of more powerful computers. Hence, we have managed to produce over 200 inversion results more than once over a very reasonable amount of time. This has helped us calculating balanced statistics

for each collected profile by combining point values from several inversion schemes and arrays. Essentially, this means that our results are evenly neutral (Mixed array, V/H filter = 1.0), favorable towards horizontal layering (Wenner array, L2-norm, V/H filter = 0.5) and favorable towards lateral variations (Dipole-Dipole array, L1-norm, V/H filter = 2.0).

Approaching our results from a statistical point of view has been extremely beneficial in all stages of this report, from visualization to interpretation. In particular, visualization is critical in terms of successful and effective presentation of inversion results but also in highlighting meaningful differentiations in the geoelectrical regime with clear color changes. We have shown that automatic color scales either in Res2DInv or other programs such as Surfer, can lead to unclear visualization but more importantly, to failed interpretations. Consequently, a custom-made color scale has been put together based on the histogram of the entire result database and on the decision, that the rainbow color sequence should be fitted logarithmically to the 1,000 to 60,000 Ωm spectrum. This was due to the fact that the number of resistivity values below 1,000 Ωm is negligible and that over 60,000 Ωm there is no need for further classification since we are talking about extremely drained fractured bedrock. Furthermore, we have determined that 12,000 Ωm is the critical resistivity below which water-saturated fractured bedrock can be found, varyingly healthy bedrock is attributed between 12,000 - 37,500 Ωm and anything over 37,500 Ωm represents extremely drained and fractured bedrock. These resistivity intervals might be rearranged based on future inputs from other information sources.

All inversion results were then exported from Res2DInv and gridded in Golden Software Surfer 15 (version 15.3.307 - 64 bit) using a Minimum Curvature method and spacing equal to 1 m for all axes. Consequently, the gridded profiles were extracted once again to ASCII format and each point value was associated with the appropriate UTM zone 32 N coordinates. Geophysicists should maintain full control and have responsibility over data gridding and since these data are scheduled to be delivered as point clouds to collaborating parties, we would like to ascertain that no new gridding will take place and differentiate the results. Another reason for creating denser point clouds than the ones exported from Res2DInv (half the electrode distance at best i.e. 5 or 2.5 m), is that they provide the possibility of creating post maps which can aid interpretation. Exporting of dense point clouds also means that they can be imported in programs such as Geosoft - Oasis Montaj (version 9.3.2) and other 3D presentation software and produce 3D views for the entire survey area.

The implementation of the aforementioned custom-made logarithmic color scale on all profiles has yielded a consistent display for the entire study area and the statistical analysis for each profile separately has led to the identification of gradual changes in the overall geoelectrical conditions along the North-South and East-West trending profiles. Generally, resistivities are lower in the southern and western counterparts of the study area representing water-saturated fractured bedrock and the extremely highly resistive top-layer indicative of drained fractured bedrock is mostly found in the northern and eastern part of Åknes. Along the North-South trend, there is a point near the end of the northernmost half of the study area where the geoelectrical regime changes keenly with an increase of ~25 % for the water-saturated part of fractured bedrock. After a maximum percentage of 35-40 % for water-saturated fractured bedrock is reached, it remains relatively constant until the end of the ERT coverage

near the fjord. Along the East-West on the other hand the decrease in resistivity is smoother and smaller in scale (20 to 30 % i.e. ~10 % difference).

The first step of interpreting the water-saturated fractured bedrock included the choice of inversion results that are more suitable for such a task and it was decided that Wenner and Mixed arrays using *Standard inversion* (L2-norm) and V/H filter equal to 0.5 are the best options. The second step included the isolation (clustering) of all resistivities below 12,000 Ωm which represent the water-saturated fractured bedrock. The third and final step further classified this water-saturated layer by dividing it in two parts at 7,500 Ωm. This was achieved with the use of classed post maps which unveiled the morphology of this layer but also its counterpart which is more prone to movement and thus more dangerous. The presentation of this interpretation stage took place in both 2D and 3D format and has shown that we are dealing with a very inhomogeneous water-saturated layer with a thickness that can reach 60 meters which is overlain by a drained fractured top layer that could be 20 meters thick.

The detection of fracture zones from the profiles conducted in Åknes was the last interpretation effort presented in this report. For this purpose, all Dipole-Dipole and Mixed array results were examined regardless of L1 or L2 norm utilized but at the same time ignoring all reprocessing with V/H filter equal to 0.5. This has led to a network of fractures which were then plotted on a map and comments were made about possible correlation between those zones. There are indications of a sub-parallel fracture system which is oriented along the East-West direction and consists of several different lineaments that cover the whole ridge.

Concluding, we believe that reprocessing of ERT data collected in past years in Åknes have added to the knowledge about the unstable rock masses and has fine-tuned the old interpretations without altering them much. Furthermore, new methods for presenting such data have been investigated and finally ERT profiling has taken one step up in presentation and entered the 3D domain. The possibility for ERT data and interpretation results to be presented in 3D space is now giving the possibility to collaborating parties to create multidisciplinary models and combine geophysical investigations with other related surveys.

In our interpretation we have classified the bedrock quality as:

Resistivity > 37.500 Ωm: Highly fractured drained bedrock
Resistivity 37.500 Ωm to 12.000 Ωm: Normal undisturbed bedrock (Healthy)
Resistivity < 12.000 Ωm: Fractured water saturated bedrock

The first group can also partly include talus (scree material) which can have the same resistivity level. It has to be emphasized that these intervals are not fixed and that there could be a gradual overlap in resistivity levels. This means that the thickness estimations given in this report are not absolute but rather indicative of the dimensions these formations could acquire.

6. REFERENCES

ABEM, 1999: ABEM Terrameter SAS 4000/SAS 1000. Instruction Manual. ABEM Printed Matter 93101. ABEM, Sweden.

ABEM, 2012: ABEM Terrameter LS. Instruction Manual. ABEM Product Number 33 3000 95, ABEM 20121025, based on release 1.11. ABEM, Sweden.

Dahlin, T., 1993: On the Automation of 2D Resistivity Surveying for Engineering and Environmental Applications. Dr. Thesis, Department of Engineering Geology, Lund Institute of Technology, Lund University. ISBN 91-628-1032-4.

Elvebakk, H., 2008: Borehullslogging, Åknes, Stranda kommune. NGU Rapport 2008.030.

Elvebakk, H., 2013: Borehullslogging i KH-08, Åknes, Stranda kommune, Møre og Romsdal. NGU Rapport 2013.032.

Ganerød, G.V., 2008: Structural mapping of the Åknes Rockslide, Møre and Romsdal County, Western Norway. NGU Rapport. 2008.042.

Ganerød, G.V., Grøneng, G., Aardal, I.B. & Kveldsvik, V. 2007: Logging of drill cores from seven boreholes at Åknes, Stranda municipality, Møre and Romsdal County. NGU Rapport 2007.020.

Ganerød, G.V., Grøneng, G., Rønning, J.S., Dalsegg, E. & Elvebakk, H. 2008: Geological Model of the Åknes Rockslide, western Norway. Engineering Geology.

Geosoft, 2018: Oasis Montaj ver. 9.3.2. Geosoft Inc. copyright © 2018.

Golden Software, 2018: Surfer 15, ver. 15.4.354 - Powerful Contouring, Gridding & 3D Surface Mapping Software. Golden Software, LLC, Colorado, USA.

Nøttveit, H.; Ganerød, G.; Grøneng, G. and Braathen, A., 2008: 3D assessment of effects caused by fault rocks and groundwater using petroleum modeling tools; Åknes rockslide, Western Norway. Landslides, February 2008.

Loke, M.H., 2017: RES2DINVx64 ver. 4.07. Rapid 2-D Resistivity & IP inversion using the least-squares method. Geotomo Software, August 2017. - www.geotomosoft.com

Rønning, J.S., Dalsegg, E., Elvebakk, H., Ganerød, G. & Tønnesen, J.F., 2006: Geofysiske målinger Åknes og Tafjord, Stranda og Nordal kommuner, Møre og Romsdal. NGU Rapport 2006.02.

Rønning, J.S., Dalsegg, E., Heincke, B.H. & Tønnesen, J.F., 2007: Geofysiske målinger på bakken ved Åknes og ved Hegguraksla, Stranda og Nordal kommuner, Møre og Romsdal. NGU Rapport 2007.026.

Schlumberger, 2017: PETREL software. © 2018 Schlumberger Limited. All rights reserved.

GEOLOGICAL
SURVEY OF
NORWAY

· NGU ·

Geological Survey of Norway
PO Box 6315, Sluppen
N-7491 Trondheim, Norway

Visitor address
Leiv Eirikssons vei 39
7040 Trondheim

Tel (+ 47) 73 90 40 00
E-mail ngu@ngu.no
Web www.ngu.no/en-gb/